GREEN SYNTHESIS OF METALLIC NANOPARTICLES USING LEAF EXTRACT OF SELECTED SILKWORM HOST PLANTS AND THEIR APPLICATIONS

A Thesis Submitted for Partial Fulfilment of the

Requirements for the degree of

DOCTOR OF PHILOSOPHY

by

SUNITA OJHA

(126106016)

Under the Supervision of

Professor Utpal Bora

Department of Biosciences and Bioengineering

Indian Institute of Technology Guwahati

Guwahati-781039, Assam, India

March 2018

INDIAN INSTITUTE OF TECHNOLOGY GUWAHATI
Department of Biosciences and Bioengineering
Guwahati-781039, Assam, India

DECLARATION

I do hereby declare that the content embodied in this thesis entitled **"Green Synthesis of Metallic Nanoparticles using Leaf Extract of Selected Silkworm Host Plants and their Applications"** is the result of investigations carried out by me under the supervision of **Professor Utpal Bora** and is submitted to Department of Biosciences and Bioengineering, Indian Institute of Technology Guwahati, Assam, India for the award of degree of *Doctor of Philosophy in Biosciences and Bioengineering*.

In keeping with the general practice of reporting scientific observations, due acknowledgements have been made wherever the work described is based on the findings of other investigators are referred, and copyright licenses have been taken from respective publishers.

March 2018

SUNITA OJHA
(Roll. No. 126106016)

INDIAN INSTITUTE OF TECHNOLOGY GUWAHATI

Department of Biosciences and Bioengineering

Guwahati-781039, Assam, India

CERTIFICATE

This is to certify that the matter embodied in this thesis entitled **"Green Synthesis of Metallic Nanoparticles using Leaf Extract of Selected Silkworm Host Plants and their Applications"** is the result of investigations carried out by **Ms. Sunita Ojha** (Roll No: 126106016) under my supervision, and is submitted to the Indian Institute of Technology Guwahati, Guwahati-781039, Assam, India for the award of degree of *Doctor of Philosophy in Biosciences and Bioengineering*. This work has not been submitted elsewhere for a degree.

March, 2018

Prof. Utpal Bora

(Thesis Supervisor)

Department of Biosciences and Bioengineering

Indian Institute of Technology Guwahati

Guwahati-781 039, India

Dedicated to

My Family, Teachers

&

Almighty God

……Sunita Ojha

ACKNOWLEDGEMENT

At the outset, I would like to express my deepest sense of gratitude to my thesis supervisor Prof. Utpal Bora for his guidance, support and direction. He has been the leading light in my endeavor for meaningful and fruitful research in the fast growing field of Biotechnology. I must acknowledge the freedom that I was given in every step of my research work. I am grateful to the chairman Prof. Aiyagari Ramesh and members of the Doctoral Committee Dr. Biplab Bose and Dr. Vaibhav V. Goud for their valuable suggestions and advices which enabled me to improve my work.

I would take this opportunity to thank Prof. Gautam Biswas, Director, IITG, for providing all the necessary facilities and a conductive academic environment. I sincerely acknowledge the financial support from Ministry of Human Resource Development (MHRD) for providing me fellowship, and Dept. of Biotechnology (DBT), Govt. of India for research grants to my supervisor.

I owe my gratitude to the Department of Biotechnology, Central Instruments Facility and Central Library for providing me all the support and necessary facilities. Also, thanks to the Dept. of Chemistry (for FTIR), Physics (for XRD), Chemical Engineering (for TGA), Center for Environment (for AAS); thanks to all the scientific staff for their kind co-operation. I extend my gratitude to NCCS, Pune for providing necessary cell lines. I would also like to thank Central Silk Board Khanapara, Guwahati, Assam, India, for providing me the leaf samples. I would like to thank Mr. Azizur Rehman for his kind cooperation in collecting leaf samples. I acknowledge S.A.I.F., NEHU, Shillong and staffs for providing me TEM facility.

My great thanks to my research group previous members Dr. Arghya Sett, Dr. Suradip Das, Dr. Manoj Gadewar, Dr. Manav Sharma, Dr. Disco Singh, Swagata Sharma, Krishna Nayani Dutta, Smita Bhattacharjee, Nipon Sarmah, Ajanta Deka, Pradiptya Das, Kasturi Goswami, current members Dr. Deepika, Ms. Papori Buragohain, Ms. Hasnahana Chetia, Mr. Debajyoti Kabiraj, Mr. Vimal Moshahari, Mr. Jon Jyoti Kalita, Ms. Biju Bharali, Ms. Dharitri Saikia, Ms. Rupanjali, Ms. Tinka

Singh, Mr. Manas Barkataki for providing me a healthy and enjoyable environment in the lab. I am immensely pleased to express my heartiest thanks to my friends Ms. Nibedita Behera, Mr. Nand kishore Roy, Ms. Anuma Singh, Ms. Karabi Saikia, Ms. Saumya Ahlawat, Ms. Rupashree Panda, Ms. Shreedevi Moharana, Ms. Madhusmita Das, Ms. Aneeta and others from all departments, centers and hostel, for the moral support. Their presence made my five years stay at IITG memorable.

This thesis has been kept on track and been seen through to completion with the immense moral support, sheer encouragement and unconditional love from my father Dr. Jaladhar Ojha, my mother Sanjukta Ojha, my elder sister Er. Namita Ojha, my brother Mr. Shubhranshu Shekhar Ojha, brother in law Er. Rajkumar Maharana, relatives, well-wishers, and teachers for their undying love and support throughout my life that installed in me the spirit of overcoming any obstacle and heightened my strength to achieve my dream in life. A special thanks to my husband Er. Padarabinda Maharana for his constant support, motivation to achieve success in my life. My heartiest thanks to my friends Saikata Sengupta, Ankita Hazarika, for their love and support in thick and thin. I owe all my achievement to them and last but not the least I thank the Almighty God for all the blessings throughout my life.

Sunita Ojha

Table of Contents

Synopsis

Particles with at least one dimension in nanoscale range i.e. 1-100 nm are known as nanoparticles. There are several methods of nanoparticle synthesis out of which green synthesis is less time consuming, low cost and environment friendly method. It involves chemical reduction of metal ions using microbes, plants, plant extract, biomass, etc. Green synthesis of nanoparticles using plant extract is fast and involves less downstream processes. Plant extract contains polyphenols, flavonoids, alkaloids and terpenoids which are the main reducing agents for nanoparticle synthesis. There are numerous reports of plant mediated metallic nanoparticle synthesis. Most of these plants are medicinally important. Apart from these, some of the silkworm host plants are also explored for nanoparticle synthesis. However, some of the primary silkworm host plants are not explored in this context despite of their medicinal and indirect economic importance.

North East India is rich in seri-biodiversity which includes silkworm varieties and their host plants. Five types of silkworms exist in North East region namely, muga (*Antheraea assamensis*), eri (*Samia cynthia ricini*), Indian tasar (*Antheraea mylitta*), oak tasar (*Antheraea proylei*) and mulberry (*Bombyx mori*) silkworms among which muga and eri are majorly produced in Assam. Silkworms feed on a variety of host plants which are categorized into primary, secondary and tertiary host plants based on silkworm feeding habit. The presence of phytochemicals in the host plants make them medicinally important. Therefore, we have selected some primary silkworm host plants of eri and muga silkworm which are not explored for nanoparticle synthesis to

our knowledge. Three selected silkworm host plants include *Ricinus communis* var *carmencita*, *Heteropanax fragrans* and *Persea bombycina*. *R. communis* (castor) is a primary host plant of eri silkworm. Red Castor or *R. communis* var *carmencita* is one of the variety of castor plants. The red castor leaves are used as anti-inflammatory and possess antimicrobial activity against *Mycobacterium tuberculosis* and *Aspergillus niger*. Similarly, *H. fragrans* (Roxb) Seem commonly known as kesseru plant is also a primary host plant of eri silkworm. These are used to treat cancer by chakma community of Bangladesh. *P. bombycina* (King ex Hook. F.) Kosterm, locally known as som, is the primary host plants of muga silkworm. In our study, we have selected these plants for the synthesis of metallic nanoparticles to widen their applications in various areas such as drug delivery, pharmaceutical sector, agriculture, environmental application, electronics, etc.

To accomplish the same, the objectives of the present research work are fixed as follows:

(i) Green synthesis of silver nanoparticles using *Ricinus communis* var. *carmencita* leaf extract and their applications.

(ii) Green synthesis of zinc oxide nanoparticles using *Heteropanax fragrans* leaf extract and their applications.

(iii) Green synthesis of iron oxide nanoparticles using *Persea bombycina* leaf extract and their applications.

Based on the objectives we have categorized the thesis into following chapters.

Chapter 1. Introduction and Review of Literature

This chapter describes the concept of nanotechnology, various types of nanoparticles and methods of nanoparticle synthesis and their applications. Various studies related to nanoparticle synthesis, particularly green synthesis and their potential applications are reviewed in this chapter. Studies related to silver, zinc oxide and iron oxide nanoparticle green synthesis have been reviewed in detail.

Chapter 2. Green Synthesis of Silver Nanoparticles using *Ricinus communis* var. *carmencita* Leaf Extract and their Applications.

In this study, we report the synthesis of silver nanoparticles (RcAgNPs) using methanolic leaf extract of *Ricinus communis* var. *carmencita*. The polyphenols present in the leaves reduce Ag^{+} ions to Ag^{0} observed by a color change in the solution. Silver nanoparticle formation was ensured by surface plasmon resonance between 400 nm to 500 nm. The RcAgNPs were found to be in a size range of 30-40 nm as confirmed from TEM analysis. X-Ray diffraction studies of RcAgNPs confirmed the face centered cubic structure of RcAgNPs. Crystallinity of the synthesized nanoparticles was further supported by UHRTEM and SAED studies. The capping of RcAgNPs with phytochemicals was studied by FTIR and TGA analysis. It also showed antibacterial activity against both gram positive and gram negative strains. RcAgNPs were found to be non-toxic against normal cell line (mouse fibroblast cell line L929) at lower concentrations (0-60 µg ml^{-1}).

Chapter 3. Green Synthesis of Zinc Oxide Nanoparticles using *Heteropanax fragrans* Leaf Extract and their Applications

In this chapter, we have used aqueous extract of Kesseru leaves (*Heteropanax fragrans*) to synthesize ZnO nanoparticles. The zinc oxide nanoparticles (KeZnONP) were characterized by UV-Visible spectroscopy, Field Emission Scanning Electron Microscopy, Transmission Electron microscopy, X-ray Diffraction, Fourier Transmission Infrared Spectroscopy and thermo-gravimetric analysis. Based on UV-visible spectroscopy result, the band gap of KeZnONP was found to be 3.24eV. Size and shape of the nanoparticles were analyzed by electron microscopes. TEM studies confirmed the nanosize and crystallinity of the nanoparticles. XRD studies confirmed the wurtzite structure of the ZnO nanoparticles. FTIR and TGA studies indicated capping and stability of the nanoparticles. The KeZnONP acted as photocatalyst in methylene blue dye degradation under UV light illumination. The rate of degradation of methylene blue (5 mg/L) by KeZnONP (1 mg/ml) at 25°C and pH 7 was calculated to be 9.79×10^{-3} min^{-1}. The nanoparticle can be reused for methylene blue treatment for multiple cycles of treatment.

Chapter 4. Green Synthesis of Iron Oxide Nanoparticles using *Persea bombycina* Leaf Extract and their Applications

This chapter outlines synthesis of iron oxide NPs using *Persea bombycina* leaf extract in alkaline condition. The iron oxide nanoparticles (PbFeONPs) were characterized by FESEM, TEM, XRD, FTIR studies. Magnetic properties were studied using VSM analysis. Cytotoxicity of the PbFeONPs was assessed by MTT assay. Microscopy studies revealed the nanoscale size of the nanoparticles. UHRTEM, SAED and XRD

studies confirmed the crystallinity of the nanoparticles. Presence of Fe_3O_4 nanoparticles was confirmed by XRD studies. VSM analysis confirmed ferromagnetic property of the iron oxide nanoparticles. From MTT assay, it was found that PbFeONPs were non-toxic to mouse fibroblast cell line at concentrations up to 50 μg/ml. These nanoparticles were used as Fenton like catalyst for the degradation of methylene blue at optimum pH condition. 90% of methylene blue at 20 mg/L concentration was degraded after 140 minutes of adding PbFeONP (0.3 mg/ml dose) along with H_2O_2 (0.1 mM). The rate of degradation of methylene blue was 18.5×10^{-3} min^{-1} . The PbFeONPs can be recycled as 90% of methylene blue was removed after 4^{th} cycle of reuse.

Chapter 5. Summary and Future Prospects

In this chapter, we have discussed the overall summary and scope for future work. RcAgNP, KeZnONP and PbFeONP have been successfully synthesized using leaf extract of silkworm host plants- *Ricinus communis* var. *carmencita*, *Heteropanax fragrans* and *Persea bombycina,* respectively. Structural characterizations confirmed their crystallinity, nanostructure, capping with phytochemicals, thermal stability and cytotoxicity of the synthesized nanoparticles. Antibacterial activity of RcAgNPs and UV absorption properties of KeZnONP can be used to formulate pharmaceutical products and cosmetics such as antibacterial cream, sunscreen lotion and powders, etc. Dye removal activity of the KeZnONP and PbFeONPs can be explored for waste water treatment.

List of Publications:

- Ojha, S., Sett, A., & Bora, U. (2017). Green Synthesis of Silver NPs by *Ricinus communis* var. *carmencita* Leaf Extract and its Antibacterial Study. *Advances in Nanosciences: Nanoscience and Nanotechnology*, 8, 1-8.
- Ojha, S., Singh, D., Sett, A., Chetia, H., Kabiraj, D. & Bora, U (2018). Nanotechnology in Crop Protection. In *Nanomaterials in Plants, Algae and Micro-organism: Concepts and Controversies (Vol 1)*. Academic Press, 345-390.

Manuscript Submitted

- Ojha, S., Saikia, D. & Bora, U. (2018). Nanopharmaceuticals: Synthesis, Characterization and Challenges. In *Nanopharmaceuticals: Principles and Applications*. Environmental Chemistry for a Sustainable World.

Manuscript under Preparation:

- Green synthesis, characterization and applications of zinc Oxide nanoparticles using *Heteropanax fragrans* leaf extract (Under Preparation)
- Green synthesis, characterization and applications of iron Oxide NPs using *Persea bombycina* leaf extract (Under Preparation)

List of Figures

List of Tables

CHAPTER 1

Introduction and Review of Literature

CHAPTER 1

Introduction and Review of Literature

1.1 Nanoscience and Nanotechnology

Nanoscience is the study of objects/particles that are in nanoscale i.e. 1-100 nm range. Nanotechnology is an upcoming branch of science that deals with functional structures designed with at least one characteristic dimension measured in nanometers. This technology has found a wide range of applications ranging from energy production to industrial production processes and biomedical applications. The term nanotechnology refers to both nanoscience and nanotechnology where nanoscience is a convergence of physics, chemistry, materials science, and biology and involved in manipulation of matter in nanoscale. Nanotechnology creates products based on the principles of nanoscience (Kumar and Kumbhat, 2016).

Nanoparticles (NPs) are solid particles that are of size 1-100 nm, atleast in one dimension (Xia et al., 2003). They are made up of several tens or hundreds of atoms or molecules and can be amorphous or crystalline. They can exist in various shapes such as spherical, rod, wire, planes, cages, stars, multipods etc. (Chen et al., 2016). Zero-dimensional nanostructures include quantum dots, NP arrays, core-shell NP, hollow-cubes and nanospheres. Whereas one-dimensional nanostructures include nanowires, nanorods, nanotubes, nanobelts, nanoribbons, and hierarchical nanostructures and two-dimensional nanostructures embrace junctions (continuous islands), branched structures, nanoprisms, nanoplates, nanosheets, nanowalls, and

nanodisks (Tiwari et al., 2012; Xia et al., 2003; Parameswaranpillai et al., 2016). Due to their nanoscale size, they have unique physical and chemical properties such as high surface area to volume ratio, high surface energy, and unique mechanical, thermal, magnetic, electrical and optical behavior compared to their bulk counterparts. These unique properties open up a wide range of applications for these NP, starting from electronics, energy harvesting and storage, communications, to biology, medicines, cosmetics clothes etc. (Hasan, 2015). The applications of NPs in different areas depend on their characteristics such as size, shape, structure, surface charge, surface area, surface porosity, and composition (Kumar and Kumbhat, 2016). However, their chemical reactivity and dispersity differ in different solvent medium. Therefore, their properties can be modulated by modifying their surface with different functional groups (Kievit et al., 2011; Nam et al., 2013).

NPs are available commercially as powders or liquid suspension. Surfactants are added to obtain a uniform and stable suspension. NPs can be used in coatings and devices. Carbon black, polymer dispersions, or micronized drugs have been produced in industrial scale long ago. Other commercialized NPs include metals (Ag, Au), metal oxides (silica oxide, titanium oxide, alumina oxide, and iron oxide), semiconductors (Cadmium telluride, gallium arsenide) and alloys (Kumar and Kumbhat, 2016).

1.2 Types of Nanoparticles

Broadly NPs are categorized into organic and inorganic NPs based on their utilization in therapy and diagnostics. The list of various types of NPs are represented in **Figure 1.1**. Organic NPs include polymeric structures, lipid based nanostructures, and

carbon nanostructures. Inorganic NPs include silica NPs, magnetic NPs, semiconductor NPs, plasmonic NPs, and upconversion NPs (Chen et al., 2016). Based on their use in pharmaceuticals, they are classified into polymeric and non-polymeric NPs. Polymeric nanostructures include polymeric nanoparticles, denderimer, micelles, drug conjugates. Non-polymeric structures include carbon nanotubes, metallic NPs, silica NPs, quantum dots (Bhatia, 2016).

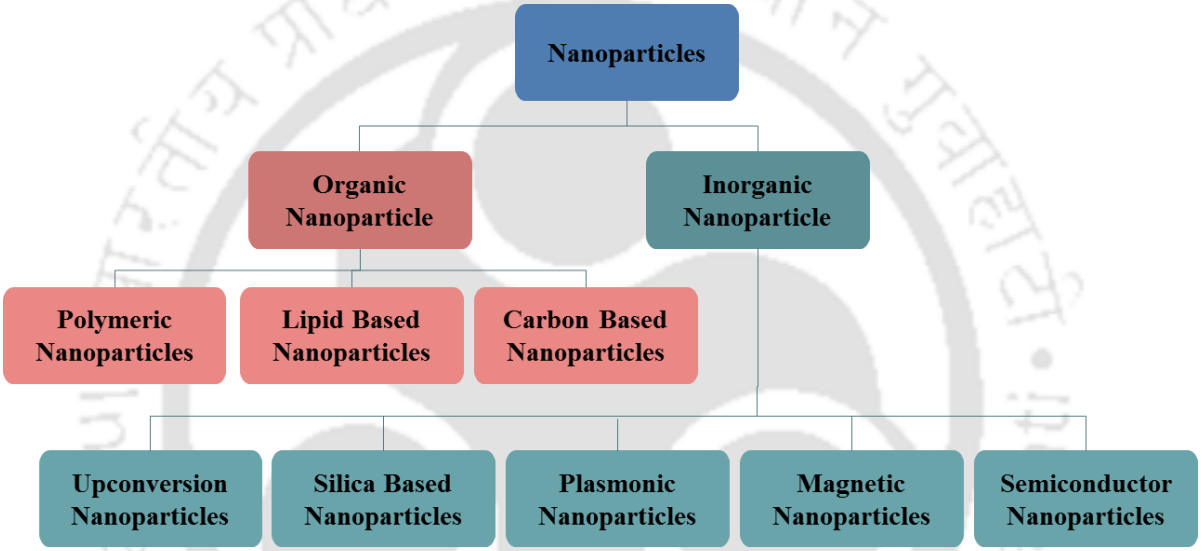

Figure 1.1 Classification of Nanoparticles (Source: Chen et al., 2016)

1.2.1 Polymeric nanoparticles

Polymeric nanoparticle is a collective term for nanospheres, nanocapsules, nanomicelle and nanogel. Nanospheres contain a solid sphere in which particles are either adsorbed on the sphere surface or encapsulated within the particle. Nanocapsules contain a solid matrix shell and a core filled with water or oil. Amphiphillic block copolymers self-assemble in an aqueous medium to form micelles (Nuruzzaman et al., 2016). Nanogels are formed from hydrophilic polymers crosslinked by Van der Waal's forces or covalent bonds. (Sultana et al., 2013)

Polymeric NPs are generally prepared by two main strategies: one is by dispersion of preformed polymers and another is by polymerization of monomers (Rao and Geckeler, 2011). The techniques involved for the preparation of polymeric NPs from preformed polymers include solvent evaporation, salting-out, dialysis and supercritical fluid technology. On the other hand, techniques involved for the preparation of polymeric NPs from monomer units are micro-emulsion, mini-emulsion, surfactant-free emulsion and interfacial polymerization (Rao and Geckeler, 2011). The polymers used are desirable to be non-toxic, non-antigenic and biodegradable for biomedical applications.

1.2.2 Lipid based nanoparticles

Three major lipid based NPs are (a) phospholipid-polymer nanomicelles, (b) lipid-bilayer vesicular nanostructures (liposomes), and (c) solid-lipid NPs (SLNs). Nanomicelle and liposomes are made up of diglycerides and the solid-lipid NPs are made up of triglycerides. Nanomicelles are made up of amphiphillic monomers that self-aggregrate above critical micellar concentration in aqueous systems (Mitra et al., 2017). Nanoliposome or submicron bilayer lipid vesicle can incorporate various types of bioactive materials ranging from pharmaceuticals to cosmetics and nutraceuticals (Mozafari, 2010). Solid-lipid NPs are of submicron size (50-1000 nm) composed of lipids which exist in solid state at room temperature. They are prepared by high pressure homogenization (hot and cold homogenization), ultrasonication (Probe and bath sonication), solvent evaporation method, solvent emulsification method, supercritical fluid method, microemulsion based method, spray drying method,

double emulsion method, precipitation technique, and film-ultrasound dispersion method (Ekambaram et al., 2012).

1.2.3 Carbon based nanoparticles

Carbon based nanostructures include fullerenes, carbon nanotubes and possess electrical and tensile strength. Fullerenes are in the form of hollow spheres, ellipsoids or tubes. Spherical fullerenes are also referred to as bucky balls. Fullerenes especially C60 have attractive electrochemical and physical properties (Bakry et al., 2007). Carbon nanotubes are allotropic crystalline forms of carbon sheets that are either single layer (Single walled carbon nanotube, SWNT) or multilayer (Multi walled carbon nanotube, MWNT) (Bhatia, 2016). These CNTs have remarkable strength and unique electrical properties (conducting, semiconducting and insulating) and are useful in biomedical applications such as sensing, imaging, and drug delivery. CNTs can facilitate conjugation through the functional groups on the surface (Chen et al., 2016).

1.2.4 Inorganic nanoparticles

Inorganic NPs have gained much importance in material science due to their potential technological importance, especially bionanotechnology owing to their size-dependent optical, magnetic, electronic, and catalytic properties. These inorganic NPs can be categorized into semiconductor nanostructures, magnetic NPs, plasmonic NPs, silica based NPs, and upconversion NPs. Quantum dots are the nanocrystals of inorganic semiconductor of sizes 3-10 nm. Semiconductor material from group II−VI (e.g., CdSe, CdS, CdTe, ZnS, ZnO, etc.), III−V (e.g., InP, InAs, GaP,

GaAs, etc.), and IV (e.g., Si, Ge, etc.) can form excellent quantum dots. Under UV or visible light quantum dots are excited to induce auto-fluorescence. They are used as optical probes in bioimaging particularly near-infrared emitting quantum dots. Plasmonic NPs are made up of novel metals such as gold and silver. They possess localized surface plasmon resonance due to the collective oscillation of surface electrons at the interface of plasmonic NPs and the surrounding dielectric medium. This phenomenon happens when resonance occurs between the frequency of incident light photons and the natural frequency of surface charge carriers. Magnetic NPs include iron oxide NPs such as Fe_3O_4, α-Fe_2O_3, and γ-Fe_2O_3, each having unique magnetic properties. Superparamagnetic iron oxide (Fe_3O_4) NPs (SPIONs) have been utilized for biosensing, bioseparation, drug and gene delivery, magnetic therapy of cancer. Silica NPs are biocompatible with tunable pore size and diameter. They can encapsulate water insoluble compounds such as drugs and organic dyes for imaging and chemotherapy. Upconversion nanomaterials are dilute guest−host systems where the guest as trivalent lanthanide ions (e.g., Er^{3+}, Ho^{3+}, Yb^{3+}, Tm^{3+}) is dispersed in an appropriate dielectric host lattice (e.g., NaYF4) with at least one dimension being less than 100 nm (Chen et al., 2016).

1.3 Applications of Nanotechnology

1.3.1 Nanotechnology in biology and medicine

NPs are used as therapeutic agents, drug and gene delivery vehicles and for diagnosis. The details have been described below:

Drug and gene delivery

NPs have many significant advantages over conventional and traditional drug delivery system (Tiruwa, 2016). Controlled and sustained release of the drug at the site of localization can be achieved by NPs. They enhance drug circulation in blood, bioavailability, and therapeutic efficacy. NPs can be administered by various routes including oral, nasal, parenteral, intra-ocular etc. At the tiny areas of body, NPs show better drug delivery as compared to other dosage forms and target to a specific cell type or receptor. Due to their small particle size, NPs overcome resistance by physiological barriers in the body and easily penetrates cell walls, blood vessels, stomach epithelium and blood–brain barrier. NPs enhance the aqueous solubility of poorly soluble drug, which improves bioavailability of the drug. By using polymers-drug release form, NPs can be modified which makes polymeric NPs an ideal drug delivery system for cancer therapy, vaccines, contraceptives, and antibiotics (Tiruwa, 2016).

RNA interference is used to study gene function through gene silencing mechanism in which mRNA is degraded in target specific manner when a sequence specific double stranded RNA is introduced into a cell. This process is blocked by many obstacles such as 1) difficulty in entering into the cell which is due to high molecular weight and negative charges, 2) degradation by nucleases, 3) difficulty in localization into cell compartment, 4) in vivo instability. These obstacles are overcome by using NPs as a vehicle for gene delivery. Cationic lipid and polymer have been used to transport nucleic acid into cells which protects the nucleic acid from enzymatic degradation. NPs can also be used for targeted delivery of the nucleic acid when

conjugated with target specific antibody. Further, it is easy to functionalize NPs so that they can bind to the specific target such as cell organelle and enter through endocytosis (Wang and Wang, 2014)

Fluorescent biological labels

Use of semiconductor nanocrystals as fluorescent probes is an emerging technique for biological staining and diagnostics. As compared to fluorophores these nanocrystals are photochemically stable and have a narrow tunable symmetric emission spectrum. Quantum dot bioconjugates are much brighter than organic dyes and stable against photo bleaching (Bruchez et al., 1998; Chan and Nie, 1998).

Tissue engineering

Nanotechnology has a therapeutic approach in tissue engineering. During bone implantation, the surface of the artificial bone should not be smooth as it causes growth of fibrous tissue between natural bones and implant that could result in inflammation and loosening of implant. Natural bone surface is not smooth and contain features of up to 100 nm. Therefore artificial bone surface should possess nanostructures that can stimulate osteoblast production. Polymeric, ceramic, and recently metallic materials demonstrated these effects. Several non-degradable particles, such as silica, lipid, dendrimer, hydroxyapatite, or gold NPs have been used as an effective protein for bone tissue regeneration (Gupta et al., 2013).

Antimicrobials

NPs as antimicrobial are of great interest as they might perform where antibiotics fail. This includes killing multidrug resistant strains and biofilm. NPs that have been

explored as antimicrobials include metals, metal oxides and organic NPs. These NPs vary in their property and so in their mode of action. Moreover, depending on the bacteria and their physiological state, the antimicrobial activity of NPs varies. Broadly, nanomaterials act along two major lethal pathways: 1) disruption of membrane potential and integrity, and 2) production of reactive oxygen species. Highly potent antimicrobial metallic and metal oxide NPs include silver (Ag), iron oxide (Fe_3O_4), titanium oxide (TiO_2), copper oxide (CuO), and zinc oxide (ZnO). Organic NPs also exhibit antimicrobial activity either by releasing antibiotics, antimicrobial peptides, or by contact killing cationic surfaces. The organic NPs having antimicrobial properties include Poly-ε-lysine, quaternary ammonium compounds, and cationic quaternary polyelectrolytes etc (Beyth et al., 2015).

Anticancer

NPs have the potential to be used as cancer diagnostics and therapeutics. They can help to overcome the challenge faced for cancer treatment in localizing drugs to the tumor sites, drug resistance by tumors and short drug circulation period. Metallic NPs such as silver, gold, iron oxide NP, titanium oxide, cerium oxide possess anti-cancer properties owing to their unique physical, chemical and biological properties. Numerous reports have been published regarding the anti-cancerous property of green synthesized metallic NPs which is reviewed well by Rao et al., 2016. AuNP has the ability to bind thiol and amine group which is used for functionalization of the AuNP for medical applications. AuNPs synthesized from *A. leptopus* exhibit good anticancer activity against MCF-7 breast cancer cells at 257.8 µg/mL (Balasubramani et al., 2015). The anti-cancerous property of AuNP is through oxidative stress induced

by the AuNPs. Iron oxide NPs bind covalently to the tumor and induce antitumor activity directly and indirectly via nontoxic wavelength radiation which is absorbed by toxic stimuli of reactive oxygen species production. Iron oxide NPs are used as an agent to treat prostate cancer and to induce magnetic hyperthermia in the brain in combination with radiation and chemotherapy. Hyperthermia leads to cell death due to increase in temperature 150-400 °C. Surface functionalization of TiO2 is preferred as anti-cancerous agent (Vinardell and Mitjans, 2015; Jain et al., 2005). Cerium oxide has the advantage of selective killing of cancerous cell through oxidative stress and radiation induced damage without harming normal cells. Silver-selenium bimetallic NP synthesized using quercetin and gallic acid presented antitumor activity against Dalton's lymphoma cells. However, the size, shape, and surface properties of the NPs are important as they influence circulation time, cellular uptake, bio-distribution, and cancer drug delivery of NPs (Rao et al., 2016).

Bioimaging

The advantages of NPs in molecular imaging includes their non-toxicity, inertness and zero binding to unspecific bio macromolecules. The optical properties of dyed NPs and intrinsically fluorescent NPs are not affected by proteins outside. They can be internalized easily depending on their size and surface properties (Wolfbeis, 2015). Au, Ag, Cu, Fe_2O_3, ZnO, Pt, Se, Gd NPs are used as contrast agents in medical imaging such as MRI and CT (Shivaramakrishnan, et al., 2017). Au and Ag nanoclusters are used for molecular imaging for the diagnosis and treatment of diseases due to their SPR (Shivaramakrishnan, et al., 2017; Li et al., 2014).

Separation and purification of biological molecules and cells

In biological research, efficient isolation of specific cells from complex mixtures is necessary. The detection of specific cell types and cells found in low frequency can be achieved by NPs which are very sensitive for the application. One such application is detection and capture of circulating tumor cells so that cancer metastasis can be detected and this will act as prognostic biomarker for metastatic breast, colorectal, and prostate cancer (Wang and Wang, 2014). Quick capture of the targeted molecules can be achieved by magnetic iron oxide with surface altered with streptavidin, carboxyl groups or amine groups through conjugation. This will lessen non-specific binding (Gupta et al., 2013).

Biosensor

Various metal NPs, metal oxide NPs, semiconductor NPs, and nanocomposites are used in electrochemical sensors and biosensors. The basic functions of these NPs involve immobilization of biomolecules (Ag, Au, SiO_2, TiO_2), catalysis of electrochemical reactions (Au, Pt); enhancement of electron transfer (Au, Ag, TiO_2, ZrO_2); labeling biomolecules (CdS, PbS, Au, Ag) acting as reactant (MnO_2). Use of NP in sensor improves sensitivity, selectivity and detection (Luo et al., 2006). AuNPs synthesized using *Syzygium aromaticum* extract were functionalized with cysteine, which when used in a urea biosensor increased the response to 60% due to increased surface area and stability of the enzyme (Kaur et al., 2012). ZnO NPs synthesized using *Corymbia citriodora* leaf extract were used in H_2O_2 biosensor. The excellent detection performance of the sensor for trace amount of H_2O_2 demonstrates that it can be used in clinical application (Zheng et al., 2016).

1.3.2 Nanotechnology in environmental remediation

Application and development of NPs in environment clean up technologies are gaining importance though their risk of ecotoxicity must be assessed. In recent years, zero valent iron, carbon nanotube and nano fibres have been applied for the remediation of contaminants such as hydrocarbons, chlorinated compounds, organic compounds and heavy metals (Patil et al., 2016).

Catalytic activity

In recent years environmental pollution caused by waste dyes has been a big issue. Physical and chemical methods including photodegradation, reverse osmosis and chemical reduction are costly, low energy efficient and lengthy. However, metallic NPs are high energy efficient catalysts for the degradation of organic dyes.

Cassia auriculata L., the flower aqueous extract mediated synthesized AgNP was an effective catalyst for the degradation of 4-nitrophenol and methyl orange (Muthu and Priya, 2017). Similar work has been carried out by Raghasudha (2016) in which they have synthesized AgNP using *Syzigium cumini* leaf extract and studied the catalytic activity of AgNP on reduction of para nitro phenol. Many reports of green synthesized AgNPs catalyzed reduction of methylene blue have been published (Edison and Sethuraman; Tripathy et al., 2013). The catalytic activity of silver nanoparticle is shape dependent (Xu et al., 2006). The most common iron oxide NPs utilized for water remediation are magnetite, hematite, maghemite, goethite, ferrihydrite due to their high catalytic activity, low toxicity and superior chemical suitability (Suib, 2013).

Water purification

Nanotechnology offers a great possibility for efficient removal of pollutants and pathogenic micro-organisms. NPs are used for detection and removal of chemical and biological substances including metals (e.g. Copper, cadmium, mercury, lead, zinc, lead), nutrients (e.g. Ammonia, phosphate, nitrate and nitrite), cyanide, organics, algae (e.g. cyanobacterial toxins) viruses, bacteria, parasites and antibiotics (Tiwari et al., 2008). Carbon based nano-adsorbent (Carbon nanotubes), metal containing NPs, zeolites and polymer nano-adsorbents are evaluated as functional materials for water purification. Metailic NPs have short intraparticle diffusion distance are compressible, abrasion resistant, photocatalytic and magnetic. They can be used for removal of heavy metals and other water pollutants; for example, use of magnetic NP (Fe_3O_4) for arsenic removal from ground water has already been established. Moreover, AgNP and TiO_2 NPs are useful as disinfectants and antibiofouling agents. TiO_2 NPs are low human toxic and chemically stable, thereforen not requiring periodic renewal. However, it needs UV lamps for its activation. Silver coatings need to be renewed as they release silver ions in the disinfection process and doesn't require extra energy for their activation (Gehrke et al., 2015). Degradation of organic contaminants such as 4-chlorocatechol by ZnO NP semiconductor films have been studied.

1.3.3 Nanotechnology in agriculture

Increase in crop productivity depends on crops resistivity towards pests, agrochemicals and varying environmental conditions. Nanotechnology is a boon to the concept of precision farming which aims for targeted delivery, firm attachment,

and controlled release of the active material. Encapsulation or entrapment of agrochemicals using polymers and dendrimer by surface ionic attachment helps in their controlled release and improves solubility and stability. Due to their antimicrobial activity, NPs of metals such as silver, zinc oxide, titanium oxide and non metals such as silica, sulfur can be used to eradicate bactericide and fungicide resistant pathogens (Chowdappa and Gowda, 2013). Polymers release the entrapped agrochemicals in response to stimulis such as pH, temperature, electric field, magnetic field etc. (Peteu et al., 2010). Recently, nanosensors were used as diagnostic tools to detect plant infection, nutrient and moisture content, pesticide residual, temperature and soil condition. These pieces of information are helpful for periodic application of nutrients, pesticides and herbicides, and timely plantation and harvesting of the crops. The nanomaterials such as carbon nanomaterials (CNMs) are absorbed through roots or by making pores in seeds and then translocated to the aerial parts (Rico et al., 2011; Husen and Siddiqui, 2014).

1.3.4 Nanotechnology for sustainable energy

Use of nanomaterials in the energy sectors for energy conversion domain is mainly focused on solar energy (mostly photovoltaic technology for local supply), hydrogen conversion and thermoelectric devices. Dye sensitized solar cells are the first nanostructured solar cells. Using nanophotocatalysts for splitting of water is the most promising method of hydrogen production. NPs are used in rechargeable batteries (nanoLi-ion batteries), and supercapacitors for sustainable electricity storage (Serrano et al., 2009).

1.3.5 Nanotechnology in electronics

Nanotechnology acts as a toolkit for electronic industry that allows to synthesize materials with special properties tuned by ultrafine particle size, crystallinity structure and surfaces. Some of the applications of nanotechnology include their use as semiconductors, in packaging IC and MEMS devices, displays, EMI shielding, conductive adhesives, and novel attachment structures (Rae, 2006)

1.4 Synthesis of Nanoparticles

Metallic NPs can be synthesized via two major approaches: top-down approach or bottom-up approach. In top down approach, a bulk metal is deconstructed to NPs using mechanical or chemical techniques, but they suffer from surface imperfections. In bottom-up approach, NPs are synthesized from atoms, molecules or clusters and are homogeneous in chemical composition. Bottom-up approach can be performed mechanically, chemically and biologically**.** Various methods of nanoparticle synthesis has been shown in **Figure 1.2**.

Top-down approach

In this approach, NPs are produced from bulk materials by high-energy ball milling, etching, sputtering, laser ablation methods, lithography, electro-explosion, electrospraying, flame pyrolysis, electrospinning. Nanomaterials are progressively removed until desired nanomaterial is obtained in the cases of nanolithography and etching techniques. In high-energy ball milling, sputtering, and laser ablation process, vacuum or inert atmosphere is required otherwise, NPs nascent synthesized tend to agglomerate (Kumar and Kumbhat, 2016).

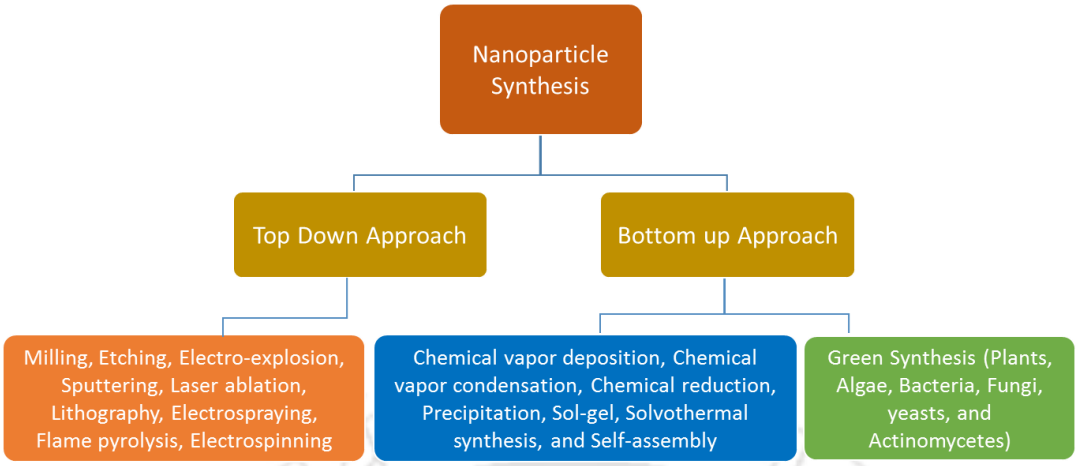

Figure 1.2 Various approaches of nanoparticle synthesis (Adapted from Keat et al., 2015; Kumar and Kumbhat, 2016)

Bottom-up approach

This approach includes chemical vapor deposition, chemical vapor condensation, plasma or flame spraying synthesis, laser pyrolysis, electro-chemical precipitation, supercritical fluid synthesis, reduction, sol–gel, solvothermal, matrix-mediated (template-assisted) processing, self-assembly and green synthesis (Kumar and Kumbhat, 2016; Keat et al., 2015). In bottom-up approach, nanoparticle synthesis employs three main components: metal precursors, reducing agents, and stabilizing or capping agents. The formation of nanoparticle involves two stages of nucleation and subsequent growth. The size of the NPs depends on these two steps. The initial nucleation and subsequent growth of the nuclei depends on various parameters such as temperature, pH, precursor, reducing agents and stabilizing agents (Tran et al., 2013).

1.4.1 Green synthesis of nanoparticles

NPs can be synthesized by physical and chemical methods. However, these approaches are expensive, high energy consuming and uses toxic and environmentally hazardous chemicals. These processes also involve generation of several byproducts and waste materials that are equally toxic. Moreover, chemical method of NPs synthesis increases reactivity and toxicity. Therefore, their use in biomedical field is sometimes questionable. Biogenic approach of NP synthesis is ecofriendly, sustainable and economical and the NPs synthesized are free of chemicals, thus, less toxic (Hussain et al., 2016). Importantly, green synthesis involves the ability of a biological entity to use its inherent biochemical processes to transform metallic ions to NPs (Baker et al., 2013). During the past decade, it has been established that a wide range of biological entities such as plants, algae, diatoms, bacteria, fungi, yeast, viruses and single cells are used to synthesize NPs (Parveen et al., 2016). Each biological entity has varying processing capabilities and different mechanism for the metal and metal oxide nanoparticle synthesis. Therefore, choice of the biological entity is important for the synthesis of nanoparticle of desired characteristics (Shah et al., 2015).

1.4.1.1 Microbe mediated nanoparticle synthesis

Microorganisms, both unicellular and multicellular, are reported to synthesize NPs through bottom-up approach by reduction/oxidation of metal ions using biomolecules such as enzymes, sugars, and proteins secreted by them. The microbe mediated synthesized NPs can be applied in various fields such as drug delivery and sensors for diagnostics owing to their less toxicity. Metallic NPs including gold, silver, alloy

and other metal NPs, oxide NPs consisting of magnetic and nonmagnetic oxide NPs, sulfide NPs, and other miscellaneous NPs are synthesized using microorganisms (Li et al., 2011).

Microbes can synthesize inorganic materials in their extracellular or intracellular region, where the former is desirable for their easy recovery (Khandel and Shahi, 2016). Usually, metal ions are trapped on the surface or inside the microbial cells due to electrostatic interaction between ions and cell membranes and then they are reduced to the NPs in presence of enzymes such as NADH and NADH dependent nitrate reductase enzymes. Some metallophillic bacteria have the genetic system which enables cell detoxification against heavy metals such as cadmium, copper, nickel ions etc. through various mechanisms such as reductive precipitation, complexation and efflux (Li et al., 2011). In case of extracellular nanoparticle synthesis, there are possibly two routes of NPs synthesis: (i) the microbes release biomolecules to the external medium which reduces the metal ions to form NPs. (ii) NPs are synthesized inside the microbe and then released to exterior (Singh et al., 2015).

1.4.1.2 Plant mediated nanoparticle synthesis

Biosynthesis of metallic nanoparticle using living plants (intracellular), plant extracts (extracellular) and phytochemicals are considered as an appropriate substitute to traditional physical and chemical methods (Iravani, 2011). Use of agricultural wastes for the nanoparticle synthesis further lowers the cost of nanoparticle synthesis many folds (Gan et al., 2012). The size of the plant mediated synthesized NPs is comparable to those obtained from physical and chemical methods (Parsons et al.,

2007). However, to control the size of the NPs, phytoconstituents such as polyphenols, proteins and organic acids are used to synthesize NPs (Basha et al., 2010; Tamuly et al., 2014).

1.4.1.2.1 Plant biomass mediated nanoparticle synthesis

Different plant species have the potential for heavy metal accumulation (Phytoextraction) and detoxification (Phytoremediation) which is exploited by the researchers to synthesize metallic NPs. Gold NPs were synthesized using *Medicago sativa* grown in a solid media first time followed by silver NPs. Other plants including *Brassica juncea, Sesbania drummondii, Chilopsis lineariz, Triticum aestivum, Avena sativa*, and *Festuca rubra* are reported to synthesize various NPs by intracellular route. The intracellular route of NP synthesis has some disadvantages such as variation in reducing and stabilizing potential of the bio-organic compounds in different parts of the plants resulting in varying degree of polydispersity and morphological variation of the NPs. Additionally, the downstream processes such as recovery of the nanoparticle and their purification are tedious jobs. Due to these drawbacks, this approach has been outdated (Dauthal and Mukhopadhyay, 2016).

1.4.1.2.2 Plant extract mediated nanoparticle synthesis

This process is extracellular in which the phyto-constituents are extracted from the plants and directly used for the nanoparticle synthesis. NP synthesis using plant extract is a fast and non-toxic method of nanoparticle synthesis (Iravani, 2011). This process has easy downstream processing, NP recovery and scale up. Biosynthesis of metallic NPs using plant extracts has is fast, nontoxic, renewable eco-benign, and

biocompatible method for the synthesis of NPs. With this approach NPs synthesized are with a more energetically favorable shape and highly reactive FCC structure. Spherical shape with preferred growth along (111) plane supports reactivity of NPs for various commercial applications (Dauthal and Mukhopadhyay, 2016). In this context green synthesis of silver, zinc oxide and iron oxide NPs are reviewed.

Plant extract mediated silver nanoparticle synthesis

Silver was initially used to stain glass yellow and as an antibacterial agent. Ancient Egyptians and Persians used silver vessels to disinfect water and food. Romans and Greeks used it for healing wounds. During World War I silver compound was used to prevent wound infection. By the 1920s, the U.S. Food and Drug Administration approved silver solution as a type of antibacterial agent (Mehlhorn, 2016).

Among other metals silver NP are of particular interest due to their superior physical and chemical properties. Their applications in color filters, optical switching, optical sensors and localized surface plasmon resonance properties make them scientifically important. Their unique optical, electrical, and thermal properties are incorporated into various industrial applications such as electronics, catalysis, and photonics. Their unique properties include broad spectrum antimicrobials, surface-enhanced Raman spectroscopy (SERS), chemical /biological sensors and biomedicine materials, biomarker and so on. These properties of silver NPs strongly depend on their morphology, crystal structure and dimensions (Ahmed et al., 2016; Natsuki et al., 2015; Khan et al., 2011). There are several methods of silver NPs synthesis including physical, chemical and biological. The chemical method of AgNP synthesis includes chemical reduction, photochemical method electrochemical method and pyrolysis

method (Swathy, 2014). In physical approach, the metallic NPs are generally synthesized by physical vapor condensation method and arc discharge method. Chemical reduction synthesis employs three main components: metal precursors, reducing agents and stabilizing or capping agents. The formation of nanoparticle involves two stages-nucleation and subsequent growth (Tran et al., 2013). The size of the NPs depends on these two steps. The initial nucleation and subsequent growth of the nuclei depends on various parameters such as temperature, pH, precursor, reducing agents ($NaBH_4$, ethyelen glycol N_2H_4, sodium citrate and N,N-dimethyformamide etc.) and stabilizing agents (Sodium dodecyl sulphate (SDS), polyvinyl pyrrolidone (PVP), tri-sodium citrate, sodium oleate etc.).

Considering the drawbacks of physico-chemical method, cost effective, eco-friendly and energy efficient method of silver nanoparticle synthesis using microorganism, plants, and biopolymers as reducing agents are emerging very fast.

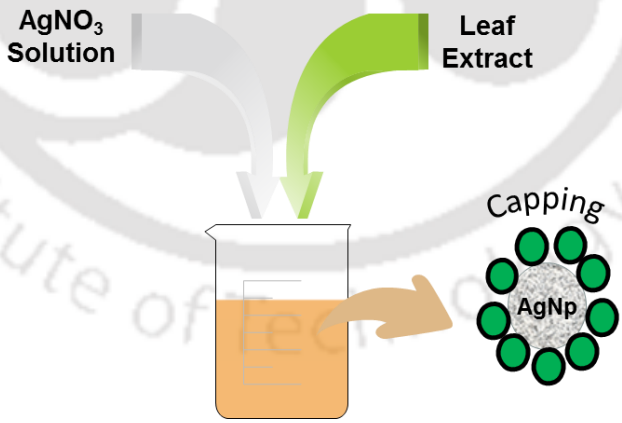

Figure 1.3 Graphical representation of green synthesis of silver nanoparticles

Green synthesis process involves reduction of metal ion by biological reducing agent. Commonly 0.1 -1.0 mM $AgNO_3$ is used as Ag^+ source (Srikar et al., 2016). Plants

synthesizing AgNPs ranged from algae to angiosperms. However, limited reports are available regarding AgNP synthesis using lower plants. A list of some of the plants used for AgNP synthesis has been reviewed in **Table 1.1**. From the list it is evident that AgNPs are synthesized by several plants which are mostly higher plants. Parts like leaves, flower, bark, root, stem, seed, and seed hull have been used for AgNP synthesis. Medicinally important plants such as *Aloe vera, Terminalia chebula, Catharanthus roseus, Ocimum tenuiflorum, Azadirachta indica, Emblica officinalis* has been used for AgNP synthesis. The mechanism of metal ion reduction has been discussed in this chapter. Briefly plant extracts contain a large number of organic chemicals such as sugars, carbohydrates, enzymes, phenols, flavanoids, terpenoids, alkaloids, gum, etc. which are capable of donating electrons to Ag^{+} to convert them Ag^{0} (Ahmed et al., 2016). These organic chemicals are responsible for both metal ion reduction and stabilization of the nanoparticle by capping as shown in (**Figure 1.3**). Ponarulselvam et al. (2012), synthesized silver nanoparticle using aqueous leaf extract of *Catharanthus roseus*. They used fresh leaves and boiled with water to prepare extract. To this extract silver nitrate solution was added which resulted in brown yellow color solution indicating silver nanoparticle formation. These silver NPs showed antiplasmoidal activity against *Plasmodium falciparum*. Silver NPs synthesized using *Azadirachta indica* leaf extract showed antibacterial activity against *Staphylococcus aureus* and *E.coli* (Ahmed et al., 2016). Aqueous extract of *A. indica* fresh leaves were prepared by boiling the leaves in water. To this extract varying concentration of 1 mM silver nitrate solution was added. Color change of the solution indicated reduction of Ag^{+} to Ag^{0}. Antibacterial activity was performed by disc diffusion method.

Applications of silver nanoparticles

The various applications of silver NPs are depicted in **Figure 1.4**. Out of these applications silver NP is more popularly known for its antimicrobial activity. There is always a demand for an alternative to antibiotics due to the growing antibiotic resistance (Khatoon et al., 2017). Two mechanisms are proposed for the antibacterial activity of metallic NPs. One is metal ion toxicity arising due to the dissolution of metal ions from the surface of the nanoparticle. Second is through oxidative stress caused by the reactive oxygen species generated from the nanoparticle surface (Dizaj et al., 2014).

Figure 1.4 Various applications of silver nanoparticles

Silver NPs possess excellent antibacterial activity against both gram positive and gram negative bacteria. The mode of action involves formation of pores in the cell wall which leads to leakage or by penetrating through ion channels and then

denaturing ribosomes thereby inhibiting expression of essential proteins and enzymes (**Figure 1.5**). Silver NPs are also effective against multi drug resistant bacteria such as Methicillin-resistant *Staphylococcus aureus*, Erythromycin-resistant *Streptococcus pyogenes*, ampicillin-resistant *Escherichia coli*, multidrug resistant *Pseudomonas aeruginosa* (Rai et al., 2012). Due to the antibacterial activity of silver nanoparticle, they are used in health industry, surgical instruments, wound dressings, bond prosthesis and heart valves, electronics, biosensing, food storage, textile coatings, respirators, household water filters, antibacterial sprays, cosmetics, detergent, dietary supplements, cutting boards, sox, shoes, cell phones, laptop keyboards and children's toys, room sprays, water cleaners, nanodevice manufacture and food storage containers (Mohammadlou et al., 2016).

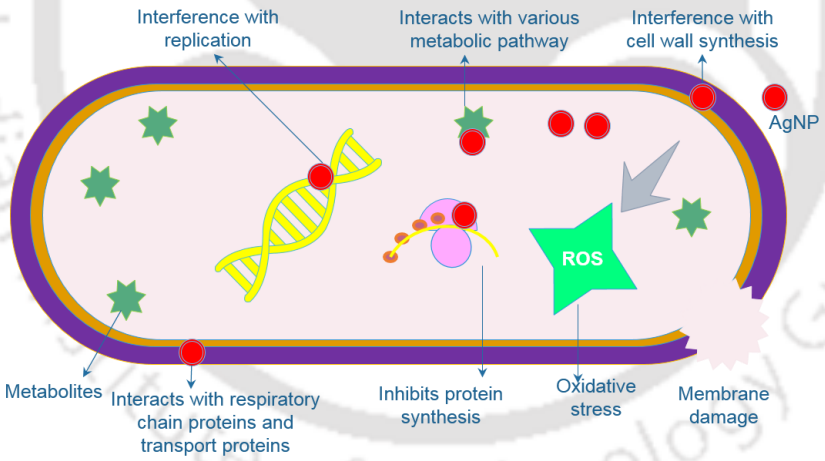

Figure 1.5 Mechanism of antibacterial activity of silver nanoparticles (Adapted from Pandey et al., 2014)

Products containing silver nanoparticle have been approved by major governing bodies such as US FDA, US EPA, Korea's Testing, SIAA of Japan and Research Institute for Chemical Industry and FITI Testing and Research Institute (Ahmed et al.,

2016). Silver NPs are also used to control plant pathogens due to their superior antimicrobial activity than the conventional plant fungicides (Shah et al., 2015). It is reported that silver NPs exhibit strong antifungal activity against *Candida* spp (Panáček et al., 2009; Mallmann et al., 2015; Nasrollahi et al., 2011). Silver nanoparticle synthesized with raspberry extract were found to inhibit growth of *Cladosporium cladosporioides* and *Aspergillus niger* (Pulit et al., 2013). Antiviral activity of mycosynthesized silver NPs against herpes simplex virus type 1 and 2 and human parainfluenza virus type 3 depending upon the size of the NPs (Gaikwad et al., 2013). Growth inhibition of bacteriophages by silver nanoparticle synthesized using *Aspergillus sps* has also been reported (Narasimha et al., 2012). Silver NPs with UV light is useful for antimicrobial applications and also protects from Leishmania parasites (Allahverdiyev et al., 2011). Silver nanoparticle are antiparasitic and can be used for effective treatment of *E. histolytica* and *C. parvum* parasites (Soliman et al., 2015). Elechiguerra et al. demonstrated that silver NPs undergo a size-dependent interaction with HIV-1, with particles exclusively in the range of 1–10 nm attached to the virus. The NPs might get attracted to the sulfur bearing groups present on the glycoproteins knobs. This suggests that the silver NPs interacts with gp120 protein of HIV-I virus (Elechiguerra et al., 2005). AgNPs synthesized using *Vitex negundo* L. extract showed 50% cell viability inhibition of human colon cancer cell lines (HCT 15) when administered at 20 µg/mL (Prabhu et al., 2013).

Table 1.1 List of plants used for silver nanoparticle synthesis and their applications

Plant	Plant part	Applications	Reference
Ailanthus excelsa	Leaf Extract	Antibacterial effect against *S. aureus*, *P. aeruginosa*, *E. coli, K. pneumonia* and anticancer effect against MCF-7 cell line	Vinmathi and Jacob, 2015
Aloe vera	Leaf Extract	--	Chandran et al., 2006
Ananas comosus	Fruit extract	--	Ahmad and Sharma, 2012
Anogeissus latifolia	Gum	Antibacterial activity against gram positive and gram negative strains	Kora et al., 2012
Asclepias curassavica	Leaf extract	--	Rajesh et al., 2014
Averrhoa carambola	Leaf Extract	--	Mishra et al., 2015
Azadirachta indica	Leaf Extract	Antibacterial activity against *S.aureus* and *E.coli*	Ahmed et al., 2016
Boswellia ovalifoliolata	Stem bark extract	--	Ankanna et al., 2010
Carica papaya	Leaf Extract	Antibacterial activity against gram positive and gram negative strains	Banala et al., 2015
Carica papaya	Fruit Extract	--	Maqdoom et al., 2013
Carica papaya	Fruit Extract	Colorimetric detection of mercury ions	Firdaus et al., 2017
Carica papaya	Leaf Extract	Antibacterial activity against *B. subtilis, E. coli, P. aeruginosa* and *S. aureus*.	Sridevi et al., 2015
Carica papaya	Callus extract	--	Mude et al., 2009
Carica papaya, Manihot esculenta, and Morinda citrifolia	Leaf Extract	Antibacterial activity against *E. coli*	Syafiuddin et al., 2017
Cassia auriculata	Leaf extract	--	Udayasoorian et al., 2011
Catharanthus roseus	Leaf Extract	Antiplasmodial activity against *P. falciparum*	Ponarulselvam et al., 2012
Centella asiatica	Leaf extract	Antibacterial activity against *S. aureus*	Rout et al., 2013
Cinnamomum camphora	Leaf Extract	--	Huang et al., 2007
Cinnamomum camphora	Leaf extract	--	Huang et al., 2007
Cinnamomum tamala	Leaf extract	Catalyst for pyranopyrazoles synthesis	Yadav and Khurana, 2015
Citrullus colocynthis	Stem derived callus extract	Antibacterial activity against *E. coli*, *V. paraheamolyticus*, *P. aeruginosa*, *Proteus vulgaris* and *L. monocytogens*.	Satyavani et al., 2011

Plant	Plant part	Applications	Reference
Clitoria ternatea, Solanum nigrum	Leaf extract	Antibacterial Effect against Common Nosocomial Pathogens	Krithiga et al., 2015
Coriandrum sativum	Leaf extract	Exhibit strong reverse saturable absorption	Sathyavathi et al., 2010
Emblica officinalis	Fruit Extract	Antibacterial activity against both gram positive and gram negative bacteria	Ramesh et al., 2015
Emblica officinalis, Terminalia catappa and Eucalyptus hybrida	Leaf extract	--	Singh et al., 2015
Eucalyptus hybrida	Leaf extract	--	Dubey et al., 2009
Euphorbia hirta and Nerium indicum	Leaf extract	Antibacterial activity against *E. coli, S. pyrogens, S. aureus, B.subtilis, S.typhi, Citrobacter* sp.	Priya et al., 2011
Jasminum grandiflorum and Cymbopogon citrullus	Leaf extract	--	Dwivedi, 2013
Jatropha curcas	Leaf Extract	Antibacterial activity against *E.coli*	Chauhan et al., 2016
Jatropha curcas	Latex	--	Bar et al., 2009
Magnolia kobus	Leaf extract	--	Song and Kim, 2009
Manihot esculenta	Leaf Extract	Larvicidal activity against *Aedes aegypti* and *Culex quinquefasciatus*	Velayutham et al., 2016
Melastoma Malabathricum	Flower Extract	Catalytic activity in methylene blue dye degradation	Krishnaprabha and Pattabi, 2015
Mentha piperita	Leaf extract	Antibacterial activity against *S. aureus* and *E. coli*.	MubarakAli et al., 2011
Musa balbisiana, Azadirachta indica, Ocimum tenuiflorum	Leaf extract	Antibacterial activity against *E. coli*, aided in plant germination and growth.	Banerjee et al., 2014
Oak plant	Fruit Hull extract	Cytotoxic against human breast cancer cells	Heydari and Rashidipour, 2015
Pelargonium graveolens,	Leaf Extract	--	Shankar et al., 2003
Quercus brantii	Leaf Extract	--	Korbekandi et al., 2015
Quercus infectoria	Leaf and fruit extract	Antibacterial activity against plant pathogenic bacteria *Pectobacterium carotovorum, Ralstonia solanacearum* , *Erwinia amylovora* and *Xanthomonas citri*	Chahardooli et al., 2014
Ricinus communis	Leaf Extract	Antibacterial activity *Bacillus fusiformis*, *E. coli*	Singh et al., 2012

Plant	Plant part	Applications	Reference
Shorea tumbuggaia	Stem Bark extract	--	Venkateswarlu et al., 2010
Solanum tricobatum, Syzygium cumini, Centella asiatica and Citrus sinensis		Antibacterial activity against pathogenic bacteria	Logeswari et al., 2013
Terminalia arjuna	Leaf Extract	Antimicrobial activity against *Escherichia coli* and *Staphylococcus aureus*	Ahmed and Ikram, 2015
Terminalia arjuna	Bark extract	Antibacterial activity against *E.coli*	Ahmed et al., 2017
Terminalia catappa	Leaf extract	--	Ankamwar, 2011
Terminalia chebula	Leaf Extract	Antibacteria activity against *Salmonella typhi, S. aureus, E.coli, Klebsiella pneumoniae*	Dwivedi, 2013
Terminalia chebula	Leaf Extract	*Pseudomonas aeruginosa, Bacilus subtilis, Staphylococcus aureus, K. pneumonia, Streptococcus sp., Salmonella sp., Escherichia coli.*	Pratibha et al., 2015
Trianthema decandra	Leaf extract	Antibacterial activity against *E. coli* and *P. aeruginosa*	Geethalakshmi and Sarada, 2010

Green synthesis of zinc oxide nanoparticles

Zinc oxide NPs are also known as oxydatum, since oxicum is permanent white, ketozinc and oxozinc. Zinc oxide NPs are described as promising, functional, strategic and versatile inorganic material with wide range of applications. As Zn and O are categorized into two and six groups of periodic table respectively, ZnO are known as II-VI semiconductor (Neumark et al., 2006). ZnO crystallizes in the wurtzite structure at ambient temperature and pressure. Further, ZnO is also known to crystallize in the cubic zinc blende and rocksalt (NaCl) structures (Coleman and Jagadish, 2006). ZnO has a unique optical, semiconducting, electrical conductivity, chemical sensing and piezoelectric properties (Fan and Lu, 2005). It is characterized by a wide band gap of 3.3eV, in the near UV-spectrum, a high free excitonic binding energy (60meV) at room temperature and a natural n-type electrical conductivity (Wang, 2004; Wang and Song, 2006; Zhang et al., 2012; Schmidt-Mende and MacManus-Driscoll, 2007). Their wide band gap affects their optical absorption and electrical conductivity properties. Their excitonic energy can persist at room temperature or even higher temperature (Janotti and Van de Walle, 2009). Their conductivity can be increased by doping ZnO with other metals. Though it shows light covalent character, Zn-O bonding is strong (Sirelkhatim et al., 2015).

Owing to its multifunctional properties and diverse applications, ZnO nanostructures have been a subject of immense research. Their potential biocompatibility, solubility in alkaline medium and the polar surfaces are currently explored in biomedical fields. Their unique features make them a potential candidate for applications in sensors,

energy harvesting, electronic devices. These beneficial properties of ZnO pave the way to adopt various methods for the synthesis of ZnO nanostructures. Depending upon the methods of synthesis, ZnO NPs have different size and morphology and thus application. Based on the desired application, size and morphology of ZnO NPs synthesis method is selected. Accordingly physical and chemical parameters such as solvent type, precursors, pH, and the temperature were optimized. Different morphologies of ZnO nanostructures synthesized include nanorods, nanosphere, nanotubes, nanowires, nanoneedles nanobelts, nanocages, nanocombs and nanosprings/nanohelixesand nanorings. Other structures of ZnO include ZnO spirals, drums, polyhedrons, disks, flowers, stars, boxes, and plates can be obtained by modulating reaction conditions (Srilekhatim et al., 2015; Wang, 2004). Each structure has unique optical, electrical and physiochemical properties and thereby application too. These nanostructures are synthesized by various physical, chemical and biological methods. Physical method of ZnO synthesis involves colloidal dispersion, vapor condensation, amorphous crystallization and physical fragmentation. Chemical method of ZnO synthesis involves thermal evaporation of ZnO powders at 1400 C, hydrothermal synthesis, sol–gel technique, simple thermal sublimation, self-combustion, polymerized complex method, vapor–liquid–solid technique, double-jet precipitation, and solution synthesis (Hussein and Shaheed, 2015; Yahya et al., 2010). To avoid the extra synthesis cost and high energy involved in physical methods and toxic chemicals used in the chemical synthesis process green approach have been adapted more recently.

Green synthesis of ZnO using plant extract has been reported by numerous researchers. One of the recent studies, ZnO green synthesis using *Moringa oleifera* has been reported by Matinise et al. in 2017. In their experiment aqueous extract of *Moringa oleifera* was prepared and zinc nitrate hexahydrate was added. After 18 h color change was visible and after drying at 100°C ZnO powder was obtained which was further characterized for their electrochemical and optical properties. The ZnO NP were of size ranging from 12.27 to 30.51 nm.

Similarly, ZnO NP synthesis using leaf extract of *Calotropis gigantea* was reported by Vidya et al., 2013. Aqueous extract of *C. gigantea* leaves was prepared by boiling the leaves in water and zinc nitrate was added when the extract was at 60°C temperature. A yellow colored paste was obtained after evaporation of the solvent. ZnO powder was obtained after heating at 400°C temperature in a furnace. After SEM and XRD analysis synthesis ZnO nanoparticle of 30-35 nm size was confirmed. Green synthesis of ZnO NP using various plant extracts has been listed in **Table 1.2.**

Applications of zinc oxide nanoparticles

ZnO NPs have a wide range of applications including UV absorption, anti-corrosive, antibacterial, antifungal treatment, antiviral, UV light emitters, photocatalyst and as an additive in many industrial products. They are also used in the fabrication of solar cells, gas sensors, luminescent materials, transparent conductor, heat mirrors and coatings (Debnath and Karmakar, 2013). Various applications of ZnO NP are shown in **Figure 1.6**.

ZnO NP was synthesized using *Calotropis procera* aqueous extract (Gawade et al., 2017). In their study, the synthesized ZnO NP powder was evaluated for the photocatalytic degradation of methyl orange. The concentration of the catalysts were varied to optimize the concentration of ZnO NP for the degradation of 20 mg/L methyl orange. The degradation efficiency was found to be 81% within 100 minutes of UV irradiation in presence of 1.5 g/dm^3 catalyst.

Figure 1.6 Various applications of zinc oxide nanoparticles (Adapted from: Kołodziejczak-Radzimska and Jesionowski, 2014).

Photocatalytic degradation of methylene blue using ZnO NPs was reported (Suresh et al., 2015). In their study they have synthesized ZnO NPs using aqueous extract of *Artocarpus gomezianus* fruit and the average size was found to be 11.53 nm. The

degradation of 5 mg/L methylene blue was carried out under UV light and sunlight using 0.5 mg/ml catalyst. The variations in catalysis at different pH conditions were evaluated. Maximum degradation was obtained at alkaline pH. The antioxidant activity of ZnO NPs was evaluated by DPPH assay and the IC_{50} value obtained was 10.8 mg/ml.

ZnO NPs were evaluated for adsorption of heavy metal from aqueous solution as nanoadsorbent. Azizi et al. synthesized ZnO NP using zerumbone extract, which is a monocyclic sesquiterpenoid found in *Zingiber zerumbe*t Smith and *Zingiber aromaticum* rhizomes (Azizi et al., 2017). Particle of size 10 -12 nm ZnO was formed which were used as nanoadsorbent for the removal of Pb(II) metal ions. Kinetic models and thermodynamics of the adsorption process was studied. The adsorption process followed pseudo second order kinetic model and the process was endothermic in nature. Pb(II) adsorption followed Langmuir isotherm with maximum adsorption capacity 19.65 mg/g under pH of 5, and temperature of 70°C.

Table 1.2 List of plants used for ZnO nanoparticles synthesis and their applications

Plant	Plant part	Applications	References
Agathosma betulina	Leaf extract	--	Thema et al., 2015
Arabic gum	Gum	Direct blue 129	Fardood et al., 2017
Artocarpus gomezianus	Fruit extract	Antioxidant activity and photocatalytic degradation of methylene blue	Suresh et al., 2015
Averrhoa carambola	Fruit juice extract	--	Nguefack Marius Borel et al., 2014
Azadirachta indica	Gum Exudates	Antifungal activity against *aspergillus fumigatus, Candida albicans*, and *Penicillum varians*	Geetha et al., 2016
Azadirachta indica (Neem)	Leaf Extract	Methylene blue	Bhuyan et al., 2015
Beta vulgaris	Root extract	Photocatalytic degradation of malachite green and methylene blue. Antioxidant activity	Kumar et al., 2015
Calotropis Gigantea	Leaf extract	--	Vidya et al., 2013
Calotropis procera	Leaf extract	Photodegradation of methyl orange	Gawade et al., 2017
Camellia sinesis	Leaf Extract	Antibacterial activity against *P. aeruginosa*, *Staphylococcus aureus*	Shah et al., 2015
Cassia fistula	Leaf Extract	Bactericidal activity against *Klebsiella aerogenes, Escherichia coli*, *Plasmodium desmolyticum* and *Staphylococcus aureus,* Antioxidant activity, photocatalytic degradation of methylene blue	Suresh et al., 2015
Celosia argentea	Leaf Extract	--	Vaishnav et al., 2017
Citrus aurantifolia	Fruit pulp	--	Samat and Nor, 2013
Corriandrum sativum	Leaf Extract	Anthracene	Hassan et al., 2015
Cuminum Cyminum	Seed extract	Alizarin Red Dye	Sirisha and Mary, 2016
Green tea (Camellia sinesis)	Leaf Extract	Antibacterial activity against gram negative bacteria and antifungal activity against *A. fumigatus, Penicillium sp, A. flavus, A. niger*	Senthilkumar and Sivakumar, 2014

Plant	Plant part	Applications	References
Hibiscus subdariffa	Leaf extract	Antibacterial activity against *Escherichia coli* and *Staphylococcus aureus* and antidiabetic activity	Bala et al., 2015
Kedrostis Foetidissima	Leaf extract	--	Devi and Dhinesh, 2016
Lantana aculeata	Leaf extract	Antifungal activity against *Aspergillus flavus, Fusarium oxysporum*	Narendhran and Sivaraj, 2016
Moringa oleifera	Leaf extract	--	Matinise et al., 2017
Nyctanthes arbor-tristis	Flower extract	Antifungal activity against *Alternaria alternate Aspergillus niger, Botrytis cinerea, Fusarium oxysporum and Penicillium expansum*	Jamdagni et al., 2016
Ocimum basilicum	Leaf extract		Salam et al., 2014
Passiflora caerulea	Leaf extract	Antibacterial activity against urinary tract infection pathogen	Santhoshkumar et al., 2017
Pyrus Pyrifolia	Leaf extract	Photocatalytic degradation of methylene blue	Parthibana and Sundaramurthy, 2015
Sesbania grandiflora	Leaf Extract	Indigo Carmine	Muthu and Rajalaxmi, 2016
Solanum nigrum	Leaf extract	Antibacterial activity against *S. aureus, S. paratyphi, V. cholerae, E. coli.*	Ramesh et al., 2015
Terminalia chebula	Fruit extract	Rhodamine B	Rana et al., 2016
Trifolium pratense	Flower extract	Antibacterial activity against *S. aureus* and *P. aeruginosa*	Dobrucka Długaszewska, 2016
Vegetable	Peel Waste	Crystal violet	Surendra et al., 2016
zerumbone	Rhizome extract	Pb(II) removal from aqueous solution	Azizi et al., 2017
Zingiber officinale	Root Extract	--	Raj and Jayalakshmy, 2015

Green synthesis of iron oxide nanoparticle

Iron oxides exist in three polymeric forms: hematite (α-Fe_2O_3), maghemite (γ-Fe_2O_3) and magnetite (Fe_3O_4). Their structures can be defined as closely packed planes of

oxygen anions and iron cations in octahedral and tetrahedral interstitial sites (Campos et al., 2015).

Hematites (α-Fe_2O_3) are weakly ferromagnetic or antiferromagnetic at room temperature and paramagnetic above 956K temperature. They exist in nature as minerals occurring widely in rocks and soils. They are easy to synthesize compared to other oxide forms as they are stable under common environmental conditions and they are the product of transformations of other iron oxide (Machala et al., 2011).

Maghemites (γ-Fe_2O_3) are ferromagnetic mineral but thermally unstable. At higher temperature 673K, they are transformed to hematite (α-Fe_2O_3). Maghemites and magnetites are easily magnetized when exposed to external magnetic field (Zboril et al., 2002; Xu et al., 2008).

β-Fe_2O_3 is a rare kind of iron oxide that exhibits paramagnetic behavior at room temperature. At temperature between 100 and 119 K Néel magnetic transition occurs and below this temperature, β-Fe_2O_3 is anti-ferromagnetically arranged. Due to thermodynamic instability, it is transformed into either α-Fe_2O_3 or γ-Fe_2O_3 when heated (Machala et al., 2011).

The epsilon form (ε-Fe_2O_3) of iron oxide can be regarded as a polymorphous intermediate presenting similarity to both γ-Fe_2O_3 and α-Fe_2O_3. It undergoes two magnetic transitions, one at 495 K and the other at 110 K. In the first one, it goes from a paramagnetic to a magnetically ordered state while at 110 K it under goes a transition to a magnetic regime.

Magnetites (Fe_3O_4) are ferromagnetic in room temperature and has an inverse spinel crystal structure which is formed by stacking planes of polyhedral model. It has a face centered cubic unit cell (Teja and Koh, 2009).

There are various techniques for iron oxide nanoparticle synthesis including microemulsions, sol–gel syntheses, sonochemical reactions, hydrothermal reactions, hydrolysis and thermolysis of precursors, flow injection syntheses, and electrospray syntheses (Basavegowda et al., 2014).

The green synthesis of iron oxide NPs using plant extracts have been reported by many researchers. Phytochemicals such as phenols, flavonoids, alkaloids etc. present in the leaf extract mediates reduction process and stabilizes the synthesized NP by capping. There are many reports of iron oxide NP synthesis using green tea which is a cheap and local resource. Stable zero valent iron oxide NPs were synthesized using green tea extract (Hoag et al., in 2009). The polyphenols present in green tea acts as both reducing agent and capping reagents for the synthesis of stable iron oxide NPs. In his study 0.1 M $FeCl_3$ was added to green tea at 2:1 ratio. Shahwan et al. (2011) also synthesized iron oxide NP using $FeCl_3$ and green tea in 2:3 ratio and pH 6. The black precipitate formed were iron oxide NPs were harvested from the solution and used as catalyst for methylene blue and methyl orange degradation. Makarov et al. (2014) used $Fe(NO_3)3{\cdot}9H_2O$ as iron precursor and green tea as the reducing agent for the synthesis of iron oxide (II and III) polyphenol complex NPs. Changing the ratio of extract to iron salts the properties of the NPs were changed as observed by Nadagouda et al. (2010). Iron oxide NPs are also synthesized using $FeCl_2$ and $FeCl_3$ in 2:1 ratio as precursor molecules. Shoajee et al.

(2016) used white tea and $FeCl_2$ and $FeCl_3$ mixture to synthesize iron oxide NPs. Besides green tea other plants extracts rich in polyphenolic content are also used for the synthesis of iron oxide NPs. Das et al., 2014 used *Datura intoxia* plant extract along with iron precursors $FeCl_2$ and $FeCl_3$ at alkaline pH for the synthesis of Fe_3O_4 NPs. Devatha et al. (2016) synthesized iron oxide NP using leaf extract of various plants *Mangifera indica, Murraya Koenigii, Azadiracta indica, Magnolia champaca*. These NPs showed satisfactory removal of total phosphates, ammonia nitrogen, and chemical oxygen demand. There are several reports of green synthesis of iron oxide NPs synthesis and has been listed in **Table 1.3**.

Applications of iron oxide nanoparticles

The various applications of iron oxide NPs are shown in **Figure 1.7**. Their magnetic properties, ultrafine structure and biocompatibility of the iron oxide NPs make them a promising candidate for various biomedical applications such as enhanced resolution contrast agents for MRI, targeted drug delivery and imaging, hyperthermia, gene therapy, stem cell tracking, molecular/cellular tracking, magnetic separation technologies (e.g., rapid DNA sequencing) early detection of inflammatory, cancer, diabetes, and atherosclerosis (Mody et al., 2010). They have unique optical, electrical and magnetic properties which are used in various applications such as production of inorganic pigments, magnetic storage media, development of gas sensors as well as electronic and optical devices, information storage, color imaging, magneto caloric refrigeration, bioprocessing, ferrofluid technology and wastewater treatment adsorbents (Campos et al., 2015). These medical applications require the NPs to have high magnetization for high resolution MR images

In catalysis, a catalyst accelerates the chemical reactions by providing a great number of active sites so that the reactant adsorb onto the surface, react and desorbs. Therefore the surface area should be small (typically 10-80 nm) so that more number of active sites will be available for the process. Nanomaterials are more effective catalysts than their bulk counterparts due to their extremely small size and large surface area. They also have unique properties which differs from their bulk counterparts. In addition to large surface area there are other features which make them a better catalyst which include their surface quality, chemical composition, and particle morphology (Chaturbedi et al., 2012). Therefore iron oxides hematite, magnetite and maghemite are extensively used in the catalysis of a number of reactions such as the synthesis of styrene, photocatalytic production of hydrogen and oxygen, removal of carbon monoxide, catalytic conversion of methane in aromatic compounds, thermal decomposition of ammonium perchlorate as well as in water treatment, catalytic decomposition of hydrogen peroxide, fuel cells and production of biodiesel (Chaturbedi et al., 2012).

Degradation of bromothymol blue iron oxide nanoparticle and zerovalent iron along with hydrogen peroxide was reported by Hoag et al. (2009). In his reports, it is evident that increase in zerovalent iron concentration increases catalysis of H_2O_2 which ultimately degrades bromothymol blue dal. Due to the generation of free radicals from H_2O_2. The catalytic activity of zerovalent iron was more than Fe-EDDS, and Fe-EDTA in their study (Hoag et al., 2009)

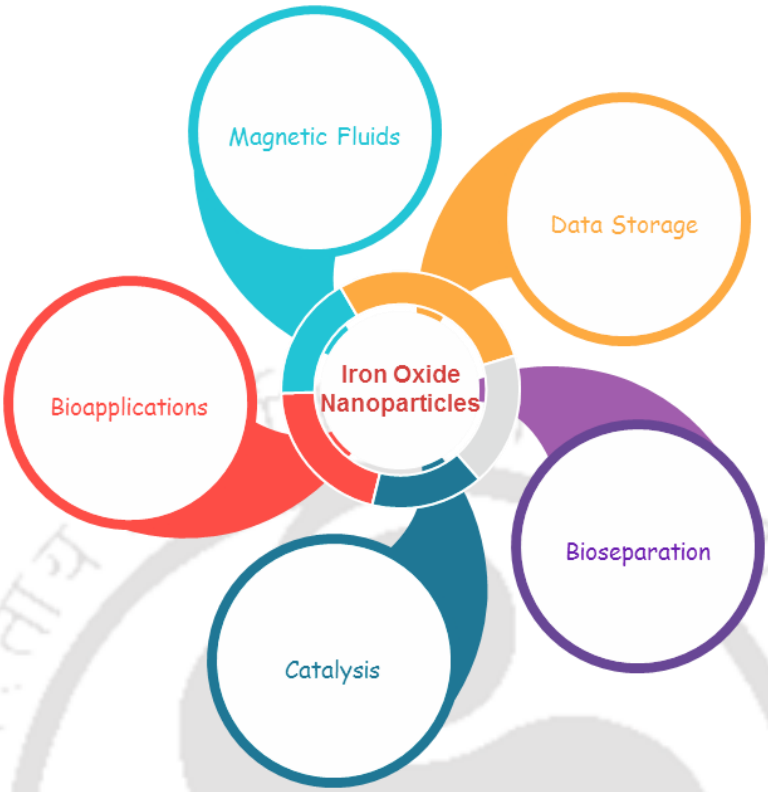

Figure 1.7 Various applications of Iron oxide nanoparticles

Degradation of methylene blue and methyl orange using zero valent iron synthesized using green tea was reported. Methylene blue and methyl orange were completely degraded at 10-200 mg/L concentration. Methylene blue degradation was faster as compared to methyl orange. Therefore, iron NPs synthesized using green tea is an effective Fenton like catalyst. Similarly, iron NPs synthesized using oolong tea were used to degrade malachite green with 75% degradation efficiency of 50 mg/L of the dye. Fenton like oxidation of monochlorobenzene using iron NPs synthesized by green tea, oolong tea and black tea was reported by Kuang et al. (2013). Luo et al. (2014) utilized grape extract to synthesize iron nanoparticles which then acted like fenton like catalyst for the degradation of acid Orange II.

Iron NPs are used as nanaoadsorbents for the removal of heavy metals. One such case is reported by Rao et al. (2013). The nanocomposite of yeast cells and iron NPs which was plant mediated synthesized proved to be a good adsorbent for hexavalent chromium removal. The sorpotion capacity of yeast cells increased three times when conjugated with iron NPs. There are many reports of heavy metal removal using iron NPs synthesized using plant extract, some of them are listed in the **Table1.3.** Adsorption capacity varies with the amount of plant extract used for the synthesis of iron NPs (Madhavi et al., 2013)

In another study, Martínez-Cabanas et al. (2016) reported arsenic adsorption by iron oxide NPs embedded in chitosan. The iron oxide NPs were synthesized using eucalyptus leaf extract. The column was packed with adsorbents and arsenic was introduced into the column. Maximum adsorption capacity of the adsorbent was found to be 147 μg/g. The adsorption was carried out for four cycles. However desorption was one of the issues that had to be resolved

Table 1.3 List of plants used for iron oxide nanoparticle synthesis and their applications

Iron Oxide NP	Plant	Plant part	Applications	References
Iron NP	*Abelmoschus esculentus*	Leaf extract	Antibacterial activity against gram positive and gram negative bacteria	Pande et al., 2015
Fe_3O_4	Carab	Leaf extract	--	Awwad and Salem, 2012
Fe_3O_4	*Caricaya Papaya*	Leaf extract	--	Latha and Gowri, 2014
γ- Fe_2O_3	*Centella asiatica*	Leaf extract	--	Pravallika et al., 2015
Fe_3O_4	*Datura Inoxia*	Leaf extract	--	Das et al., 2014
Iron oxide NP	*Desmodium gangeticum*	Root extract	--	Meyyappan et al., 2015
Hematite (α-Fe_2O_3)	*Eucalyptus globulus*	Leaf extract	As(V) removal by iron oxide NP encapsulated in chitosan matrix	Martínez-Cabanas et al., 2016
Iron-polyphenol complex	Eucalyptus leaves	Leaf extract	--	Wang, 2013
Iron-polyphenol complex	*Eucalyptus tereticornis, Melaleuca nesophila, and Rosemarinus officinalis.*	Leaf extract	Used as Fenton-like catalyst for decolorization of acid black 194.	Wang et al, 2014
Fe_3O_4 FeOOH	Grape	Leaf extract	Decolorization of azo dyes such as acid Orange	Luo et al., 2014
Fe_3O_4, FeOOH	Green tea	Leaf extract	Decolorization of Methylene blue and methyl orange	Shahwan et al., 2011
nZVI Iron	Green Tea		Degradation of bromothymol blue	Haog et al., 2009
Fe_3O_4 and Fe_2O_3	Green tea and eucalyptus	Leaf extract	Nitrates removal	Wang et al., 2014
Fe_2O_3	*Hordeum vulgare and Rumex acetosa*	Leaf extract	--	Makarov et al., 2014
Fe_3O_4	*Jatropha Gosspifolia*	Leaf extract	--	Karkuzhali and Yogamoorthi, 2015
Fe_3O_4	*Kappaphycus alvarezii*	sea weed extract	--	Yew et al., 2016
β-Fe_2O_3	*Mansoa alliacea*	Leaf extract	--	Prasad, 2016
Fe_3O_4	*Mimosa pudica*	Root extract	--	
NZVI Iron	Oak, pomegranate, green tea			Machado et al., 2013
Fe_2O_3	*Ocimum sanctum*	Leaf extract	--	Balamurughan et al., 2014
α-Fe_2O_3, γ-Fe_2O_3	*Omani mango*	Leaf extract	Heavy oil viscosity treatment	Al-Ruqeishi et al., 2016
zero-valent iron (α-Fe), maghemite (γ-Fe_2O_3), magnetite (Fe_3O_4)	Oolong tea	Tea extract	Degradation of malachite green	Huang et al., 2014

Iron Oxide NP	Plant	Plant part	Applications	References
zero-valent iron (α-Fe), maghemite (γ-Fe_2O_3), magnetite (Fe_3O_4)	Oolong tea, Black tea and Green tea	Tea extract	Monochlorobenzene degradation	Kuang et al., 2013
Fe_3O_4	*Padina pavonica* (Linnaeus) Thivy and *Sargassum acinarium* (Linnaeus) Setchell 1933	sea weed extract	Used for Pb (II) removal when entrapped in calcium alginate beads.	El-Kassas et al., 2016
Fe_2O_3	*Passiflora foetida*	Leaf extract	Antibacterial activity against gram positive and gram negative bacteria	Suganya et al., 2016
Fe^0/Fe_3O_4	*Punica granatum*	Leaf extract	Removal of Cr(VI) by Fe^0/Fe_3O_4 nanocomposite-modified cells of *Yarrowia lipolytica*	Rao et al., 2013
Iron oxide NP	*S. jambos* (L.) Oolong tea, *A. moluccana* (L.), etc	Leaf extract	Removal of chromium	Xiao et al., 2016
Fe_3O_4	Shanghai white tea (*Camelia sinensis*)	Leaf extract	--	Shojaee et al., 2016
Fe_3O_4	*Syzygium cumini*	Seed Extract	--	Venkateswarlu et al., 2014
NZVI Iron	Tea polyphenols		--	Nadagouda et al., 2010
Iron oxide NP	*Terminalia chebula*	Fruit extract	--	Kumar et al., 2013
Fe_3O_4	*Tridax procumbens*	Leaf extract	Bactericidal activity against *Pseudomonas aeruginosa*	Senthil and Ramesh, 2012
Fe_3O_4	*Wrightia tinctoria*	Leaf extract	Antibacterial activity against gram positive and gram negative bacteria	Sravanthi et al., 2016

1.4.1.2.3 Phytochemical mediated nanoparticle synthesis

In this context, researchers are focused on the identification of particular phyto-constituent that are responsible for the NPs. It is predicted that polyphenols and flavonoids play active role in synthesis and stabilization of NPs (Dauthal and Mukhopadhyay, 2016).

1.4.1.2.4 Plant mediated synthesis of bimetallic nanoparticles

Bimetallic nanoparticle display unique optical electronic, biological and chemical properties from their monometallic counterparts due to the synergic effects of both the metals. Very few studies have been reported in this context (Dauthal and Mukhopadhyay, 2016).

1.4.1.3 Mechanism of plant mediated nanoparticle synthesis

Green synthesis of the NPs require three constituents such as reducing agents, stabilizing agent and a solvent medium (Vijayaraghavan and Nalini, 2010). Green synthesis involving plant extract for NP synthesis, the extract plays dual role of reducing and stabilizing agents. The exact mechanism of nanoparticle synthesis has not been interpreted yet. However, it is believed that plant extract containing polyphenols (flavonoids, phenolic acids, and terpenoids), organic acids, proteins and polysaccahrides act as bioreducing and stabilizing agents synergistically (Dauthal and Mukhopadhyay, 2016).

Flavonoids

These are water soluble plant secondary metabolites with 15 carbon structure and subdivided into six subgroups: anthoxanthins, flavanones, flavanonols, flavans, anthocyanidins, and isoflavonoid. They have molecular oxygen scavenging activity or reducing or antioxidant activity which is directly related to their electron or hydrogen donating ability (Pietta, 2000). Metal ions are reduced by free hydrogens, liberated during tautomeric transformation of the flavonoids from enol to keto-form. Enol-form to keto-form transformation of luteolin and rosmarinic acid in the *Ocimum basilicum* extract is responsible for the formation of silver NPs from Ag^{+} ions (Ahmad et al., 2010). Some flavonoids (quercetin and myricetin) can chelate metal ions with their carbonyl groups and π electrons. Quercitin can chelate ions with carbonyl and hydroxyl groups at the C3 and C5 positions and the catechol group at the C3' and C4' positions (Makarov et al., 2014). These groups chelate various metal ions such as Fe^{2+}, Fe^{3+}, Cu^{2+}, Zn^{2+}, Al^{3+}, Cr^{3+}, Pb^{2+}, and Co^{2+}. Flavonoids are adsorbed onto the nascent nanoparticle and involved in the nucleation and aggregation of the NPs. Moreover, flavonoids and flavonoid glycoside can induce the formation of metal NPs (Makarov et al., 2014).

Phenolic Acids

Polyphenols have a phenolic ring and an organic acid as a functional group. Phenolic acids such as gallic acid, caffeic acid, ellagic acid, lignan (phyllanthin), flavonoid glycosides (apiin), and tannin (bayberry tannin), and protocatechuic acid are reported to be used as bioreducing agents for metallic nanoparticle synthesis due to the metal-chelating ability of highly nucleophilic aromatic rings. Caffeic acid has a strong

reducing activity due to the extra conjugation in the propanoic acid side chain which facilitates electron delocalization by resonance (Dauthal and Mukhopadhyay, 2016).

Terpenoids

Terpenoids such as citronellol, geraniol, linalool, eugenol, and methyl chavicol are low molecular weight organic compounds and possess metal reducing capacity. The hydroxyl group of eugenol releases proton and this activity is inducted by electron withdrawing methoxy and allyl group at ortho and para position (Makarov et al., 2014).

Proteins and aminoacids

Bioreduction of metal ions using protein is complicated due to their complex structure. However, it is reported that cyclic peptides present in the *Jatropha curcas* latex are capable of reducing and capping silver ions (Bar et al., 2009). Tyrosine amino acid is capable of reducing silver ions through ionization of its phenolic group which results in formation of semiquinone structure of tyrosine (Roy et al., 2014; Selvakannan et al., 2004). Similarly glutamic acid and tryptophan also has reductive properties (Wangoo et al., 2008; Selvakannan et al., 2004; Si et al., 2007). According to Gruen, 1975 aminoacids such as lysine, cysteine, arginine and methionine are capable of binding silver ions. Aspartate is capable of reducing tetrachloroauric acid to form NPs (Saikat et al., 2002). Among all the 20 α-aminoacids, tryptophan has the strongest reducing capacity for Au ions and histidine has the strongest binding affinity for Au ions (Tan et al., 2010). The aminoacids bind to the metal ions through the carbonyl or amino groups of the main chain or through the side chain.

Organic acids

Plants produce several secondary metabolites when exposed to various metals or other unfavorable conditions. Organic acids and alkaloids of plant secondary metabolites also has metal reducing properties. Example one alkaloid pedicellamide isolated from *Piper pedicellatum* (Tamuly et al., 2014) and ascorbic acid from *Citrus.sinesis* peel has reducing properties (Konwarh et al., 2011).

Sugars

Sugars present in the plant extracts are also involved in the bioreduction of metal ions. Monosaccharides such as glucose (linear and containing an aldehyde group) can act as reducing agent. Monosaccharides containing keto-group such as fructose also acts as an antioxidant only when it has undergone tautomeric transformation from ketone to an aldehyde. The reducing capacity of disaccharides and polysaccharide depends on their monomer unit and its ability to adopt an open chain form so that it can get access to the metal ions. Therefore lactose and maltose has reducing ability whereas sucrose doesn't have. Similarly glucose is a strong reducing agent than fructose and is involved in synthesis of metal NPs of various morphology (Ahmad et al., 2010).

1.4.1.4 Factors influencing green synthesis of metallic nanoparticles

During the synthesis of NPs with the use of metal ions and plant extract various other factors such as pH, reactant concentration, time and temperature influence the size, shape and yield of the NPs (Shah et al., 2015).

Influence of pH

The pH of the reaction medium is crucial for the nanoparticle synthesis (Gardea-Torresdey et al., 1999). The shape and the size of the nanoparticle vary with the varying pH conditions. In a study, gold NPs synthesized using *Avena sativa* biomass had higher particle size at acidic pH conditions and smaller particle size at higher pH conditions (Armendariz et al., 2004). This was explained by the presence of more accessible functional groups present at higher pH conditions (pH 3 and pH 4) leading more particle nucleation whereas less accessible functional group at lower pH conditions (pH 2) leads to aggregation of the particles. In another study the number of silver NPs increased with increasing concentration of *Cinnamon zeylanicum* bark extract and pH. The shape of the silver NPs became spherical (Sathishkumar et al., 2009). However, size of the palladium NPs slightly increased at increased pH when synthesized using *Cinnamon zeylanicum* bark extract (Sathishkumar et al., 2009)

Influence of reactant concentration

The concentrations of metal ion and plant extract influence the size, shape and number of the particles. The shape of the gold NPs changed from triangular to spherical with the increasing concentration of chloroauric acid (Huang et al., 2007). Similarly the ratio of triangular gold NP and spherical gold NP along with their size varied with varying concentration of *Aloe vera* leaf extract (Chandran et al., 2006).

Influence of reaction time

The reaction time is crucial for the synthesis of the NPs as the size, shape and number varies with time of the reaction. The size of silver nanoparticle increased from 10 to 35 nm with increase in time span from 30 min to 4 h (Prathna et al., 2011)

Influence of reaction temperature

It is well known that the temperature is crucial factor in any synthesis reaction of NPs. The yield of NPs along with their size and shape differs with the reaction temperature. The size of the silver NPs decreased from 35 to 10 nm when the temperature of the reaction was increased from 25 °C to 60 °C (Kaviya et al., 2011).

1.5 Characterization of Nanoparticles

The NPs synthesized from above all the techniques either via top down approach or bottom up approach are characterized by several techniques to determine various properties such as particle size, size distribution, shape and surface area because the application of NPs are dependent on these properties (Shah et al., 2015).

During the synthesis of nanoparticles from metal salts in aqueous medium in chemical and biological process the first qualitative indication of nanoparticle formation is a color change (Singh et al., 2015). Colloidal particles thus formed can be detected by a laser beam that passes through the colloidal solution and detects the presence of nanoparticle in a solution. This effect is called as tyndall effect (Shah et al., 2015). The NPs are separated from the solution by centrifugation and then prepared for advanced characterization.

The techniques used to determine the nature, surface properties, composition, purity, stability, and morphology of any NPs include UV-visible spectroscopy (UV-vis), dynamic light scattering (DLS), atomic force microscopy (AFM), transmission electron microscopy (TEM), scanning electron microscopy (SEM), energy dispersive spectroscopy (EDS), X-ray diffraction (XRD), Fourier transform infrared spectroscopy (FT-IR), Raman spectroscopy, atomic absorption spectroscopy, X-ray photoelectron spectroscopy, neutron activation analysis and thermogravimetric analysis (Anandalakshmi et al., 2015; Singh et al., 2015). Microscopy techniques such as SEM, TEM and AFM are the direct methods of characterizing the shape and morphology of the NPs. Spectroscopy studies such as UV-visible, DLS, XRD, EDS, FT-IR and Raman are indirect methods of determining composition, structure, crystal phase, and properties of NPs (Joshi et al., 2008; Singh et al., 2015). In UV-visible spectroscopy both types of radiations interact with the nanoparticle excite electrons to higher state from ground state, resulting a characteristic peak for particles in 2 nm to 100 nm range. Silver NPs has absorbance between 420-500 nm. DLS spectroscopy is used to determine the size distribution and quantify the surface charge of the particle in a liquid medium. XRD of nanoparticle produces a diffraction pattern which is compared with standard crystallographic database to determine structural information. XRD data analysis gives information about crystallite size, structure, crystallinity, preferred orientation and phase composition of the sample. Raman spectroscopy is used to study the vibrational, rotational and other low frequency modes in the system. XPS is a quantitative spectroscopic technique which is a surface chemical analysis technique used to estimate the empirical formula or

elemental composition, chemical state and electronic state of the surface elements of the particles (Joshi et al., 2008).

1.6 RESEARCH GAP

From the above review, it is evident that green synthesis of NPs using plants has been explored a lot in recent years. Some of these plants are edible and have medicinal value. In this context, exploration of silkworm primary host plant is limited though there are reports of NPs synthesis using some host plants of silkworms such as *Quercus sp., Terminalia arjuna, Terminalia chebula, Terminalia catappa, Jatropha curcas, Carica papaya, Emblica officinalis, Centella asiatica Syzygium cumini, Centella asiatica, Ailanthus excels, Anogeissus latifolia, Manihot esculenta, Cinnamomum camphora, Cinnamomum tamala, Averrhoa carambola, Melastoma Malabathricum*. Northeastern region of India is rich in diversity of sericigenous insects and their host plants. Among the five types of silkworms namely muga (*Antheraea assamensis*), eri (*Samia cynthia ricini*), Indian tasar (*Antheraea mylitta*), Oak tasar (*Antheraea proylei*) and mulberry (*Bombyx mori*) silkworm, muga silk and eri silk is majorly produced in Assam. A brief introduction on the host plants of eri and muga silkworm has been mentioned here.

Briefly, the host plants of silkworms vary in secondary metabolite composition which affects the feeding habit of the silkworms. The plants which are the most preferred by a silkworm are known as primary host plants and the less and least preferred plants are known as secondary and tertiary host plants, respectively for that particular silkworm. Muga silkworm (*A. assamensis*) is polyphagous in nature so, it feeds on 15 variety of host plants among which two species, som (*Persea bombycina* King ex.

Hook) and sualu (*Litsea monopetela* Persoon) are regarded as its primary host plants. *Litsea salicifolia* Roxburgh ex. Nees and *Litsea citrata* Blume, are considered to be secondary host plants. Tertiary host plants of muga silkworm include *Actinodaphnae obovata* Nees (Blume), *A. anquistifolia* (Blume) Nees, *Cinnamomum glaucescans* (Nees) Drury, *C. glanduliferum* (Wallich) Meisner, *Litsea nitida* (Roxburgh) Hooker f., all of which belong to Lauraceae family. Tree species rarely eaten by this insect belonging to other families include, *Michelia champaca* L. (Magnoliaceae) and *Magnolia sphenocarpa* Hooker f. and Thomson, *Celastrus monospermus* Roxburgh (Celastraceae); *Gmelia arborea* Roxburgh (Verbanaceae), *Zanthozylum rhesta* (Roxburgh) D.C. (Rutaceae); *Zizyphus jujuba* (Rhamnaceae) etc. (Neog et al. 2006). Som has the best nutritional composition among the four, followed by sualu and mejankori (Singha et al., 2016). There are 51 varieties of som plants (PB001-PB051) out of which *Nahorpotia* (Acc. PB 003) & *Kothalpotia* (Acc. PB 006) are the most preferred diploid genotypes and Gadadhar (PB012) is most promising polyploid variety (URL: http://www.cmerti.res.in/faq.html). In upper Assam area (Dibrugarh, Sibsagar, Jorhat and Lakhimpur Districts), som is naturally abundant and commercially exploited for reeling cocoon production. Soalu one of the primary host plant muga is naturally distributed in the foothills of lower Assam spreading up to Garo hills ranges of Meghalaya (URL: http://www.cmerti.res.in/faq.html).

Similarly, eri silkworm (*Samia cynthia ricini* (Boisd.)) is polyphagous in nature and feeds on wide range of plants over 30 species (Radhika et al., 2017; Bindroo et al., 2007). The primary host plants of eri silkworm includes castor plants (*Ricinus communis*) and kesseru plants (*Heteropanax fragrans*) (Fukuda et al., 1961; Watt,

2014). There are different varieties of castor plants present based on the stem color, bloom, seed color, seed shape etc. Castor plant has many high yielding and improved varieties such as: TNV-5, CO-1, RC-8, GCM-2, GCM-4 and Aruna (Singha et al., 2016). These high yielding varieties are nutritionally superior to indigenous variety i.e., Red, Red petiole, Green and Powdery. The moisture and starch content of castor gradually decreases from tender to mature leaves while total nitrogen, crude protein, total mineral, crude fibre, and total soluble sugar content increases steadily with the maturity of leaves (Singha et al., 2016). The cultivation of castor plants requires flat and sloping land rich in humus. Likewise kesseru plantation requires high flat and sloping lands. Tapioca (*Manihot esculenta*) and payam (*Evodia flaxinifolia*) are the secondary host plants and these plants can be used for commercial production of eri silk. Rest of the plant species like barkesseru (*Ailanthus excelsa*), papaya (*Carica papaya*), Jatropha (*Jatropha curcas*), barpat (*A. grandis*), gulancha (*Plumeria acutifolia*), gamari (*Gmelina arborea*) etc. (Radhika et al., 2017) are tertiary host plants, on which the silkworm could complete its lifecycle. Eri silkworm could also survive on certain non-host plants species if met with starvation due to non-availability of its food plants. The major factor for healthy growth and development of silkworm is the nutritious balanced foods, as it provide the ultimate source of energy to the insects. The quality and quantity of the product is dependent on the quality of the leaves, the sole food of silkworm (Talukdar et al., 2015).

The silkworm host plants not only have the only role to serve as food for these silkworms but also have other importance for the human society such as their medicinal value, bioenergy source etc. Warrier and Nambiar, (1993) has listed the

medicinal properties of *Ricinus communis*, the primary host plant of eri silkworm. The roots are astringent, acrid, thermogenic, carminative, anthelmintic, emollient, diuretic, aphrodisiac, galactagogue, sudorific, expectorant, and depurative. They are used in gastropathy (gulma, amadosa, and constipation), inflammations, fever, ascites, strangury, bronchitis, cough, leprosy, skin diseases, vitiated conditions of vata, colic, coxalgia, and lumbago. The leaves are useful in burns, nyctalopia, strangury, for bathing and fomantations in vitiated conditions of vata in rheumatoid arthiritis, urodynia and arthralgia due to their diuretic, antihelmintic and galactagogue properties. *R. communis* flowers are medicinally important as they are used in urodynia and glandular tumors. The seeds are equally medicinally important as they are acrid thermogenic, digestive, antirheumatic (Scarpa, and Guerci, 1982), cathartic and aphrodisiac and they are used to treat arthralgia. The oil extracted from the seeds is laxative (Hoareau and DaSilva, 1999), antipyretic, thermogenic and effective purgative for all ailments acused by vata and kapha. It is recommended for scrotocele, ascites, intermittent fever, colonites, lumbago, coxalgia and coxitis. *Heteropanax fragrans* (Roxb) Seem. commonly known as kesseru plant serves as an host plant to eri silkworm when there is a scarcity of primary host plant *Ricinus communis*. These are used to treat cancer by Chakma community of Bangladesh (Changmai et al., 2015) Similarly, muga silkworm primary host plant *Persea bombycina* plants has also medicinal properties as their leaves are used to cure piles (Das, 2016).

Despite their medicinal importance, these plants which serve food for the economical silkworm have been least explored. Therefore we have selected the three host plants

red castor (*Ricinus communis var. carmencita*), kesseru (*Heteropanax fragrans*) and som (*Persea bombycina*) for green synthesis of metallic NPs.

1.7 CONCLUSION

Green synthesis of NPs are cost effective, ecofriendly and less time consuming method of nanoparticle synthesis. These NPs can be used in various applications such as medicine, environment remediation, agriculture etc. as there are no toxic chemicals involved in the synthesis process. We have explored silkworm host plants for the synthesis silver, zinc oxide and iron oxide NPs to be used in various applications such as antibacterial activity, and dye removal.

1.8 References

Ahmad, N., & Sharma, S. (2012). Green synthesis of silver nanoparticles using extracts of *Ananas comosus*. *Green and Sustainable Chemistry*, *2*(4), 141-147.

Ahmad, N., Sharma, S., Alam, M. K., Singh, V. N., Shamsi, S. F., Mehta, B. R., & Fatma, A. (2010). Rapid synthesis of silver nanoparticles using dried medicinal plant of basil. *Colloids and Surfaces B: Biointerfaces*, 81(1), 81-86.

Ahmed, Q., Gupta, N., Kumar, A., & Nimesh, S. (2017). Antibacterial efficacy of silver nanoparticles synthesized employing *Terminalia arjuna* bark extract. *Artificial cells, Nanomedicine, and Biotechnology*, 45(6), 1192-1200.

Ahmed, S., & Ikram, S. (2015). Silver nanoparticles: one pot green synthesis using *Terminalia arjuna* extract for biological application. *Journal of Nanomedicine & Nanotechnology*, *6*(4), 1-6

Ahmed, S., Ahmad, M., Swami, B. L., & Ikram, S. (2016). A review on plants extract mediated synthesis of silver nanoparticles for antimicrobial applications: a green expertise. *Journal of advanced research*, 7(1), 17-28.

Ahmed, S., Ahmad, M., Swami, B. L., & Ikram, S. (2016). Green synthesis of silver nanoparticles using Azadirachta indica aqueous leaf extract. *Journal of Radiation Research and Applied Sciences*, *9*(1), 1-7.

Allahverdiyev, A. M., Abamor, E. S., Bagirova, M., Ustundag, C. B., Kaya, C., Kaya, F., & Rafailovich, M. (2011). Antileishmanial effect of silver nanoparticles and their enhanced antiparasitic activity under ultraviolet light. *International Journal of Nanomedicine*, 6, 2705-2714.

Al-Ruqeishi, M. S., Mohiuddin, T., & Al-Saadi, L. K. (2016). Green synthesis of iron oxide nanorods from deciduous Omani mango tree leaves for heavy oil viscosity treatment. *Arabian Journal of Chemistry*, 1-7.

Anandalakshmi, K., Venugobal, J., & Ramasamy, V. (2015). Characterization of silver nanoparticles by green synthesis method using *Pedalium murex* leaf extract and their antibacterial activity. *Applied Nanoscience*, 6(3), 399.

Ankamwar, B. (2011). Biosynthesis of silver nanoparticles using leaf extract of *Terminalia catappa*. *Nano Science & Nano Technology*: *An Indian Journal*, 5(3), 131-134.

Ankanna, S., TNVKV, P., Elumalai, E. K., & Savithramma, N. (2010). Production of biogenic silver nanoparticles using *Boswellia ovalifoliolata* stem bark. *Digest Journal of Nanomaterials Biostructures*, *5*(2), 369-372.

Armendariz, V.; Herrera, I.; Peralta-Videa, J.R.; Jose-Yacaman, M.; Troiani, H.; Santiago, P.; Gardea-Torresdey, J.L. (2004). Size controlled gold nanopartilce formation by Avena sativa biomass: Use of plants in nanobiotechnology. *Journal of Nanoparticle Research*, 6, 377–382.

Awwad, A. M., & Salem, N. M. (2012). A green and facile approach for synthesis of magnetite nanoparticles. *Nanoscience and Nanotechnology*, 2(6), 208-213.

Azizi, S., Mahdavi Shahri, M., & Mohamad, R. (2017). Green Synthesis of Zinc Oxide Nanoparticles for Enhanced Adsorption of Lead Ions from Aqueous Solutions: Equilibrium, Kinetic and Thermodynamic Studies. *Molecules*, 22, 1-14

Baker, S., Harini, B. P., Rakshith, D., & Satish, S. (2013). Marine microbes: invisible nanofactories. *Journal of Pharmacy Research*, 6(3), 383-388.

Bakry, R., Vallant, R. M., Najam-ul-Haq, M., Rainer, M., Szabo, Z., Huck, C. W., & Bonn, G. K. (2007). Medicinal applications of fullerenes. *International Journal of Nanomedicine*, 2(4), 639-649.

Bala, N., Saha, S., Chakraborty, M., Maiti, M., Das, S., Basu, R., & Nandy, P. (2015). Green synthesis of zinc oxide nanoparticles using Hibiscus subdariffa leaf extract: effect of temperature on synthesis, anti-bacterial activity and anti-diabetic activity. *RSC Advances*, *5*(7), 4993-5003.

Balamurughan, M. G., Mohanraj, S., Kodhaiyolii, S., & Pugalenthi, V. (2014). *Ocimum sanctum* leaf extract mediated green synthesis of iron oxide nanoparticles: spectroscopic and microscopic studies. *Journal of Chemical and Pharmaceutical Sciences*, National Conference on Green Engineering and Technologies for Sustainable Future-2014, 201-204.

Balasubramani, G., Ramkumar, R., Krishnaveni, N., Pazhanimuthu, A., Natarajan, T., Sowmiya, R., & Perumal, P. (2015). Structural characterization, antioxidant and anticancer properties of gold nanoparticles synthesized from leaf extract (decoction) of Antigonon leptopus Hook. & Arn. *Journal of Trace Elements in Medicine and Biology*, 30, 83-89.

Banala, R. R., Nagati, V. B., & Karnati, P. R. (2015). Green synthesis and characterization of *Carica papaya* leaf extract coated silver nanoparticles through

X-ray diffraction, electron microscopy and evaluation of bactericidal properties. *Saudi Journal of Biological Sciences*, 22(5), 637-644.

Banerjee, P., Satapathy, M., Mukhopahayay, A., & Das, P. (2014). Leaf extract mediated green synthesis of silver nanoparticles from widely available Indian plants: synthesis, characterization, antimicrobial property and toxicity analysis. *Bioresources and Bioprocessing*, *1*(1), 1-10.

Bar, H., Bhui, D. K., Sahoo, G. P., Sarkar, P., De, S. P., & Misra, A. (2009). Green synthesis of silver nanoparticles using latex of *Jatropha curcas*. *Colloids and surfaces A: Physicochemical and engineering aspects*, 339(1), 134-139.

Basavegowda, N., Magar, K. B. S., Mishra, K., & Lee, Y. R. (2014). Green fabrication of ferromagnetic Fe 3 O 4 nanoparticles and their novel catalytic applications for the synthesis of biologically interesting benzoxazinone and benzthioxazinone derivatives. *New Journal of Chemistry*, *38*(11), 5415-5420.

Basha, S. K., Govindaraju, K., Manikandan, R., Ahn, J. S., Bae, E. Y., & Singaravelu, G. (2010). Phytochemical mediated gold nanoparticles and their PTP 1B inhibitory activity. *Colloids and Surfaces B: Biointerfaces*, 75(2), 405-409.

Beyth, N., Houri-Haddad, Y., Domb, A., Khan, W., & Hazan, R. (2015). Alternative antimicrobial approach: nano-antimicrobial materials. Evidence-based complementary and alternative medicine, 2015, 1-16.

Bhatia, S. (2016). Nanoparticles Types, Classification, Characterization, Fabrication Methods and Drug Delivery Applications. In Natural Polymer Drug Delivery Systems. Springer International Publishing

Bhuyan, T., Mishra, K., Khanuja, M., Prasad, R., & Varma, A. (2015). Biosynthesis of zinc oxide nanoparticles from *Azadirachta indica* for antibacterial and photocatalytic applications. *Materials Science in Semiconductor Processing*, 32, 55-61.

Bindroo, B. B., Singh, N. T., Sahu, A. K., & Chakravorty, R. (2007). Eri silkworm host plants. *Indian Silk*, 5, 13-16.

Bruchez, M., Moronne, M., Gin, P., Weiss, S., & Alivisatos, A. P. (1998). Semiconductor nanocrystals as fluorescent biological labels. *Science*, 281(5385), 2013-2016.

Campos, E. A., Pinto, D. V. B. S., Oliveira, J. I. S. D., Mattos, E. D. C., & Dutra, R. D. C. L. (2015). Synthesis, characterization and applications of iron oxide nanoparticles-A short review. *Journal of Aerospace Technology and Management*, 7(3), 267-276.

Chahardooli, M., Khodadadi, E., & Khodadadi, E. (2014). Green synthesis of silver nanoparticles using oak leaf and fruit extracts (Quercus) and its antibacterial activity against plant pathogenic bacteria. *International Journal of Biosciences*, 4(3), 97-103.

Chan, W. C., & Nie, S. (1998). Quantum dot bioconjugates for ultrasensitive nonisotopic detection. *Science*, 281(5385), 2016-2018.

Chandran, S. P., Chaudhary, M., Pasricha, R., Ahmad, A., & Sastry, M. (2006). Synthesis of gold nanotriangles and silver nanoparticles using Aloe vera plant extract. *Biotechnology progress*, 22(2), 577-583.

Changmai, M., Chetia J., Upadhyaya, S., Yadav, R. N. S., Bhuyan, M. (2015) Phytochemical and biochemical analysis of two host plants of eri silkworm, *Samia ricini* (D.) *International Journal of Pharmaceutical Sciences Review and Research*, 32(2), 187-192.

Chaturvedi, S., Dave, P. N., & Shah, N. K. (2012). Applications of nano-catalyst in new era. *Journal of Saudi Chemical Society*, *16*(3), 307-325.

Chauhan, N., Tyagi, A. K., Kumar, P., & Malik, A. (2016). Antibacterial potential of Jatropha curcas synthesized silver nanoparticles against food borne pathogens. *Frontiers in microbiology*, 7, 1-13.

Chen, G., Roy, I., Yang, C., & Prasad, P. N. (2016). Nanochemistry and nanomedicine for nanoparticle-based diagnostics and therapy. *Chemical reviews*, 116(5), 2826-2885.

Chowdappa, P., & Gowda, S. (2013). Nanotechnology in crop protection: Status and scope. *Pest Management in Horticultural Ecosystems*, 19(2), 131-151.

Coleman, V. A., & Jagadish, C. (2006). Basic properties and applications of ZnO. *Zinc Oxide Bulk, Thin Films and Nanostructures: Processing, Properties, and Applications*, 1-20.

Das, A. K., Marwal A. & Verma, R. (2014) *Datura Inoxia* Leaf Extract Mediated One Step Green Synthesis and Characterization of Magnetite (Fe_3O_4) Nanoparticles. *Research and Reviews: Journal of Pharmaceutics and Nanotechnology*, 2(2), 21-24

Das, R. (2016) Biodiversity of Ethnomedicinal Plants used by the Ethnic Tribal People of Barpeta District of Assam, North East India. *Asian Journal of Pharmaceutical Science & Technology*, 6(1), 27-32.

Dauthal, P., & Mukhopadhyay, M. (2016). Noble metal nanoparticles: Plant-mediated synthesis, mechanistic aspects of synthesis, and applications. *Industrial & Engineering Chemistry Research*, 55(36), 9557-9577.

Debanath, M. K., & Karmakar, S. (2013). Study of blueshift of optical band gap in zinc oxide (ZnO) nanoparticles prepared by low-temperature wet chemical method. *Materials Letters*, 111, 116-119.

Devatha, C. P., Thalla, A. K., & Katte, S. Y. (2016). Green synthesis of iron nanoparticles using different leaf extracts for treatment of domestic waste water. *Journal of Cleaner Production*, 139, 1425-1435.

Devi R.S. & Dhinesh, R. (2016) Rapid Green Synthesis of Zinc Oxide Nanoparticles Using *Kedrostis Foetidissima* (Jacq.)Cogn Leaf. *International Journal of Innovative Research in Science, Engineering and Technology*, 5(11), 19281-19285.

Dizaj, S. M., Lotfipour, F., Barzegar-Jalali, M., Zarrintan, M. H., & Adibkia, K. (2014). Antimicrobial activity of the metals and metal oxide nanoparticles. *Materials Science and Engineering: C*, 44, 278-284.

Dobrucka, R., & Długaszewska, J. (2016). Biosynthesis and antibacterial activity of ZnO nanoparticles using *Trifolium pratense* flower extract. *Saudi Journal of Biological Sciences*, 23(4), 517-523.

Dubey, M., Bhadauria, S., & Kushwah, B. S. (2009). Green synthesis of nanosilver particles from extract of Eucalyptus hybrida (safeda) leaf. *Digest Journal of Nanomaterials and Biostructures*, 4(3), 537-543.

Dwivedi, R. (2013). Green synthesis of Silver Nanoparticle using *Terminalia chebula* and Assessment of its Antimicrobial Activity. *International Journal of Pure and Applied Bioscience*, 1(6), 1-6.

Dwivedi, R. (2014). Silver Nanoparticles Ecofriendly Green Synthesis by Using Two Medicinal Plant Extract. *International Journal of Bio-Technology and Research*, *3*, 61-68.

Edison, T. J. I., & Sethuraman, M. G. (2012). Instant green synthesis of silver nanoparticles using *Terminalia chebula fruit* extract and evaluation of their catalytic activity on reduction of methylene blue. *Process Biochemistry*, 47(9), 1351-1357.

Ekambaram, P., Sathali, A. A. H., & Priyanka, K. (2012). Solid lipid nanoparticles: a review. *Scientific reviews and chemical communications*, 2(1), 80-102.

Elechiguerra, J. L., Burt, J. L., Morones, J. R., Camacho-Bragado, A., Gao, X., Lara, H. H., & Yacaman, M. J. (2005). Interaction of silver nanoparticles with HIV-1. *Journal of nanobiotechnology*, 3(1), 1-10.

El-Kassas, H. Y., Aly-Eldeen, M. A., & Gharib, S. M. (2016). Green synthesis of iron oxide (Fe_3O_4) nanoparticles using two selected brown seaweeds: characterization and application for lead bioremediation. *Acta Oceanologica Sinica*, 35(8), 89-98.

Fan, Z., & Lu, J. G. (2005). Zinc oxide nanostructures: synthesis and properties. *Journal of nanoscience and nanotechnology*, 5(10), 1561-1573.

Fardood, S. T., Ramazani, A., Moradi, S., & Asiabi, P. A. (2017). Green synthesis of zinc oxide nanoparticles using Arabic gum and photocatalytic degradation of direct blue 129 dye under visible light. *Journal of Materials Science: Materials in Electronics*, 1-6.

Firdaus, M., Andriana, S., Alwi, W., Swistoro, E., Ruyani, A., & Sundaryono, A. (2017). Green synthesis of silver nanoparticles using *Carica Papaya* fruit extract under sunlight irradiation and their colorimetric detection of mercury ions. *In Journal of Physics: Conference Series*, 817(1), IOP Publishing.

Fukuda, T., Higuchi, Y., & Matsuda, M. (1961). Artificial food for Eri-silkworm raising. *Agricultural and Biological Chemistry*, 25(5), 417-420.

Gaikwad, S., Ingle, A., Gade, A., Rai, M., Falanga, A., Incoronato, N., Russo, L., Galdiero, S. & Galdiero, M. (2013). Antiviral activity of mycosynthesized silver nanoparticles against herpes simplex virus and human parainfluenza virus type 3. *International Journal of Nanomedicine*, 8, 4303-4314.

Gan, P. P., Fong, S., & Li, Y. (2012). Potential of plant as a biological factory to synthesize gold and silver nanoparticles and their applications. *Reviews in Environmental Science and Biotechnology*, 11(2), 169-206.

Gardea-Torresdey, J.L.; Tiemann, K.J.; Gamez, G.; Dokken, K.; Tehuacamanero, S.; Jose-Yacaman, M. (1999). Gold nanoparticles obtained by bio-precipitation from gold (III) solutions. *Journal of Nanoparticle Research*, 1, 397–404.

Gawade, V. V., Gavade, N. L., Shinde, H. M., Babar, S. B., Kadam, A. N., & Garadkar, K. M. (2017). Green synthesis of ZnO nanoparticles by using *Calotropis procera* leaves for the photodegradation of methyl orange. *Journal of Materials Science: Materials in Electronics*, 1-7.

Geetha, A., Sakthivel, R., & Mallika, J. (2016). A Single pot Green synthesis of ZnO nanoparticles using aqueous gum exudates of *Azadirachta indica* and its antifungal activity, *International Research Journal of Engineering and Technology*, 3(9), 300-306.

Geethalakshmi, R., & Sarada, D. V. L. (2010). Synthesis of plant-mediated silver nanoparticles using *Trianthema decandra* extract and evaluation of their antimicrobial activities. *International Journal of Engineering Science and Technology*, *2*(5), 970-975.

Gehrke, I., Geiser, A., & Somborn-Schulz, A. (2015). Innovations in nanotechnology for water treatment. *Nanotechnology, science and applications*, 8, 1-17.

Gruen, L. C. (1975). Interaction of amino acids with silver (I) ions. *Biochimica et Biophysica Acta (BBA)-Protein Structure*, *386*(1), 270-274.

Gupta, V., Gupta, A.R. & Kant, V. (2013). Synthesis, Characterization and Biomedical Applications of Nanoparticles. *Science International*, 1(5), 167-174

Hasan, S. (2015). A review on nanoparticles: their synthesis and types. *Research Journal of Recent Sciences*. 4, 1-3

Hassan, S. S., El Azab, W. I., Ali, H. R., & Mansour, M. S. (2015). Green synthesis and characterization of ZnO nanoparticles for photocatalytic degradation of anthracene. *Advances in Natural Sciences: Nanoscience and Nanotechnology*, 6(4), 1-11.

Heydari, R., & Rashidipour, M. (2015). Green synthesis of silver nanoparticles using extract of oak fruit hull (Jaft): synthesis and in vitro cytotoxic effect on MCF-7 cells. *International Jjournal of Breast Cance*r, 2015, 1-6.

Hoag, G. E., Collins, J. B., Holcomb, J. L., Hoag, J. R., Nadagouda, M. N., & Varma, R. S. (2009). Degradation of bromothymol blue by 'greener'nano-scale zero-valent iron synthesized using tea polyphenols. *Journal of Materials Chemistry*, 19(45), 8671-8677.

Hoareau, L., & DaSilva, E. J. (1999). Medicinal plants: a re-emerging health aid. Electronic *Journal of Biotechnology*, 2(2), 3-4.

Huang, J.; Li, Q.; Sun, D.; Lu, Y.; Su, Y.; Yang, X.; Wang, H.; Wang, Y.; Shao, W.; He, N.; (2007) et al. Biosynthesis of silver and gold nanoparticles by novel sundried *Cinnamomum camphora* leaf. *Nanotechnology*, 18, 1–11.

Huang, L., Weng, X., Chen, Z., Megharaj, M., & Naidu, R. (2014). Synthesis of iron-based nanoparticles using oolong tea extract for the degradation of malachite green. *Spectrochimica Acta Part A: Molecular and Biomolecular Spectroscopy*, 117, 801-804.

Husen, A., & Siddiqi, K. S. (2014). Carbon and fullerene nanomaterials in plant system. *Journal of Nanobiotechnology*, 12(1), 1-10.

Hussain, I., Singh, N. B., Singh, A., Singh, H., & Singh, S. C. (2016). Green synthesis of nanoparticles and its potential application. *Biotechnology letters*, 38(4), 545.

Hussein, F. H., & Shaheed, M. A. (2015). Preparation and Applications of Titanium Dioxide and Zinc Oxide Nanoparticles. *Journal of Environmental Analytical Chemistry*, 2(1), 1-3.

Iravani, S. (2011). Green synthesis of metal nanoparticles using plants. *Green Chemistry*, *13*(10), 2638-2650.

Jain, T. K., Morales, M. A., Sahoo, S. K., Leslie-Pelecky, D. L., & Labhasetwar, V. (2005). Iron oxide nanoparticles for sustained delivery of anticancer agents. *Molecular Pharmaceutics*, 2(3), 194-205.

Jamdagni, P., Khatri, P., & Rana, J. S. (2016). Green synthesis of zinc oxide nanoparticles using flower extract of Nyctanthes arbor-tristis and their antifungal activity. *Journal of King Saud University-Science*.

Janotti, A., & Van de Walle, C. G. (2009). Fundamentals of zinc oxide as a semiconductor. *Reports on Progress in Physics*, 72(12), 126501.

Joshi. M., Bhattacharyya, A. and Ali, S.W. (2008). Characterization techniques for nanotechnology applications in textiles. *Indian Journal of Fibre and Textile Research*, 33, 304-317

Karkuzhali, & Yogamoorthi, A. (2015) Biosynthesis Of Iron Oxide Nanoparticles Using Aquous Extract of *Jatropha Gosspifolia* As Source Of Reducing Agent. *International Journal of NanoScience and Nanotechnology*, 6(1), 47-55.

Kaur, B., Markan, M., & Singh, M. (2012). Green synthesis of gold nanoparticles from *Syzygium aromaticum* extract and its use in enhancing the response of a colorimetric urea biosensor. *BioNanoScience*, 2(4), 251-258.

Kaviya, S.; Santhanalakshmi, J.; Viswanathan, B.; Muthumary, J.; Srinivasan, K. (2011). Biosynthesis of silver nanoparticles using *Citrus sinensis* peel extract and its antibacterial activity. *Spectrochimica Acta Part A: Molecular and Biomolecular Spectroscopy,* 79, 594–598.

Keat, C. L., Aziz, A., Eid, A. M., & Elmarzugi, N. A. (2015). Biosynthesis of nanoparticles and silver nanoparticles. *Bioresources and Bioprocessing*, 2, 1-11.

Khan, M. A. M., Kumar, S., Ahamed, M., Alrokayan, S. A., & AlSalhi, M. S. (2011). Structural and thermal studies of silver nanoparticles and electrical transport study of their thin films. *Nanoscale Research Letters*, *6*(1), 1-8.

Khandel, P., & Shahi S. K. (2016) Microbes mediated synthesis of metal nanoparticles: current status and future prospects. *International Journal of Nanomaterials and Biostructures*, 6(1), 1-24.

Khatoon, N., Mazumder, J. A., and Sardar, M. (2017) Biotechnological Applications of Green Synthesized Silver Nanoparticles. *Journal of Nanosciences: Current Research*. 2(1), 1-8

Kievit, F. M., & Zhang, M. (2011). Surface engineering of iron oxide nanoparticles for targeted cancer therapy. *Accounts of Chemical Research*, 44(10), 853-862.

Kołodziejczak-Radzimska, A., & Jesionowski, T. (2014). Zinc oxide—from synthesis to application: a review. *Materials*, *7*(4), 2833-2881.

Konwarh, R.; Gogoi, B.; Philip, R.; Laskar, M. A.; Karak, N. (2011). Biomimetic preparation of polymer-supported free radical scavenging, cytocompatible and antimicrobial "green" silver nanoparticles using aqueous extract of *Citrus sinensis* peel. *Colloids Surface B: Biointerfaces*, 84, 338− 345.

Kora, A. J., Beedu, S. R., & Jayaraman, A. (2012). Size-controlled green synthesis of silver nanoparticles mediated by gum ghatti (*Anogeissus latifolia*) and its biological activity. *Organic and Medicinal Chemistry Letters*, 2(1), 1-10.

Korbekandi, H., Chitsazi, M. R., Asghari, G., Bahri Najafi, R., Badii, A., & Iravani, S. (2015). Green biosynthesis of silver nanoparticles using *Quercus brantii* (oak) leaves hydroalcoholic extract. *Pharmaceutical Biology*, 53(6), 807-812.

Krishnaprabha, M. & Pattabi, M. (2017, May). Biogenic synthesis of fluorescent silver nanoparticles using *Melastoma Malabathricum* flower extract. In AIP Conference Proceedings 1832(1), AIP Publishing.

Krithiga, N., Rajalakshmi, A., & Jayachitra, A. (2015). Green synthesis of silver nanoparticles using leaf extracts of *Clitoria ternatea* and *Solanum nigrum* and study of its antibacterial effect against common nosocomial pathogens. *Journal of Nanoscience*, *2015*, 1-8.

Kuang, Y., Wang, Q., Chen, Z., Megharaj, M., & Naidu, R. (2013). Heterogeneous Fenton-like oxidation of monochlorobenzene using green synthesis of iron nanoparticles. *Journal of Colloid and Interface Science*, 410, 67-73.

Kumar, K. M., Mandal, B. K., Kumar, K. S., Reddy, P. S., & Sreedhar, B. (2013). Biobased green method to synthesise palladium and iron nanoparticles using *Terminalia chebula* aqueous extract. *Spectrochimica Acta Part A: Molecular and Biomolecular Spectroscopy*, 102, 128-133.

Kumar, M. P., Suresh, D., Nagabhushana, H., & Sharma, S. C. (2015). Beta vulgaris aided green synthesis of ZnO nanoparticles and their luminescence, photocatalytic and antioxidant properties. *The European Physical Journal Plus*, 130, 1-7.

Kumar, N., & Kumbhat, S. (2016). Essentials in Nanoscience and Nanotechnology. John Wiley & Sons.

Latha, N., & Gowri, M. (2014). Biosynthesis and characterisation of Fe_3O_4 nanoparticles using *Caricaya papaya* leaves extract. *International Journal of Scientific Research*, 3(11), 1551-1556.

Li, X., Xu, H., Chen, Z. S., & Chen, G. (2011). Biosynthesis of nanoparticles by microorganisms and their applications. *Journal of Nanomaterials*, 2011.

Li, Z., Sun, Q., Zhu, Y., Tan, B., Xu, Z. P., & Dou, S. X. (2014). Ultra-small fluorescent inorganic nanoparticles for bioimaging. *Journal of Materials Chemistry B*, 2(19), 2793-2818.

Liu, L. (2009). Emerging Nanotechnology Power Nanotechnology R&D and Business Trends in the Asia

Logeswari, P., Silambarasan, S., & Abraham, J. (2013). Ecofriendly synthesis of silver nanoparticles from commercially available plant powders and their antibacterial properties. *Scientia Iranica*, 20(3), 1049-1054.

Luo, F., Chen, Z., Megharaj, M., & Naidu, R. (2014). Biomolecules in grape leaf extract involved in one-step synthesis of iron-based nanoparticles. *RSC Advances*, 4(96), 53467-53474.

Luo, X., Morrin, A., Killard, A. J., & Smyth, M. R. (2006). Application of nanoparticles in electrochemical sensors and biosensors. *Electroanalysis*, 18(4), 319-326.

Machado, S., Pinto, S. L., Grosso, J. P., Nouws, H. P. A., Albergaria, J. T., & Delerue-Matos, C. (2013). Green production of zero-valent iron nanoparticles using tree leaf extracts. *Science of the Total Environment*, 445, 1-8.

Machala, L., Tuček, J., & Zboril, R. (2011). Polymorphous transformations of nanometric iron (III) oxide: a review. *Chemistry of Materials*, 23(14), 3255-3272.

Madhavi, V., Prasad, T. N. V. K. V., Reddy, A. V. B., Reddy, B. R., & Madhavi, G. (2013). Application of phytogenic zerovalent iron nanoparticles in the adsorption of hexavalent chromium. *Spectrochimica Acta Part A: Molecular and Biomolecular Spectroscopy*, *116*, 17-25.

Makarov, V. V., Love, A. J., Sinitsyna, O. V., Makarova, S. S., Yaminsky, I. V., Taliansky, M. E., & Kalinina, N. O. (2014). “Green” nanotechnologies: synthesis of metal nanoparticles using plants. *Acta Naturae*, 6(1 (20)) 35-44.

Makarov, V. V., Makarova, S. S., Love, A. J., Sinitsyna, O. V., Dudnik, A. O., Yaminsky, I. V., Taliansky, M.E. & Kalinina, N. O. (2014). Biosynthesis of stable iron oxide nanoparticles in aqueous extracts of *Hordeum vulgare* and *Rumex acetosa* plants. *Langmuir*, *30*(20), 5982-5988.

Mallmann, E. J. J., Cunha, F. A., Castro, B. N., Maciel, A. M., Menezes, E. A., & Fechine, P. B. A. (2015). Antifungal activity of silver nanoparticles obtained by green synthesis. *Revista do Instituto de Medicina Tropical de São Paulo*, 57(2), 165-167.

Mandal, S., Selvakannan, P. R., Phadtare, S., Pasricha, R., & Sastry, M. (2002). Synthesis of a stable gold hydrosol by the reduction of chloroaurate ions by the amino acid, aspartic acid. *Journal of Chemical Sciences*, *114*(5), 513-520.

Maqdoom, F., Sabeen, H., & Zarina, S. (2013). Papaya fruit extract: A potent source for synthesis of bionanoparticle. *Journal of Environmental Research and Development*, 7(4A), 1518-1522.

Martínez-Cabanas, M., López-García, M., Barriada, J. L., Herrero, R., & de Vicente, M. E. S. (2016). Green synthesis of iron oxide nanoparticles. Development of magnetic hybrid materials for efficient As (V) removal. *Chemical Engineering Journal*, 301, 83-91.

Matinise, N., Fuku, X. G., Kaviyarasu, K., Mayedwa, N., & Maaza, M. (2017). ZnO nanoparticles via *Moringa oleifera* green synthesis: Physical properties & mechanism of formation. *Applied Surface Science*, 406, 339-347.

Mehlhorn, H. (Ed.). (2016). *Nanoparticles in the fight against parasites* (Vol. 8). Springer.

Meyyappan A., Banu A. S. & Kurian G. A. (2015) One step synthesis of iron oxide nanoparticles via chemical and green route– an effective comparison. *International Journal of Pharmacy and Pharmaceutical Sciences*, 7(1), 70-74.

Mishra, P. M., Sahoo, S. K., Naik, G. K., & Parida, K. (2015). Biomimetic synthesis, characterization and mechanism of formation of stable silver nanoparticles using *Averrhoa carambola* L. leaf extract. *Materials Letters*, 160, 566-571.

Mitra, A. K., Cholkar, K., & Mandal, A. (Eds.). (2017). Emerging Nanotechnologies for Diagnostics, Drug Delivery and Medical Devices. William Andrew.

Mody, V. V., Siwale, R., Singh, A., & Mody, H. R. (2010). Introduction to metallic nanoparticles. *Journal of Pharmacy and Bioallied Sciences*, 2(4), 282-289.

Mohammadlou, M., Maghsoudi, H., & Jafarizadeh-Malmiri, H. (2016). A review on green silver nanoparticles based on plants: Synthesis, potential applications and eco-friendly approach. *International Food Research Journal*, 23(2) 446-463.

Mozafari, M. R. (2010). Nanoliposomes: preparation and analysis. Liposomes: Methods and Protocols, Volume 1: Pharmaceutical Nanocarriers, 29-50.

MubarakAli, D., Thajuddin, N., Jeganathan, K., & Gunasekaran, M. (2011). Plant extract mediated synthesis of silver and gold nanoparticles and its antibacterial activity against clinically isolated pathogens. *Colloids and Surfaces B: Biointerfaces*, *85*(2), 360-365.

Mude, N., Ingle, A., Gade, A., & Rai, M. (2009). Synthesis of silver nanoparticles using callus extract of Carica papaya—a first report. *Journal of Plant Biochemistry and Biotechnology*, 18(1), 83-86.

Muthu, C. R. R. and Rajalaxshmi, A. (2016) A.Green Synthesis, Characterization of ZnO nanoparticles and Ceion doped ZnO nanoparticles assisted *Sesbania Grandiflora* for photocatalytic application. *Research Journal of Material Sciences*, 4(2), 1-6.

Muthu, K., & Priya, S. (2017). Green synthesis, characterization and catalytic activity of silver nanoparticles using *Cassia auriculata* flower extract separated fraction. *Spectrochimica Acta Part A: Molecular and Biomolecular Spectroscopy*, 179, 66-72.

Nadagouda, M. N., Castle, A. B., Murdock, R. C., Hussain, S. M., & Varma, R. S. (2010). In vitro biocompatibility of nanoscale zerovalent iron particles (NZVI) synthesized using tea polyphenols. *Green Chemistry*, 12(1), 114-122.

Nam, J., Won, N., Bang, J., Jin, H., Park, J., Jung, S., Park, Y. & Kim, S. (2013). Surface engineering of inorganic nanoparticles for imaging and therapy. *Advanced drug delivery reviews*, 65(5), 622-648.

Narasimha, G., Khadri, H., & Alzohairy, M. (2012). Antiviral properties of silver nanoparticles synthesized by *Aspergillus* spp. *Der Pharmacia Lettre*, 4(2), 649-651.

Narendhran, S., & Sivaraj, R. (2016). Biogenic ZnO nanoparticles synthesized using L. aculeata leaf extract and their antifungal activity against plant fungal pathogens. *Bulletin of Materials Science*, 39(1), 1-5.

Nasrollahi, A., Pourshamsian, K. H., & Mansourkiaee, P. (2011). Antifungal activity of silver nanoparticles on some of fungi. *International Journal of Nano Dimension*, 1(3), 233-239.

Natsuki, J., Natsuki, T., & Hashimoto, Y. (2015). A review of silver nanoparticles: synthesis methods, properties and applications. *International Journal of Material Science and Application*, 4, 325-332.

Neumark, G., Gong, Y., & Kuskovsky, I. (2006). Doping Aspects of Zn-Based Wide-Band-Gap Semiconductors. In Springer Handbook of Electronic and Photonic Materials. Springer US.

Nguefack Marius Borel, N., Foba-Tendo, J., Yufanyi, D. M., Peter Etape, E., Eko, J. N., & John Ngolui, L. (2014). *Averrhoa carambola*: A Renewable Source of Oxalic Acid for the Facile and Green Synthesis of Divalent Metal (Fe, Co, Ni, Zn, and Cu) Oxalates and Oxide Nanoparticles. *Journal of Applied Chemistry*, 2014, 1-9.

Nuruzzaman, M., Rahman, M. M., Liu, Y., & Naidu, R. (2016). Nanoencapsulation, nano-guard for pesticides: a new window for safe application. *Journal of Agricultural and Food Chemistry*, 64(7), 1447-1483.

Panáček, A., Kolář, M., Večeřová, R., Prucek, R., Soukupová, J., Kryštof, V., Hamal, P., Zbořil, R. & Kvítek, L. (2009). Antifungal activity of silver nanoparticles against *Candida* spp. *Biomaterials*, 30(31), 6333-6340.

Pande, N.S., Jaspal, D.K., Malviya, A. & Jayachandran V.P. (2015) Green route synthesis of iron nanoparticles and antibacterial studies. *International Journal of Advances in Science Engineering and Technology*, 3(2), 98-102.

Parameswaranpillai, J., Hameed, N., Kurian, T., & Yu, Y. (Eds.). (2016). Nanocomposite Materials: Synthesis, Properties and Applications. CRC Press.

Parsons, J. G., Peralta-Videa, J. R., & Gardea-Torresdey, J. L. (2007). Use of plants in biotechnology: synthesis of metal nanoparticles by inactivated plant tissues, plant extracts, and living plants. *Developments in Environmental Science*, 5, 463-485.

Parthibana, C., & Sundaramurthy, N. (2015). Biosynthesis, characterization of ZnO nanoparticles by using *Pyrus pyrifolia* leaf extract and their photocatalytic activity. *International Journal of Innovative Research in Science, Engineering and Technology*, 4(10), 9710-9718.

Parveen, K., Banse, V., & Ledwani, L. (2016, April). Green synthesis of nanoparticles: Their advantages and disadvantages. *In AIP Conference Proceedings*,1724(1) 020048 AIP Publishing.

Patil, S. S., Shedbalkar, U. U., Truskewycz, A., Chopade, B. A., & Ball, A. S. (2016). Nanoparticles for environmental clean-up: a review of potential risks and emerging solutions. *Environmental Technology & Innovation*, 5(2016), 10-21.

Peteu, S. F., Oancea, F., Sicuia, O. A., Constantinescu, F., & Dinu, S. (2010). Responsive polymers for crop protection. *Polymers*, 2(3), 229-251.

Pietta, P. G. (2000). Flavonoids as antioxidants. *Journal of Natural Products*, *63*(7), 1035-1042.

Ponarulselvam, S., Panneerselvam, C., Murugan, K., Aarthi, N., Kalimuthu, K., & Thangamani, S. (2012). Synthesis of silver nanoparticles using leaves of *Catharanthus roseus* Linn. G. Don and their antiplasmodial activities. *Asian Pacific Journal of Tropical Biomedicine*, *2*(7), 574-580.

Prabhu, D., Arulvasu, C., Babu, G., Manikandan, R., & Srinivasan, P. (2013). Biologically synthesized green silver nanoparticles from leaf extract of *Vitex negundo* L. induce growth-inhibitory effect on human colon cancer cell line HCT15. *Process Biochemistry*, 48(2), 317-324.

Prasad, A. S. (2016). Iron oxide nanoparticles synthesized by controlled bio-precipitation using leaf extract of garlic vine (*Mansoa alliacea*). *Materials Science in Semiconductor Processing*, 53, 79-83.

Prathibha S., Packiyam E. J. E., Bhat P. R., Jayadev K. & Shetty S. (2015) Green synthesis of silver nanoparticles from fruit extracts of *Terminalia chebula* Retz. and their antibacterial activity. *International Journal of Research in Biosciences*, 4(2), 29-35.

Prathna, T. C., Chandrasekaran, N., Raichur, A. M., & Mukherjee, A. (2011). Kinetic evolution studies of silver nanoparticles in a bio-based green synthesis process. *Colloids and Surfaces A: Physicochemical and Engineering Aspects*, 377(1), 212-216.

Pravallika, P. L., Mohan, G. K. & Venkateswara, (2015) K. R. Green synthesis & characterization of iron oxide magnetic nanoparticles using *Centella asiatica* plant-a theranostic agent. *International Journal of Engineering Research-Online*, 3(1), 52-59.

Priya, M. M., Selvi, B. K., & Paul, J. A. (2011). Green synthesis of silver nanoparticles from the leaf extracts of *Euphorbia hirta* and *Nerium indicum*. *Digest Journal of Nanomaterials & Biostructures*, *6*(2), 869-877.

Pulit, J., Banach, M., Szczygłowska, R., & Bryk, M. (2013). Nanosilver against fungi. Silver nanoparticles as an effective biocidal factor. *Acta Biochimica Polonica*, 60(4), 795-798.

Radhika, S. A., Sakthivel, N., & Sahayaraj, K. (2017) Acceptance of tertiary and non-food plants by eri silkworm, *Samia cynthia ricini* boisduval (lepidoptera: saturniidae). *Munis Entomology & Zoolo*gy 12(1), 127-132.

Rae, A. (2006). Real life applications of nanotechnology in electronics. *OnBoard Technology*, *2006*, 28.

Raghasudha, M. (2016). Green synthesis of silver nano particles and study of catalytic activity. *International Journal of Modern Chemistry and Applied Science*, 3(1), 306-308.

Rai, M. K., Deshmukh, S. D., Ingle, A. P., & Gade, A. K. (2012). Silver nanoparticles: the powerful nanoweapon against multidrug-resistant bacteria. *Journal of Applied Microbiology*, 112(5), 841-852.

Raj, L. A., & Jayalakshmy, E. (2015). Biosynthesis and characterization of zinc oxide nanoparticles using root extract of *Zingiber officinale*. *Oriental Journal of Chemistry*, *31*, 51-56.

Rajesh T.P., Narendhar, C., Sivakumar, P. A., Mohanambal, V. & Dheeran, R. (2014). Green synthesis of silver nanoparticles from leaf extracts of *Asclepias curassavica,* National Conference on Plant Metabolomics (Phytodrugs – 2014), *Journal of Chemical and Pharmaceutical Sciences,* 90-94.

Ramesh, M., Anbuvannan, M., & Viruthagiri, G. (2015). Green synthesis of ZnO nanoparticles using *Solanum nigrum* leaf extract and their antibacterial activity. *Spectrochimica Acta Part A: Molecular and Biomolecular Spectroscopy*, 136, 864-870.

Ramesh, P. S., Kokila, T., & Geetha, D. (2015). Plant mediated green synthesis and antibacterial activity of silver nanoparticles using *Emblica officinalis* fruit extract. *Spectrochimica Acta Part A: Molecular and Biomolecular Spectroscopy*, 142, 339-343.

Rana, N., Chand, S., & Gathania, A. K. (2016). Green synthesis of zinc oxide nano-sized spherical particles using *Terminalia chebula* fruits extract for their photocatalytic applications. *International Nano Letters*, 6(2), 91.

Rao, A., Bankar, A., Kumar, A. R., Gosavi, S., & Zinjarde, S. (2013). Removal of hexavalent chromium ions by *Yarrowia lipolytica* cells modified with phyto-inspired Fe^0/Fe_3O_4 nanoparticles. *Journal of Contaminant Hydrology*, 146, 63-73.

Rao, J. P., & Geckeler, K. E. (2011). Polymer nanoparticles: preparation techniques and size-control parameters. *Progress in Polymer Science*, 36(7), 887-913.

Rao, P. V., Nallappan, D., Madhavi, K., Rahman, S., Jun Wei, L., & Gan, S. H. (2016). Phytochemicals and biogenic metallic nanoparticles as anticancer agents. *Oxidative Medicine and Cellular Longevity*, 2016, 1-15.

Rico, C. M., Majumdar, S., Duarte-Gardea, M., Peralta-Videa, J. R., & Gardea-Torresdey, J. L. (2011). Interaction of nanoparticles with edible plants and their possible implications in the food chain. *Journal of Agricultural and Food Chemistry*, 59(8), 3485-3498.

Rout, A., Jena, P. K., Parida, U. K., & Bindhani, B. K. (2013). Green synthesis of silver nanoparticles using leaves extract of *Centella asiatica* L. For studies against human pathogens. *International Journal of Pharma and Biosciences*, 4(4), 661-74.

Roy, B.; Mukherjee, S.; Mukherjee, N.; Chowdhury, P.; Sinha Babu, S. P. (2014). Design and green synthesis of polymer inspired nanoparticles for the evaluation of their antimicrobial and antifilarial efficiency. *RSC Advances*, 4, 34487−34499

Salam, H. A., Sivaraj, R., & Venckatesh, R. (2014). Green synthesis and characterization of zinc oxide nanoparticles from *Ocimum basilicum* L. var. purpurascens Benth.-Lamiaceae leaf extract. *Materials Letters*, 131, 16-18.

Samat, N. A., & Nor, R. M. (2013). Sol–gel synthesis of zinc oxide nanoparticles using *Citrus aurantifolia* extracts. *Ceramics International*, 39, S545-S548.

Santhoshkumar, J., Kumar, S. V., & Rajeshkumar, S. (2017). Synthesis of zinc oxide nanoparticles using plant leaf extract against urinary tract infection pathogen. *Resource-Efficient Technologies,* 1-7.

Sathishkumar, M., Sneha, K., Kwak, I. S., Mao, J., Tripathy, S. J., & Yun, Y. S. (2009). Phyto-crystallization of palladium through reduction process using *Cinnamom zeylanicum* bark extract. *Journal of Hazardous materials*, *171*(1), 400-404.

Sathishkumar, M., Sneha, K., Won, S. W., Cho, C. W., Kim, S., & Yun, Y. S. (2009). *Cinnamon zeylanicum* bark extract and powder mediated green synthesis of nano-crystalline silver particles and its bactericidal activity. *Colloids and Surfaces B: Biointerfaces*, *73*(2), 332-338.

Sathyavathi, R., Krishna, M. B., Rao, S. V., Saritha, R., & Rao, D. N. (2010). Biosynthesis of silver nanoparticles using *Coriandrum sativum* leaf extract and their application in nonlinear optics. *Advanced science letters*, *3*(2), 138-143.

Satyavani, K., Ramanathan, T., & Gurudeeban, S. (2011). Green synthesis of silver nanoparticles by using stem derived callus extract of bitter apple (*Citrullus colocynthis*). *Digest Journal of Nanomaterials Biostructures*, *6*(3), 1019-1024.

Scarpa, A., & Guerci, A. (1982). Various uses of the castor oil plant (*Ricinus communis* L.) a review. *Journal of ethnopharmacology*, 5(2), 117-137.

Schmidt-Mende, L., & MacManus-Driscoll, J. L. (2007). ZnO–nanostructures, defects, and devices. *Materials Today*, 10(5), 40-48.

Selvakannan, P. R., Mandal, S., Phadtare, S., Gole, A., Pasricha, R., Adyanthaya, S. D., & Sastry, M. (2004). Water-dispersible tryptophan-protected gold nanoparticles prepared by the spontaneous reduction of aqueous chloroaurate ions by the amino acid. *Journal of Colloid and Interface Science*, *269*(1), 97-102.

Selvakannan, P. R., Swami, A., Srisathiyanarayanan, D., Shirude, P. S., Pasricha, R., Mandale, A. B., & Sastry, M. (2004). Synthesis of aqueous Au core− Ag shell nanoparticles using tyrosine as a pH-dependent reducing agent and assembling phase-transferred silver nanoparticles at the air− water interface. *Langmuir*, *20*(18), 7825-7836.

Senthil, M., & Ramesh, C. (2012). Biogenic synthesis of Fe_3O_4 nanoparticles using *Tridax procumbens* leaf extract and its antibacterial activity on *Pseudomonas aeruginosa*. *Digest Journal of Nanomaterials & Biostructures*, 7(4), 1-6.

Senthilkumar, S. R., & Sivakumar, T. (2014). Green tea (*Camellia sinensis*) mediated synthesis of zinc oxide (ZNO) nanoparticles and studies on their antimicrobial activities. *International Journal of Pharmacy and Pharmaceutical Sciences*, 6(6), 461-465.

Serrano, E., Rus, G., & Garcia-Martinez, J. (2009). Nanotechnology for sustainable energy. *Renewable and Sustainable Energy Reviews*, 13(9), 2373-2384.

Shah, M., Fawcett, D., Sharma, S., Tripathy, S. K., & Poinern, G. E. J. (2015). Green synthesis of metallic nanoparticles via biological entities. *Materials*, 8(11), 7278-7308.

Shah, R. K., Boruah, F., & Parween, N. (2015). Synthesis and characterization of ZnO nanoparticles using leaf extract of *Camellia sinesis* and evaluation of their antimicrobial efficacy. *International Journal of Current Microbiology and Applied Sciences*, 4(8), 444-450.

Shahwan, T., Sirriah, S. A., Nairat, M., Boyacı, E., Eroğlu, A. E., Scott, T. B., & Hallam, K. R. (2011). Green synthesis of iron nanoparticles and their application as a Fenton-like catalyst for the degradation of aqueous cationic and anionic dyes. *Chemical Engineering Journal*, 172(1), 258-266.

Shankar, S. S., Ahmad, A., & Sastry, M. (2003). Geranium leaf assisted biosynthesis of silver nanoparticles. *Biotechnology progress*, 19(6), 1627-1631.

Shivaramakrishnan, B., Gurumurthy, B., & Balasubramanian, A. (2017). Potential biomedical applications of metallic nanobiomaterials: a review. *International Journal of Pharmaceutical Sciences and Research*, 8(3), 985-1000.

Shojaee, S., & Mahdavi Shahri, M. (2016). Green synthesis and characterization of iron oxide magnetic nanoparticles using Shanghai White tea (*Camelia sinensis*) aqueous extract. *Journal of Chemical and Pharmaceutical Research*, 8(5), 138-143.

Si, S., & Mandal, T. K. (2007). Tryptophan-Based Peptides to Synthesize Gold and Silver Nanoparticles: A Mechanistic and Kinetic Study. *Chemistry-A European Journal*, *13*(11), 3160-3168.

Singh, A., Mittal, S., Shrivastav, R., Dass, S., & Srivastava, J. N. (2012). Biosynthesis of Silver Nanoparticles using *Ricinus communis* L. leaf extract and its antibacterial activity. *Digest Journal of Nanomaterials and Biostructures*, 7(3), 1157-1163.

Singh, R., Shedbalkar, U. U., Wadhwani, S. A., & Chopade, B. A. (2015). Bacteriagenic silver nanoparticles: synthesis, mechanism, and applications. *Applied Microbiology and biotechnology*, 99(11), 4579

Singh, V., Shrivastava, A., & Wahi, N. (2015). Biosynthesis of silver nanoparticles by plants crude extracts and their characterization using UV, XRD, TEM and EDX. *African Journal of Biotechnology*, 14(33), 2554-2567.

Singha, T. A., Dutta, L. C., & Borgahain, A. (2016). Nutritional status of Muga and Eri silkworm host plants-A review. *International Journal of Scientific Research*, 4(8).

Sirelkhatim, A., Mahmud, S., Seeni, A., Kaus, N. H. M., Ann, L. C., Bakhori, S. K. M., Hasan, H. & Mohamad, D. (2015). Review on zinc oxide nanoparticles: antibacterial activity and toxicity mechanism. *Nano-Micro Letters*, 7(3), 219-242.

Sirisha, S. A. D., & Mary, A. (2016) Green Synthesis of Nanoparticle of zinc and treatment of nanobeads for waste water of alizarin red dye. *International Journal of Environmental Research and Development*, 6(1), 11-16

Soliman, M. I., Saad, A. H. A., Azzam, A. M., & Mostafa, A. B. (2015). Antiparasitic activity of silver and copper oxide nanoparticles against *Entamoeba histolytica* and *Cryptosporidium parvum* cysts. *Journal of the Egyptian Society of Parasitology*, 45(3), 593-602.

Song, J. Y., & Kim, B. S. (2009). Rapid biological synthesis of silver nanoparticles using plant leaf extracts. *Bioprocess and Biosystems Engineering*, *32*(1), 79-84.

Sravanthi, M., Kumar, D. M., Ravichandra, M., Vasu, G. & Hemalatha K.P.J. (2016) Green Synthesis and Characterization of Iron Oxide Nanoparticles using *Wrightia tinctoria* Leaf Extract and their Antibacterial Studies. *International Journal of Current Research and Academic Review*, 4(8), 30-44.

Sridevi A., Sandhya A. & Suvarnalatha D. P. (2015) Characterization and antibacterial studies of leaf assisted silver nanoparticles from *Carica papaya*: a green synthetic approach. *International Journal of Pharmacy and Pharmaceutical Sciences*, 7(5), 143-146.

Srikar, S. K., Giri, D. D., Pal, D. B., Mishra, P. K., & Upadhyay, S. N. (2016). Green synthesis of silver nanoparticles: a review. *Green and Sustainable Chemistry*, 6(1), 34.

Suganya, D., Rajan, M.R., & Ramesh, R. (2016) Green synthesis of iron oxide nanoparticles from leaf extract of *Passiflora foetida* and its antibacterial activity. *International Journal of Current Research*, 8(11), 42081-42085

Suib, S. L. (Ed.). (2013). New and future developments in catalysis: Catalysis for remediation and environmental concerns. Newnes.

Sultana, F., Imran-Ul-Haque, M., Arafat, M., & Sharmin, S. (2013). An Overview of Nanogel Drug Delivery System. *Journal of Applied Pharmaceutical Science*, 3, 95–105.

Surendra, T. V., Roopan, S. M., Al-Dhabi, N. A., Arasu, M. V., Sarkar, G., & Suthindhiran, K. (2016). Vegetable Peel Waste for the Production of ZnO Nanoparticles and its Toxicological Efficiency, Antifungal, Hemolytic, and Antibacterial Activities. *Nanoscale Research Letters*, 11(1), 546.

Suresh, D., Nethravathi, P. C., Rajanaika, H., Nagabhushana, H., & Sharma, S. C. (2015). Green synthesis of multifunctional zinc oxide (ZnO) nanoparticles using *Cassia fistula* plant extract and their photodegradative, antioxidant and antibacterial activities. *Materials Science in Semiconductor Processing*, 31, 446-454.

Suresh, D., Shobharani, R. M., Nethravathi, P. C., Kumar, M. P., Nagabhushana, H., & Sharma, S. C. (2015). *Artocarpus gomezianus* aided green synthesis of ZnO nanoparticles: luminescence, photocatalytic and antioxidant properties. *Spectrochimica Acta Part A: Molecular and Biomolecular Spectroscopy*, 141, 128-134.

Swathy, B. (2014). A review on metallic silver nanoparticles. *IOSR Journal of Pharmacy*, 4, 38-44.

Syafiuddin, A., Hadibarata, T., Salim, M. R., Kueh, A. B. H., & Sari, A. A. (2017). A purely green synthesis of silver nanoparticles using *Carica papaya*, *Manihot esculenta*, and *Morinda citrifolia*: synthesis and antibacterial evaluations. *Bioprocess and Biosystems Engineering*, 1-13.

Talukdar, K., Rajkhowa, R. C., Sarma S, K. J., & Rahman, A. (2015). Quantification and Electrophoretic Profile of Haemolymph Proteins of Muga Silkworm

(*Antheraea Assamensis* Ww) Larvae Reared On Two Major Host Plants (*Litsea Monopetala* and *Persea Bombycina*) For Two Different Crops (Seasons). *Journal of Entomology and Zoology Studies*, 3(4), 473-475

Tamuly, C., Hazarika, M., Bordoloi, M., Bhattacharyya, P. K., & Kar, R. (2014). Biosynthesis of Ag nanoparticles using pedicellamide and its photocatalytic activity: An eco-friendly approach. *Spectrochimica Acta Part A: Molecular and Biomolecular Spectroscopy*, 132, 687-691.

Tan, Y. N., Lee, K. H., & Su, X. (2011). Study of single-stranded DNA binding protein–nucleic acids interactions using unmodified gold nanoparticles and its application for detection of single nucleotide polymorphisms. *Analytical chemistry*, *83*(11), 4251-4257.

Teja, A. S., & Koh, P. Y. (2009). Synthesis, properties, and applications of magnetic iron oxide nanoparticles. *Progress in crystal growth and characterization of materials*, 55(1), 22-45.

Thema, F. T., Manikandan, E., Dhlamini, M. S., & Maaza, M. (2015). Green synthesis of ZnO nanoparticles via *Agathosma betulina* natural extract. *Materials Letters*, 161, 124-127.

Tiruwa, R. (2016). A review on nanoparticles-preparation and evaluation parameters. Indian *Journal of Pharmaceutical and Biological Research*, 4(2), 27.

Tiwari, D. K., Behari, J., & Sen, P. (2008). Application of Nanoparticles in Waste Water Treatment. *World Applied Sciences Journal*, 3 (3), 417-433.

Tiwari, J. N., Tiwari, R. N., & Kim, K. S. (2012). Zero-dimensional, one-dimensional, two-dimensional and three-dimensional nanostructured materials for advanced electrochemical energy devices. *Progress in Materials Science*, 57(4), 724-803.

Tran, Q. H., Nguyen, V. Q. & Le, Anh-Tuan. (2013) Silver nanoparticles: synthesis, properties, toxicology, applications and perspectives. *Advances in Natural Sciences: Nanoscience and Nanotechnology*, 4, 1-20.

Tripathi, R. M., Kumar, N., Shrivastav, A., Singh, P., & Shrivastav, B. R. (2013). Catalytic activity of biogenic silver nanoparticles synthesized by *Ficus panda* leaf extract. *Journal of Molecular Catalysis B: Enzymatic*, 96, 75-80.

Udayasoorian, C., Kumar, R. V., & Jayabalakrishnan, M. (2011). Extracellular synthesis of silver nanoparticles using leaf extract of *Cassia auriculata*. *Digest Journal of Nanomaterials Biostructures*, *6*(1), 279-283.

Vaishnav, J., Subha, V., Kirubanandan, S., Arulmozhi, M., & Renganathan, S. (2017). Green synthesis of zinc oxide nanoparticles by Celosia argentea and its characterization. *Journal of Optoelectronics and Biomedical Materials Vol*, *9*(1), 59-71.

Velayutham, K., Ramanibai, R., & Umadevi, M. (2016). Green synthesis of silver nanoparticles using *Manihot esculenta* leaves against *Aedes aegypti* and *Culex quinquefasciatus*. *The Journal of Basic & Applied Zoology*, 74, 37-40.

Venkateswarlu, P., Ankanna, S., Prasad, T. N. V. K. V., Elumalai, E. K., Nagajyothi, P. C., & Savithramma, N. (2010). Green synthesis of silver nanoparticles using

Shorea tumbuggaia stem bark. *International Journal of Drug Development and Research* 2(4), 720-723.

Venkateswarlu, S., Kumar, B. N., Prasad, C. H., Venkateswarlu, P., & Jyothi, N. V. V. (2014). Bio-inspired green synthesis of Fe_3O_4 spherical magnetic nanoparticles using *Syzygium cumini* seed extract. *Physica B: Condensed Matter*, 449, 67-71.

Vidya, C., Hiremath, S., Chandraprabha, M. N., Antonyraj, M. L., Gopal, I. V., Jain, A., & Bansal, K. (2013). Green synthesis of ZnO nanoparticles by *Calotropis gigantea*. Proceedings of National Conference on „Women in Science & Engineering" (NCWSE 2013), SDMCET Dharwad, *International Journal of Current Engineering and Technology*, 118-120.

Vijayaraghavan, K., & Nalini, S. P. (2010). Biotemplates in the green synthesis of silver nanoparticles. *Biotechnology Journal*, *5*(10), 1098-1110.

Vinardell, M. P., & Mitjans, M. (2015). Antitumor activities of metal oxide nanoparticles. *Nanomaterials*, 5(2), 1004-1021.

Vinmathi, V., & Jacob, S. J. P. (2015). A green and facile approach for the synthesis of silver nanoparticles using aqueous extract of *Ailanthus excelsa*. *Bulletin of Materials Science*, 38(3), 625-628.

Wang, E. C., & Wang, A. Z. (2014). Nanoparticles and their applications in cell and molecular biology. *Integrative Biology*, 6(1), 9-26.

Wang, T., Lin, J., Chen, Z., Megharaj, M., & Naidu, R. (2014). Green synthesized iron nanoparticles by green tea and eucalyptus leaves extracts used for removal of nitrate in aqueous solution. *Journal of Cleaner Production*, *83*, 413-419.

Wang, Z. (2013). Iron complex nanoparticles synthesized by eucalyptus leaves. *ACS Sustainable Chemistry & Engineering*, 1(12), 1551-1554.

Wang, Z. L. (2004). Nanostructures of zinc oxide. *Materials Today*, 7(6), 26-33.

Wang, Z. L. (2004). Zinc oxide nanostructures: growth, properties and applications. *Journal of Physics: Condensed Matter*, 16(25), R829-R858.

Wang, Z. L., & Song, J. (2006). Piezoelectric nanogenerators based on zinc oxide nanowire arrays. *Science*, 312(5771), 242-246.

Wang, Z., Fang, C., & Megharaj, M. (2014). Characterization of iron–polyphenol nanoparticles synthesized by three plant extracts and their fenton oxidation of azo dye. *ACS Sustainable Chemistry & Engineering*, *2*(4), 1022-1025.

Wangoo, N., Bhasin, K. K., Mehta, S. K., & Suri, C. R. (2008). Synthesis and capping of water-dispersed gold nanoparticles by an amino acid: bioconjugation and binding studies. *Journal of Colloid and Interface Science*, *323*(2), 247-254.

Warrier, P. K., & Nambiar, V. P. K. (1993). Indian medicinal plants: a compendium of 500 species (Vol. 5). Orient Blackswan.

Watt, G. (2014). A dictionary of the economic products of India. Cambridge University Press.

Wolfbeis, O. S. (2015). An overview of nanoparticles commonly used in fluorescent bioimaging. *Chemical Society Reviews*, 44(14), 4743-4768.

Xia, Y., Yang, P., Sun, Y., Wu, Y., Mayers, B., Gates, B., Yin, Y., Kim, F. & Yan, H. (2003). One-dimensional nanostructures: synthesis, characterization, and applications. *Advanced Materials*, 15(5), 353-389.

Xiao, Z., Yuan, M., Yang, B., Liu, Z., Huang, J., & Sun, D. (2016). Plant-mediated synthesis of highly active iron nanoparticles for Cr (VI) removal: Investigation of the leading biomolecules. *Chemosphere*, 150, 357-364.

Xu, H., Wang, X., & Zhang, L. (2008). Selective preparation of nanorods and micro-octahedrons of Fe_2O_3 and their catalytic performances for thermal decomposition of ammonium perchlorate. *Powder Technology*, 185(2), 176-180.

Xu, R., Wang, D., Zhang, J., & Li, Y. (2006). Shape-dependent catalytic activity of silver nanoparticles for the oxidation of styrene. *Chemistry–An Asian Journal*, 1(6), 888-893.

Yadav, S., & Khurana, J. M. (2015). *Cinnamomum tamala* leaf extract-mediated green synthesis of Ag nanoparticles and their use in pyranopyrazles synthesis. *Chinese Journal of Catalysis*, 36(7), 1042-1046.

Yahya, N., Daud, H., Tajuddin, N. A., Daud, H. M., Shafie, A., & Puspitasari, P. (2010). Application of ZnO nanoparticles EM wave detector prepared by sol-gel and self-combustion techniques. *Journal of Nano Research*, 11(2010), 25-34.

Yew, Y. P., Shameli, K., Miyake, M., Kuwano, N., Khairudin, N. B. B. A., Mohamad, S. E. B., & Lee, K. X. (2016). Green synthesis of magnetite (Fe_3O_4) nanoparticles using seaweed (*Kappaphycus alvarezii*) extract. *Nanoscale Research Letters*, *11*(1), 1-7.

Zboril, R., Mashlan, M., & Petridis, D. (2002). Iron (III) oxides from thermal processes synthesis, structural and magnetic properties, Mössbauer spectroscopy characterization, and applications. *Chemistry of Materials*, 14(3), 969-982.

Zhang, Y., Ram, M. K., Stefanakos, E. K., & Goswami, D. Y. (2012). Synthesis, characterization, and applications of ZnO nanowires. *Journal of Nanomaterials*, 2012, 1-22.

Zheng, Y., Wang, Z., Peng, F., & Fu, L. (2016). Application of biosynthesized ZnO nanoparticles on an electrochemical H_2O_2 biosensor. *Brazilian Journal of Pharmaceutical Sciences*, 52(4), 781-786.

CHAPTER 2

Green Synthesis of Silver Nanoparticles using *Ricinus communis* var. *carmencita* Leaf Extract and their Applications

CHAPTER 2

Green Synthesis of Silver Nanoparticles using *Ricinus communis* var. *carmencita* Leaf Extract and their Applications

2.1 INTRODUCTION

Silver nanoparticles (AgNPs) are one of the metallic nanoparticles which have unique properties such as optical, electrical, thermal high electrical conductivity and biological properties. Due to these properties AgNPs are used in several applications, such as food industry, household, and healthcare-related products, consumer products, medical device coatings, optical sensors and cosmetics. They are used as antibacterial agents, diagnostics, orthopedics, drug delivery and as anticancer agents. AgNPs possess higher bactericidal activity due to its larger surface area whereas Ag^+ ion as an anti-bacterial agent is delimited by its easy inactivation through complexation and precipitation, (Lee et al., 2014; Salem et al., 2015). AgNPs also inhibit bacterial cell division causing membrane damage and increased cell permeability which finally leads to cell death (Ma et al., 2011). Further bacterial proliferation also decreases when the functional groups present on nanoparticle (NP) surface interact with bacterial membrane proteins, phospholipids, lipoproteins and lipotechoic acids and decline their colonization and surface adherence (Arakha et al., 2015). AgNPs are non-toxic to animal cells, therefore they are regarded as safe and effective bactericidal agent (Abdel-Aziz et al., 2014). Considering their wide applications, synthesis of AgNPs of unique size with a characteristic dispersity and composition is a key area of research (Iravani et al., 2014). Besides other physical

and chemical methods, AgNPs can be synthesized by biological method which is cost effective and ecofriendly process. Plants and microorganisms are explored as biological source for nanoparticle synthesis which is referred as 'green synthesis' of nanoparticles (Banerjee et al., 2014). Microorganisms trap metal ions from environment and convert them to nanoparticles by enzymatic process. Plants contain strong reducing agents such as polyphenols, terpenoids, phenolic acids, alkaloids, sugars and proteins which are the key players for bio reduction of silver ions (Ag^{+}) due to presence of several −OH groups (Rodríguez-León et al., 2013). Recent reports suggest the synthesis of AgNPs using *Averrhoa carambola* fruit extract and *Solidago altissima* leaf extract having antibacterial and photocatalytic properties (Gavade et al., 2015; Kumar et al., 2016). Moreover green synthesis of AgNPs has also been carried out using an endophytic fungi *Penicillium* species of *Glycosmis mauritiana* (Govindappa et al., 2016). The extract from *Padina tetrastromaticai* and carbohydrates secreted from microalgae *Chlorella vulgaris* has also been used to synthesize AgNPs having anticancer activities (Selvi et al., 2016; Ebrahiminezhad et al., 2016).

In this paper we have exploited *Ricinus communis* var. *carmencita* leaf extract as 'green chemical' to synthesize silver nanoparticle (RcAgNP). We further characterized its physical, optical and biological properties along with its antibacterial activity against gram positive and gram negative strains.

2.2 OUTLINE OF THE RESEARCH STUDY

i) Green synthesis of silver nanoparticles using leaf extract of *Ricinus communis* var. *carmencita*.

ii) Characterization of the synthesized silver nanoparticles using various biophysical techniques.

iii) Evaluation of antibacterial activity against gram negative and gram positive strains

2.3 EXPERIMENTAL SECTION

2.3.1 Preparation of leaf extract

Ricinus communis var. *carmencita* leaves were collected from the IIT Guwahati campus, Guwahati, India. Leaves were cleaned, dried in shade and ground to fine powder. Methanolic extract of the leaves was prepared by cold maceration process (Raaman, 2006). The extract was evaporated to dryness under reduced pressure and stored for further characterization.

2.3.2 Estimation of total phenolic content of leaf extract

Total phenolic content of *R. communis* leaf extract was estimated using Folin-Ciocalteu reagent as described by Stankovic (2013). 0.5 ml of leaf extract (1 mg/ml) was mixed with 2.5 ml of 10% Folin-Ciocalteu reagent. Another 2.5 ml of sodium carbonate was added followed by incubation at 45°C for 45 minutes. Then absorbance was measured at 765 nm using Elisa Plate Reader (Tecan i-control, 1.11.1.0). Different concentrations of gallic acid standard (10-100 µg/ml) was

prepared in methanol. The total phenolic content of the extract was determined from the linear equation obtained from gallic acid standard curve (Alhakmani et al., 2014).

2.3.3 Silver nanoparticle using *Ricinus communis* var. *carmencita l*eaf extract

In a 1 ml reaction mixture, 10 µg/ml leaf extract (in methanol) was added to 1 mM silver nitrate solution (in MiliQ) at different ratio starting from 1:1 to 1:3. The solution was mixed by gentle shaking and kept at room temperature for 24 hours. Then absorbance was scanned from 300-800 nm wavelength by UV-Visible spectrophotometer (Tecan i-control, 1.11.1.0)

After 24 hours, the reaction mixture was centrifuged at 13,000 rpm for 10 mins to pellet down the *R. communis* assisted synthesized silver nanoparticles (RcAgNPs). Then the pellet was washed with deionized water to remove leaf extract residues. This step was repeated twice and the pellet was lyophilized to obtain RcAgNPs in powder form to be used for further characterization.

2.3.4 Characterization of RcAgNPs

UV-Visible spectroscopy

In a 1 ml reaction volume, varying ratio (1:1, 1:2 and 1:3) of leaf extract and silver nitrate solution were mixed and kept for 24 hours at room temperature. Absorbance of synthesized silver nanoparticle was measured at UV-Visible spectrum i.e. 300-800 nm wavelength using UV-Visible spectrophotometer (Tecan i-control, 1.11.1.0).

Microscopy studies

The morphology of the RcAgNPs was studied using Field Emission Scanning Electron Microscopy (FESEM) (Make-ZEISS). RcAgNPs were used in powdered form for FESEM studies. Transmission Electron Microscopy (TEM) studies were carried out to analyze the size and crystallinity of the NPs. The RcAgNPs were suspended in deionized water and sonicated. A drop of dispersed RcAgNP was placed on a copper grid and kept at 37°C for drying. TEM (Make: JEOL, Model: JEM-100 CX II) was performed to confirm the size of the NPs.

X-Ray Diffraction (XRD) studies

A thin film of uniformly water suspended RcAgNP was prepared on a glass slide and kept for drying. X-Ray diffraction studies of the RcAgNP thin film was carried out in X-Ray Diffractometer at 2theta/theta scanning mode (operational voltage 50 kV and current 180 mA, CuKα radiation λ=1.540A0 with 20 per minute scanning rate).

Fourier Transform Infrared Spectroscopy (FTIR) analysis

Leaf extract dissolved in methanol was used for FTIR analysis. RcAgNPs were suspended in water and sonicated to get a uniform suspension. FTIR analysis of leaf extract and RcAgNPs was carried out using IRAffinity-1 (Shimadzu) by ATR method in transmittance mode from 600 cm^{-1} to 4000 cm^{-1} with resolution at 4.0 cm^{-1}.

Thermogravimetric (TGA) analysis

The STA7200 Thermal analysis system, Hitachi was used to perform TGA studies. The RcAgNPs in powder form obtained after lyophilization was used for TGA. An alumina crucible tied with another crucible (reference) was cleaned with acetone and

kept next to the other without touching. 8.6 mg of RcAgNP was kept in the crucible and subjected to heat at 10°C/min increasing rate from 40°C to 900°C with constant flow of nitrogen gas at a flow rate 40 ml/min. Nitrogen gas level was checked regularly in between the analysis.

2.3.5 Cell viability assay

Cytotoxicity of RcAgNP was assessed by MTT (3-[4, 5-dimethylthiazole-2-yl]-2, 5-diphenyl tetrazolium bromide) tetrazolium reduction assay in mouse fibroblastic cell line L929 as mentioned in Sett et al. (2016). In a 96 well plate, each well was seeded with 1×10^4 cells in 100µl cell culture medium (DMEM: Dulbecco's Modified Eagle Medium) with 10% fetal bovine serum. A series of RcAgNP dilutions (5-100 µg/ml) was prepared in serum free culture medium from 1 mg/ml stock suspension for the treatment. After 24 hours of seeding each well was treated with 100 µl of UV sterilized uniformly suspended RcAgNP. Negative control did not contain any test material. After 24 and 48 hours of incubation the culture medium was discarded and 100 µl of MTT prepared in serum free culture medium at 0.5 mg/ml concentration was added and kept for 4 hours incubation. Blue formazan crystals formed thereafter was solubilized in 100 µl of DMSO. Ten minutes later absorbance was measured at 570 nm with reference wavelength at 690 nm using Elisa Plate Reader (Tecan i-control, 1.11.1.0). Cell viability assay was expressed with the following equation

$$\text{Viability (\%)} = N_T/N_C \times 100 \quad (1)$$

Where N_T and N_C are absorbance of NP treated and untreated control cells, respectively.

2.3.6 Applications of RcAgNPs

Antibacterial studies

Antibacterial studies were carried out using resazurin with two Gram negative strains (*Enterobacter aerogenes*, *Enterococcus coli*) and three Gram positive strains (*Bacillus subtilis*, *Streptococcus zooepidemicus*, *Staphylococcus aureus*).

Antibacterial assay by resazurin method

The antibacterial activity of RcAgNP were evaluated by resazurin method as described by Sarker et al. (2007) with some modifications. Both gram positive and gram negative strains were tested for antibacterial activity of RcAgNPs. A uniform number of bacterial cells i.e. 5 $\times 10^5$ cfu/ml was maintained in this assay. RcAgNPs were suspended in deionized water at a concentration of 1 mg/ml. The nanoparticle suspension was sonicated to disperse NPs uniformly. Various dilutions of RcAgNPs were prepared from 1 mg/ml stock suspension. Resazurin solution was prepared by dissolving 270 mg resazurin in 40 ml water. Sterile 96 well plate was used for the assay. Each well contained 50 µl of the nanoparticle, 10 µl of resazurin solution, 30 µl of Luria Bertani broth and 10 µl bacterial suspension. Positive control contained kanamycin of same concentrations as that of NPs along with other components. One set without NPs or antibiotic and another set without bacteria were considered as negative controls. The plates were sealed with parafilm and kept at 37°C for 24 hours in static condition.

Growth Curve Analysis of RcAgNP treated E. aerogenes

Growth curve analysis of *Enterobacter aerogenes* treated with different concentrations of RcAgNPs (0, 20, 50, 100 µg/ml) was carried out to understand their growth pattern under RcAgNP treatment. Bacteria was inoculated in Luria Bertani broth and kept overnight at 37°C temperature and shaking at 180 rpm. Then growth medium was inoculated to obtain 5×10^5 cfu/ml of bacterial cells. Uniformly dispersed nanoparticle from 1 mg/ml stock suspension was diluted to obtain desired dilution. Bacterial culture without any treatment was considered as negative control and kept along with the treated ones at 37°C and 180 rpm. Absorbance was measured at 600 nm for 10 hours starting from the 0^{th} hour i.e. just after the nanoparticle addition.

2.4 RESULTS AND DISCUSSIONS

2.4.1 Estimation of total phenolic content of *R. communis* var. *carmencita* leaf extract and RcAgNP synthesis

Total phenolic content of the leaf extract was estimated by Folin Ciocalteu's reagent. The total phenolic content of varying gallic acid concentration was estimated and a standard curve was plotted (**Figure 2.1**). The total phenolic content of the *R. Communis* leaf extract was calculated from the standard curve and found to be 12.42 GAE/mg.

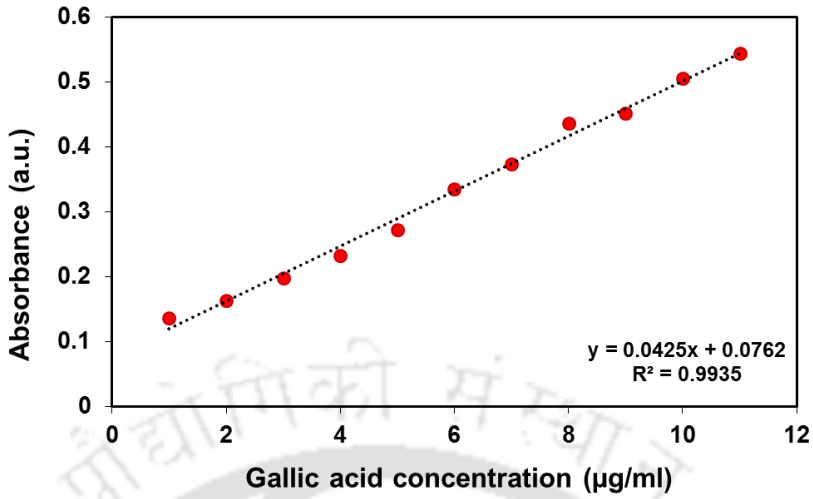

Figure 2.1 Gallic acid standard curve of total phenolic content.

The color change of silver nitrate solution from clear solution to golden yellow color upon addition of *Ricinus communis* var. *carmencita* leaf extract indicates the reducing potency of phytochemicals present in it which is related to the total phenolic content of the leaves.

2.4.2 Characterization of RcAgNPs

UV-Visible spectroscopic analysis

The color of the silver nitrate solution was changed from transparent to golden yellow color when leaf extract was added at an optimal ratio. This color change is due to the excitation of surface plasmonic vibrations of silver NPs (Awwad et al., 2013). Absorbance spectra of all the prepared solutions containing varying ratios of leaf extract (10 µg/ml) and silver nitrate (1 mM) has been depicted in **Figure 2.2**. Absorbance peak at 442 nm wavelength indicated the SPR of the synthesized silver NPs in the solution containing leaf extract and silver nitrate at 1:3 ratio (Ahmed et al., 2016).

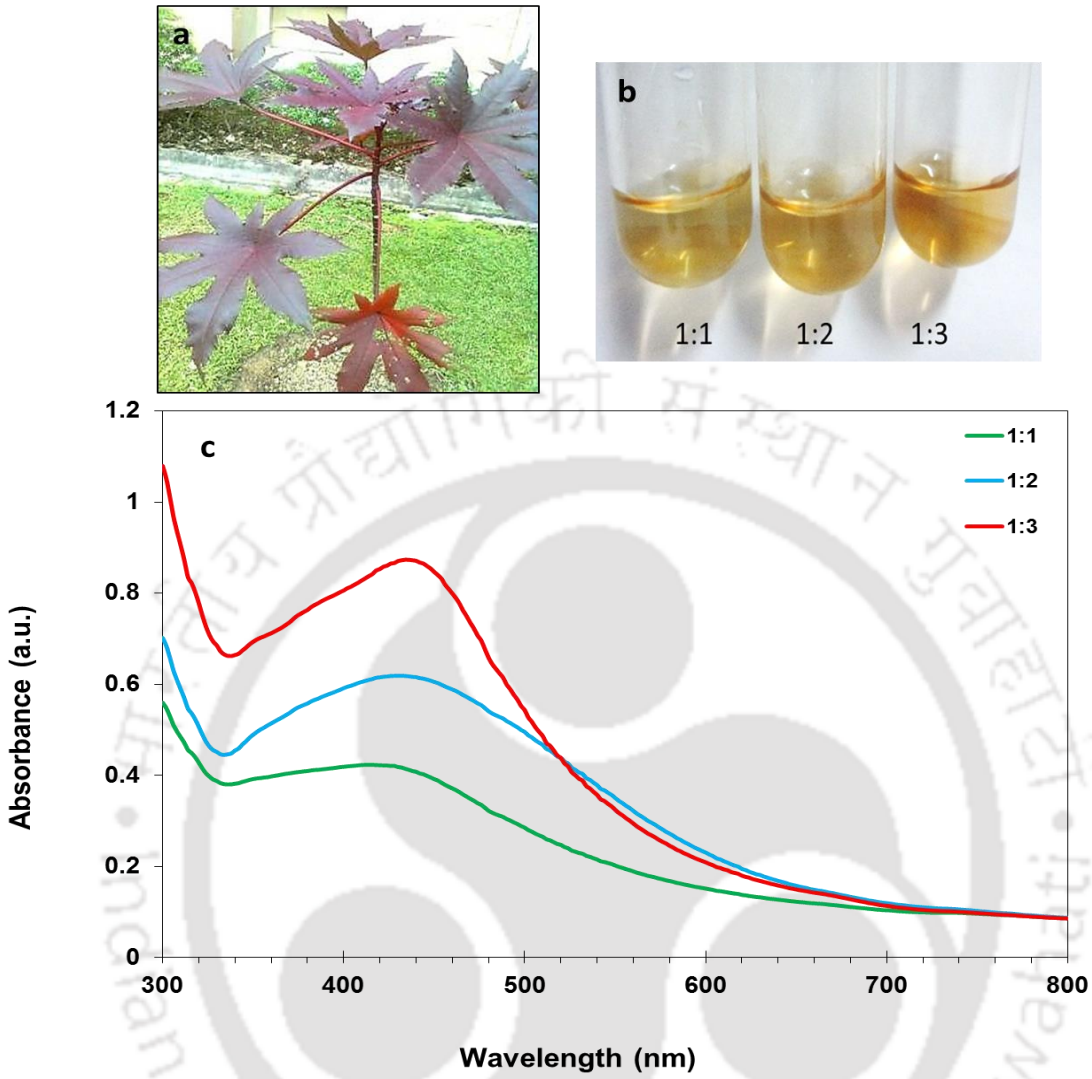

Figure 2.2 Green synthesis of RcAgNPs (a) *Ricinus communis* var. *carmencita* plant, (b) Golden color of silver NPs in solution and (c) UV-Visible absorption spectra of nanoparticle synthesized at different ratios of leaf extract to $AgNO_3$ solution at room temperature.

The absorbance peak reached maximum at the SPR region after 24 h of addition of all the components which articulates maximum reduction of silver ions after 24 h (**Figure 2.3).** UV–Vis absorption spectrum of the reaction mixture was measured for

24 h at 2 h interval. From the absorbance spectra it was observed that the absorbance of NPs intensified with time at 430 nm. Highest absorbance was recorded at 24 h of the synthesis of nanoparticle at room temperature. The peak at 430 nm indicates surface plasmon resonance of silver NPs and hence formation of AgNP (Ahmed et al., 2016). Increased intensity of the peak with time suggests complete reduction of Ag^{+} ions to Ag^{0}. Secondary metabolites present in plant extract varies even when same amount of extract has been used each time for nanoparticle synthesis. This could be the reason for the change in peak position from **figure 2.2**.

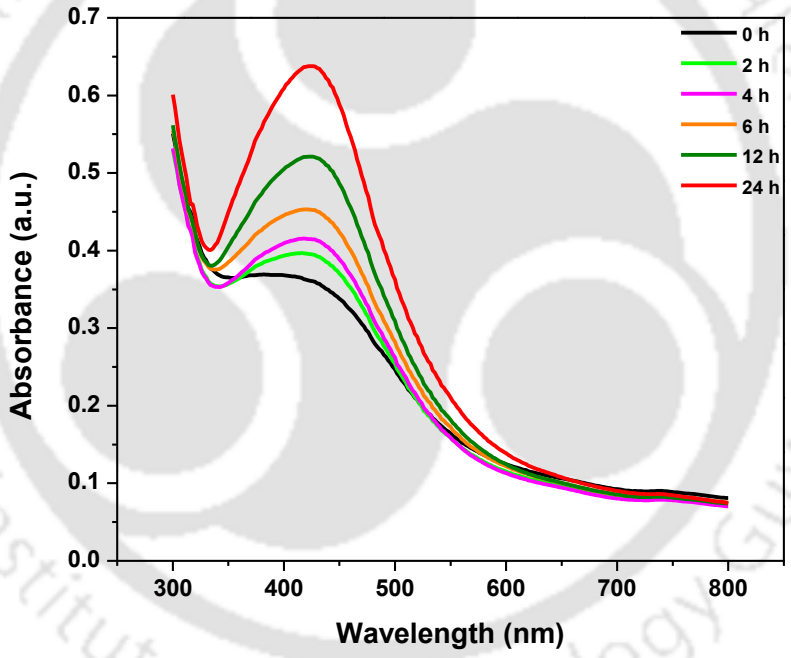

Figure 2.3 UV-Visible absorption spectrum of RcAgNPs synthesized using leaf extract and silver nitrate solution at 1:3 ratio in different time intervals.

Microscopy studies

FESEM and TEM study was performed and the images are shown in **Figure 2.4.** RcAgNPs synthesized were mostly seen in spherical shape (**Figure 2.4a, 2.4b**). The

average size was found to be 30-40 nm when analyzed under Transmission electron microscope (Model: JEM-2100). Lattice fringes with 0.13 nm spacing were observed on the nanoparticle surface in ultra-high resolution TEM (UHRTEM) images (**Figure 2.4c**) which correspond to the (220) crystal planes of silver nanoparticle (Tapia et al., 2016). Selected area electron diffraction pattern image (**Figure 2.4d**) showed concentric rings with bright spots due to Bragg's reflection arising from separate crystals thereby affirming the crystallinity of the RcAgNPs (Sathyaseelan et al., 2013).

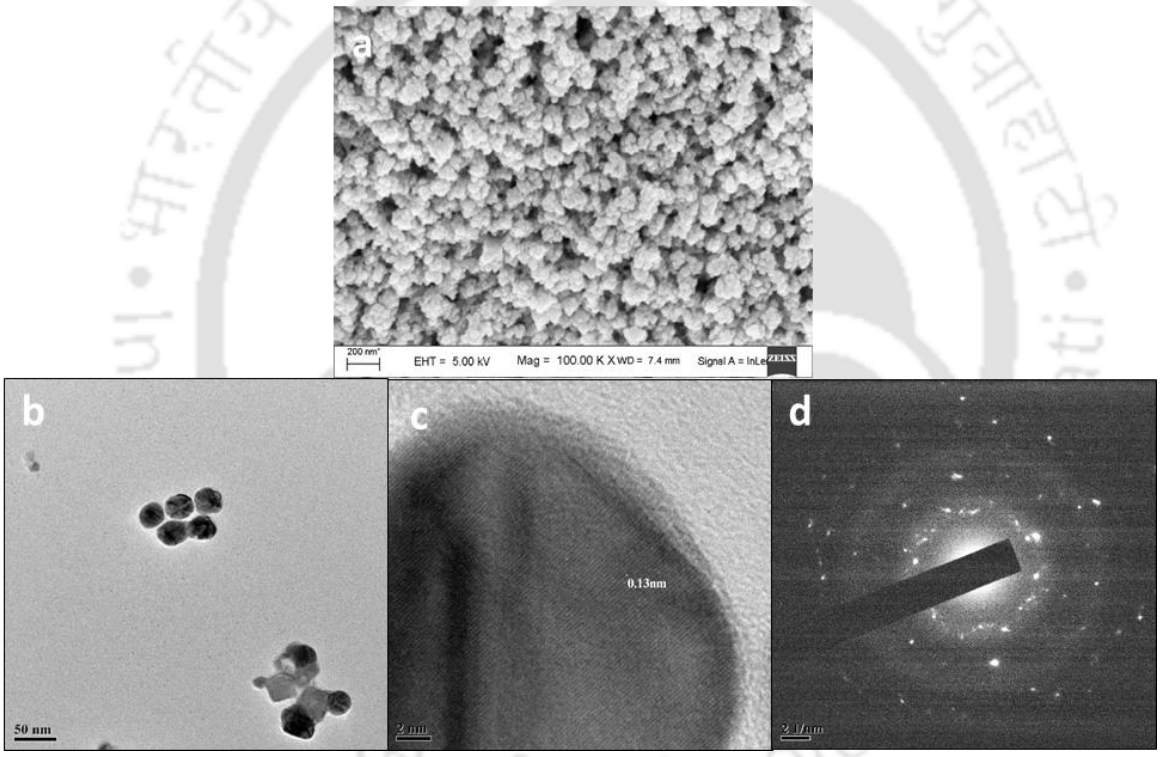

Figure 2.4 Images of RcAgNPs (a) FESEM, (b) TEM, (c) UHRTEM and (d) SAED.

XRD analysis

X-ray diffraction pattern of RcAgNP is presented in **Figure 2.5**. XRD analysis of RcAgNPs showed presence of Bragg's peaks at 2θ values 27.81°, 32.19°, 38.16°, 44.43°, 46.23°, 54.93°, 57.39, 64.65°, 77.61° corresponding to (210), (122), (111),

(200), (231), (142), (241), (220) and (311) planes of silver metals based on face centered cubic structure as described in (Meng, 2015; Khan et al., 2011). Thus the XRD studies confirm the crystallinity of RcAgNPs.

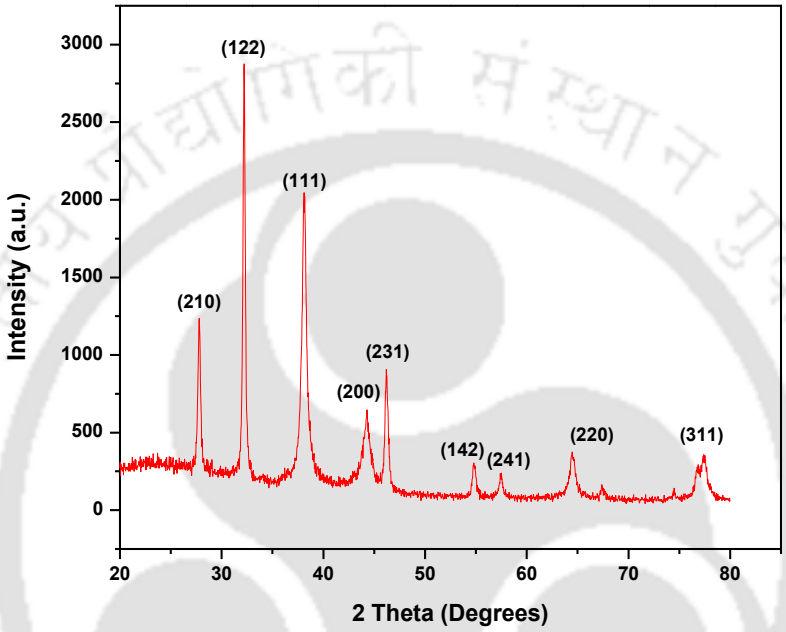

Figure 2.5 XRD image of RcAgNPs.

FTIR analysis

During green synthesis of NPs, the phenolic constituents reduce metal ions to nanoparticle and stabilizes the nanoparticle by capping them. The stability of RcAgNP is characterized by FTIR studies of RcAgNPs and leaf extract to distinguish plant phenolic compound capping on RcAgNPs surface. **Figure 2.6** shows peaks at 3435 cm^{-1} and 3443 cm^{-1} in *R. communis* extract and RcAgNPs, respectively corresponds to O-H group. Peaks at 1634 cm^{-1} and 1631 cm^{-1} *R. communis* extract and RcAgNPs, respectively correspond to amide (N-H) groups. Peaks at 2054 and 2046 cm^{-1}

corresponds to C=O stretch. (http://www2.ups.edu/faculty/hanson/Spectroscopy/IR/IRfrequencies.html, https://webspectra.chem.ucla.edu/irtable.html). The O-H stretch may arise due to the presence moisture on the nanoparticle surface and in the plant extract. Presence of functional groups RcAgNP ensures capping of the nanoparticle with plant extract constituents and thus ensures nanoparticle stability.

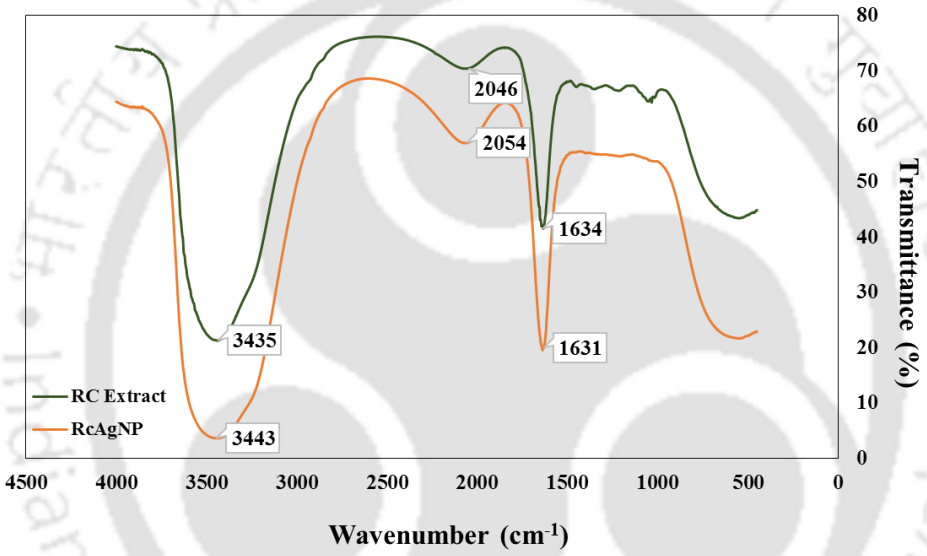

Figure 2.6 FTIR analysis of RcAgNPs and *Ricinus communis* var. *carmencita* leaf extract.

TGA analysis

Thermal analysis was carried out to study thermal characteristics of RcAgNPs. TGA analysis reports change in mass with temperature, which in turn indicates thermal stability, material purity and moisture content of the NPs. From the TGA curve as shown in **Figure 2.7**, it is visible that loss of nanoparticle mass was two stage process.

In the first stage 12% of the initial weight of NPs was lost between 200°C to 440°C and in the second stage, 15% weight was lost between 440°C to 900°C. There was almost no loss of weight till 180°C. The results suggests that the organic compounds or phytochemicals responsible for the reduction of Ag^{+} to Ag^{0} could be thermally unstable which is lost at higher temperature (Sett et al., 2016). Thus it can be inferred that the surface of the NPs contained bio-organic compounds which confirms stability of nanoparticles in solution (Patra et al., 2016).

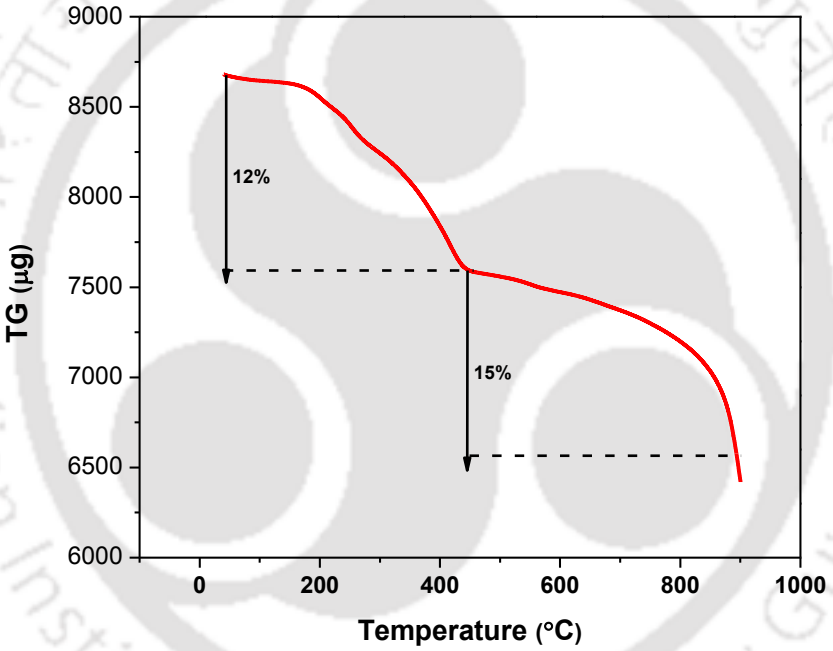

Figure 2.7 TGA analysis of RcAgNPs.

2.4.3 Cell viability assay

MTT is widely used for cytotoxic, cell viability and proliferation studies in cell biology. When dissolved in water MTT gives a yellowish color solution. The MTT is reduced to water insoluble purple colored precipitate called formazan by reducing agents

present in the metabolically active cells (Stockert et al., 2012). When DMSO was added after the nanoparticle treatment the formazan present in viable cell were dissolved. The dead cells could not reduce MTT to formazan due to inactivation of mitochondrial enzymes, therefore no purple color was present in the dead cells. In this colorimetric assay, the intensity of purple color is directly related to the number of viable cells (Riss et al., 2016). In this study after 24 and 48 hours of the RcAgNP treatment at 0-60 µg/ml concentration, 80% and 75% mouse fibroblast cells were alive, respectively **(Figure 2.8)**. This results infers that RcAgNPs were non-toxic to normal cells at lower concentration and hence can be used in biomedical applications.

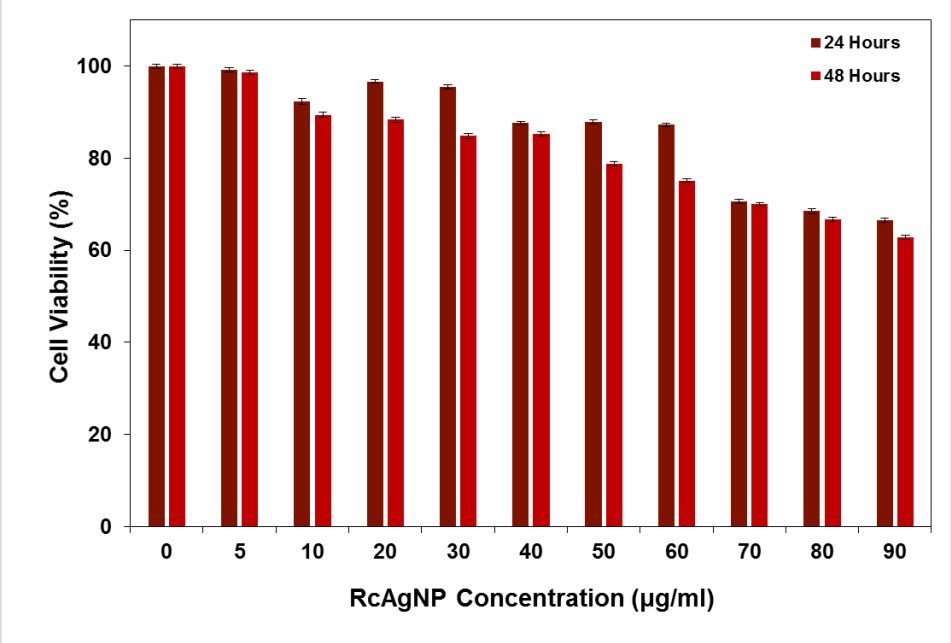

Figure 2.8 Cytotoxicity assay of RcAgNP in L929 cell line at 24 hours and 48 hours.

2.4.4 Applications of RcAgNPs

Antibacterial assay

Antibacterial activity of RcAgNP against gram positive and gram negative bacteria such as *Enterobacter aerogenes*, *Escherichia coli*, *Bacillus subtilis*, *Streptococcus zooepidemicus* and *Staphylococcus aureus* were evaluated using resazurin method. The minimum inhibitory concentration of the RcAgNPs were determined and compared with a positive control, kanamycin. Bacterial growth pattern in presence of RcAgNP was also studied in this context.

Resazurin Method

Resazurin is an indicator dye which is used to determine cell viability. The colour of resazurin indicates bacterial growth. Oxidoreductase enzymes present in viable cells reduce non-fluorescent and non-toxic resazurin dye to resorfurin which is pink in colour. Resorufin on further reduction becomes hydroresorufin which is colourless (Sarker et al., 2007). Therefore blue colour indicates no bacterial growth whereas pink colour denotes presence of viable bacterial cells (**Figure 2.9**). The MICs of RcAgNP and kanamycin for bacterial strains at 5×10^5 cfu/ml were listed in **Table no. 2.1**. Membrane damage and distorted morphology in RcAgNP treated *E. aerogenes* was observed in FESEM images (**Figure 2.9**) whereas the untreated bacterial cells had intact cell membrane.

From the resazurin antibacterial assay, it can be inferred that RcAgNPs possess bactericidal activity against both gram positive and gram negative strains listed above. RcAgNPs has the maximum inhibition against *B. subtilis* and *S. aureus* in

comparison to other strains used in this experiment. RcAgNP inhibited growth of *E. aerogenes* at 100 µg/ml. However RcAgNP inhibited *E. coli* and *S. zooepidemicus* growth at a little higher concentration. Interestingly kanamycin had lesser inhibitory effect on *S. zooepidemicus* at 10 µg/ml which was the MIC value for RcAgNP. A bar graph in Figure 2.10 compares the MIC values of RcAgNPs and kanamycin against the five bacterial strains.

The mechanism of antibacterial activity of silver nanoparticle involves inhibition of bacterial cell division causing membrane damage and increased cell permeability which finally leads to cell death (Ma et al., 2011). The functional groups present on AgNPs surface interact with bacterial membrane proteins, phospholipids, lipoproteins and lipotechoic acids, declining their colonization and surface adherence which results in decreased bacterial proliferation (Arakha et al., 2015). Inhibition of cell wall synthesis in *S. aureus* results in increased permeability and disturbed respiration (Song et al., 2006). In *E.coli* the NPs adhere and penetrate into the cell membrane and induces pits formation in the cell membrane (Sondi and Salopek-Sondi, 2004). The AgNPs once inside the cell interacts with phosphorous and sulphur containing compounds such as DNA and proteins and impairs DNA replication along with other functions. They release Ag^{+} ions which interacts with respiratory chain proteins, transport proteins and membrane protein channels and impair the regular functions of the bacteria. This causes increased cell permeability and massive proton loss through membrane leading to cell death. ROS production induced by AgNPs leads to increased oxidative stress which attacks membrane lipids resulting in bacterial cell death (Pandey et al., 2014).

Growth curve of RcAgNP treated bacteria

Figure 2.11 shows growth curve of *E. aerogenes* treated with RcAgNPs at different concentrations (0, 20, 50, 100 µg/ml) for 10 hours. From the growth curve it was evident that growth of *E. aerogenes* increased with time in case of negative control, however, *E. aerogenes* treated with nanoparticle had inhibited growth as their log phase is delayed as compared to control. The log phase was significantly delayed in case of *E. aerogenes* treated with 50 µg/ml and it is absent at 100 µg/ml. Absorbance at 0^{th} hour of 100 µg/ml treated bacteria was higher due to the absorbance of nanoparticle suspended in the culture. It is also observed that at 50 µg/ml growth of the *E. aerogenes* was inhibited similar to 100 µg/ml but, after 8^{th} hour some of the viable bacteria could resist the nanoparticle treatment and started to grow.

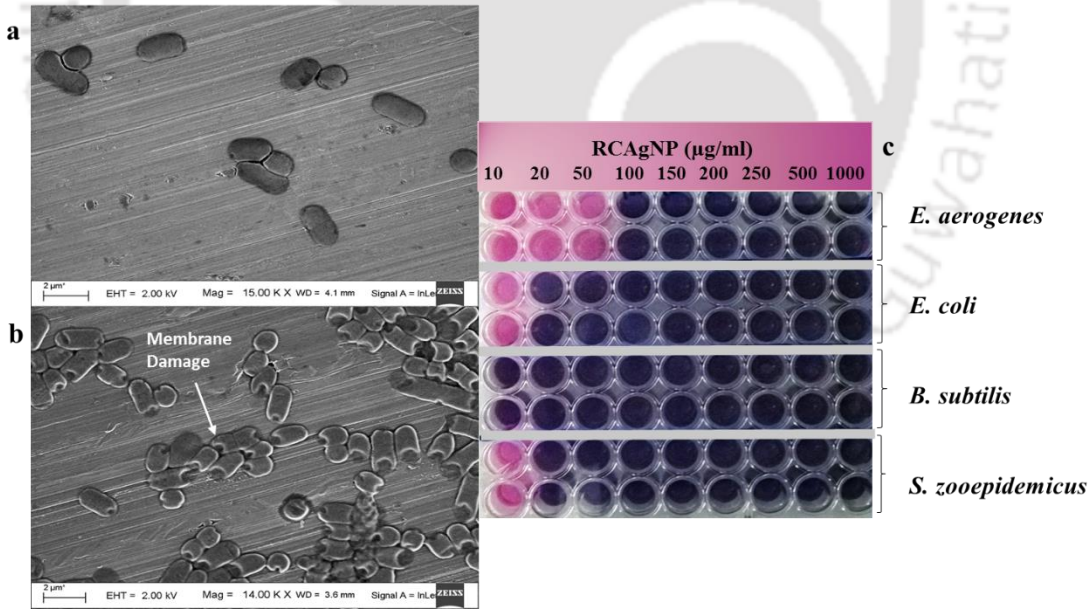

Figure 2.9. Antibacterial activity of RcAgNPs (a) FESEM image of untreated *E. aerogenes*, (b) FESEM image RcAgNP treated *E. aerogenes*, (c) Antibacterial assay by resazurin method.

Table 2.1 List of minimum inhibitory concentrations of RcAgNP and kanamycin against bacterial strains.

Sl. No.	Bacterial Strain (5×10^5 cfu/ml)	MIC of RcAgNP (µg/ml)	MIC of Kanamycin (µg/ml)
1	*Enterobacter aerogenes* (MTCC No. 2824)	100	10
2	*Escherichia coli* (MTCC No. 443)	20	10
3	*Bacillus subtilis* (BS168GW)	10	10
4	*Streptococcus zooepidemicus* (SZ3523)	20	250
5	*Staphylococcus aureus* (NCIM 2901)	10	10

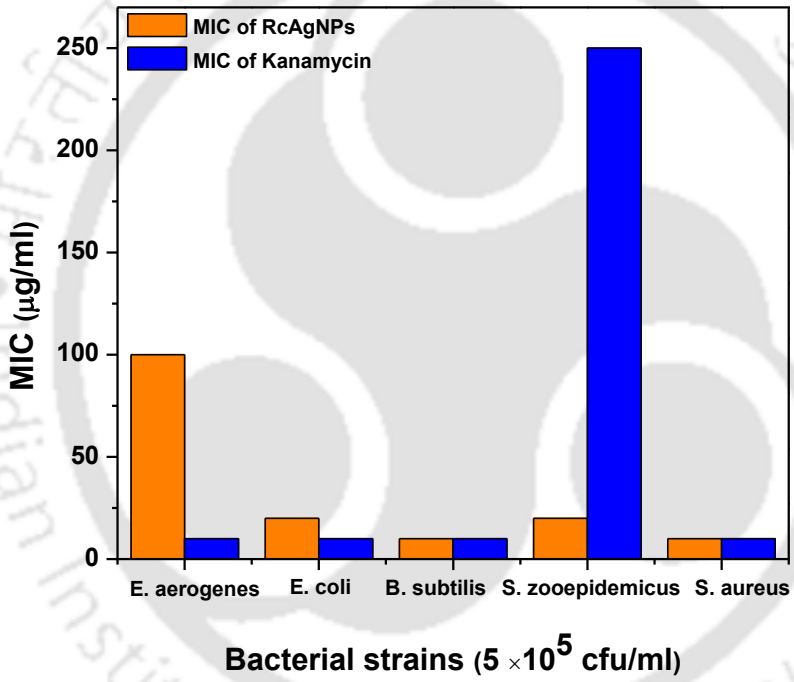

Figure 2.10 Bar graph showing minimum inhibitory concentrations of RcAgNPs and kanamycin against bacterial strains.

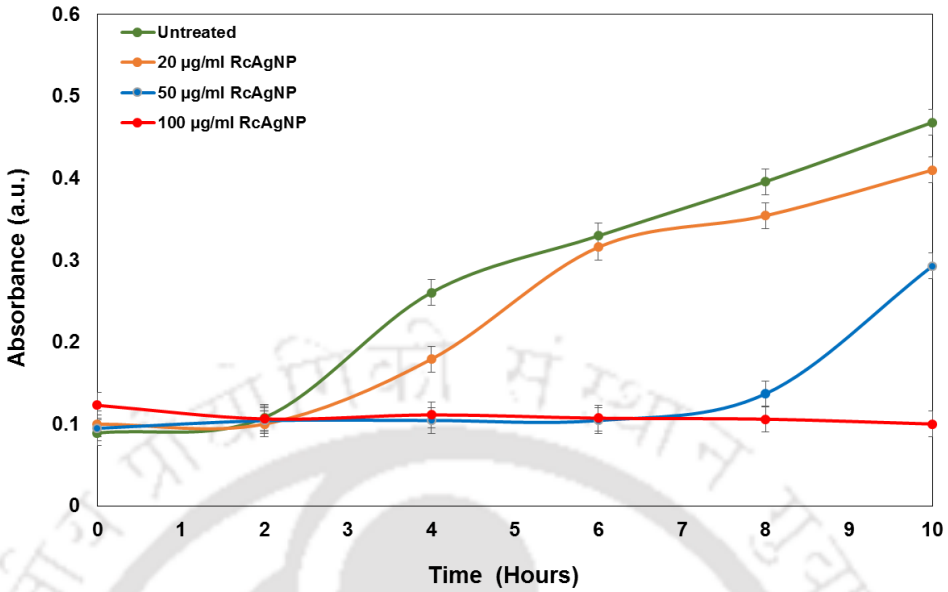

Figure 2.11 Growth curve of *E. aerogenes* treated with RcAgNP at 20, 50 and 100 µg/ml concentrations.

2.5 CONCLUSION

Ricinus communis var *carmencita*, primary host plant of eri silkworm is explored as a sustainable green chemical to synthesize silver nanoparticle. Essentially its phenolic elements are pivotal for silver ion reduction. The silver NPs thus synthesized were characterized by various biophysical techniques. The NPs were mostly round in shape as observed from FESEM and TEM analysis. The nanosize of RcAgNPs were found to be in 30-40 nm range. UHRTEM, SAED and XRD studied confirmed the crystallinity of the NPs. FTIR analysis showed capping of the nanoparticle which ensures stability of the NPs synthesized. Capping and thermal stability of the nanoparticle was ensured by TGA studies. Although the antibacterial activity of silver and silver NPs is well-known but their activity depend on the size of the NPs.

Antibacterial activity of the RcAgNPs was evaluated against gram positive and gram negative bacteria by resazurin reduction assay and the results found to be noteworthy. The toxicity of RcAgNPs were evaluated by MTT assay and was found to be non-toxic to normal mouse fibroblast cell lines at lower concentrations.

Surface modifications and functionalization of RcAgNPs can lower their toxicity so that they can be used in various biomedical applications such as antimicrobial formulations, drug delivery, diagnostics etc.

2.6 REFERENCES

Abdel-Aziz, M. S., Shaheen, M. S., El-Nekeety, A. A., & Abdel-Wahhab, M. A. (2014). Antioxidant and antibacterial activity of silver nanoparticles biosynthesized using *Chenopodium murale* leaf extract. *Journal of Saudi Chemical Society*, 18(4), 356-363.

Ahmed, S., Ahmad, M., Swami, B. L., & Ikram, S. (2016). Green synthesis of silver nanoparticles using *Azadirachta indica* aqueous leaf extract. *Journal of Radiation Research and Applied Sciences*, *9*(1), 1-7.

Alhakmani, F., Khan, S. A., & Ahmad, A. (2014). Determination of total phenol, in-vitro antioxidant and anti-inflammatory activity of seeds and fruits of *Zizyphus spina-christi* grown in Oman. Asian Pacific *Journal of Tropical Biomedicine*, 4, S656-S660.

Arakha, M., Pal, S., Samantarrai, D., Panigrahi, T. K., Mallick, B. C., Pramanik, K., Mallick, B & Jha, S. (2015). Antimicrobial activity of iron oxide nanoparticle upon modulation of nanoparticle-bacteria interface. *Scientific reports*, 5, 1-12.

Awwad, A. M., Salem, N. M., & Abdeen, A. O. (2013). Green synthesis of silver nanoparticles using carob leaf extract and its antibacterial activity. *International Journal of Industrial Chemistry*, 4(1), 1-6.

Banerjee, P., Satapathy, M., Mukhopahayay, A., & Das, P. (2014). Leaf extract mediated green synthesis of silver nanoparticles from widely available Indian plants: synthesis, characterization, antimicrobial property and toxicity analysis. *Bioresources and Bioprocessing*, 1(1), 1-10.

Ebrahiminezhad, A., Bagheri, M., Taghizadeh, S. M., Berenjian, A., & Ghasemi, Y. (2016). Biomimetic synthesis of silver nanoparticles using microalgal secretory carbohydrates as a novel anticancer and antimicrobial. *Advances in Natural Sciences: Nanoscience and Nanotechnology*, 7(1), 1-8.

Gavade, S. M., Nikam, G. H., Dhabbe, R. S., Sabale, S. R., Tamhankar, B. V., & Mulik, G. N. (2015). Green synthesis of silver nanoparticles by using carambola fruit extract and their antibacterial activity. *Advances in Natural Sciences: Nanoscience and Nanotechnology*, 6(4), 1-6.

Govindappa, M., Farheen, H., Chandrappa, C. P., Rai, R. V., & Raghavendra, V. B. (2016). Mycosynthesis of silver nanoparticles using extract of endophytic fungi, Penicillium species of *Glycosmis mauritiana*, and its antioxidant, antimicrobial, anti-inflammatory and tyrokinase inhibitory activity. *Advances in Natural Sciences*: *Nanoscience and Nanotechnology*, 7(3), 1-9.

Iravani, S., Korbekandi, H., Mirmohammadi, S. V., & Zolfaghari, B. (2014). Synthesis of silver nanoparticles: chemical, physical and biological methods. *Research in Pharmaceutical Sciences*, 9(6), 385-406.

Khan, M. A. M., Kumar, S., Ahamed, M., Alrokayan, S. A., & AlSalhi, M. S. (2011). Structural and thermal studies of silver nanoparticles and electrical transport study of their thin films. *Nanoscale Research Letters*, 6(1), 1-8.

Kumar, V. A., Uchida, T., Mizuki, T., Nakajima, Y., Katsube, Y., Hanajiri, T., & Maekawa, T. (2016). Synthesis of nanoparticles composed of silver and silver chloride for a plasmonic photocatalyst using an extract from a weed *Solidago*

altissima (goldenrod). *Advances in Natural Sciences: Nanoscience and Nanotechnology*, 7(1), 1-12.

Lee, W., Kim, K. J., & Lee, D. G. (2014). A novel mechanism for the antibacterial effect of silver nanoparticles on *Escherichia coli*. *Biometals*, 27(6), 1191-1201.

Ma, J., Zhang, J., Xiong, Z., Yong, Y. & Zhao, X.S. (2011) . Preparation , characterization and antibacterial properties of silver-modified graphene oxide, *Journal of Material Chemistry,* 10, 3350-3352.

Meng, Y. (2015). A sustainable approach to fabricating Ag nanoparticles/PVA hybrid nanofiber and its catalytic activity. *Nanomaterials*, 5(2), 1124-1135.

Pandey, J. K., Swarnkar, R. K., Soumya, K. K., Dwivedi, P., Singh, M. K., Sundaram, S., & Gopal, R. (2014). Silver nanoparticles synthesized by pulsed laser ablation: as a potent antibacterial agent for human enteropathogenic gram-positive and gram-negative bacterial strains. *Applied Biochemistry and Biotechnology*, *174*(3), 1021-1031.

Patra, J. K., & Baek, K. H. (2016). Green synthesis of silver chloride nanoparticles using Prunus persica L. outer peel extract and investigation of antibacterial, anticandidal, antioxidant potential. *Green Chemistry Letters and Reviews*, 9(2), 132-142.

Raaman, N. (2006). Phytochemical techniques. New India Publishing.

Riss, T. L., Moravec, R. A., Niles, A. L., Duellman, S., Benink, H. A., Worzella, T. J., & Minor, L. (2016). Cell viability assays.

Rodríguez-León, E., Iñiguez-Palomares, R., Navarro, R. E., Herrera-Urbina, R., Tánori, J., Iñiguez-Palomares, C., & Maldonado, A. (2013). Synthesis of silver nanoparticles using reducing agents obtained from natural sources *(Rumex hymenosepalus* extracts). *Nanoscale research letters*, 8(1), 1-9.

Salem, W., Leitner, D. R., Zingl, F. G., Schratter, G., Prassl, R., Goessler, W., Reidl, J. & Schild, S. (2015). Antibacterial activity of silver and zinc nanoparticles against *Vibrio cholerae* and enterotoxic *Escherichia coli*. *International Journal of Medical Microbiology*, 305(1), 85-95.

Sarker, S. D., Nahar, L., & Kumarasamy, Y. (2007). Microtitre plate-based antibacterial assay incorporating resazurin as an indicator of cell growth, and its application in the in vitro antibacterial screening of phytochemicals. *Methods*, 42(4), 321-324.

Sathyaseelan, B., Baskaran, I., & Sivakumar, K. (2013). Phase transition behavior of nanocrystalline Al_2O_3 powders. *Soft Nanoscience Letters*, 3(4), 69-74.

Selvi, B. C. G., Madhavan, J., & Santhanam, A. (2016). Cytotoxic effect of silver nanoparticles synthesized from Padina tetrastromatica on breast cancer cell line. *Advances in Natural Sciences: Nanoscience and Nanotechnology*, 7(3), 1-8.

Sett, A., Gadewar, M., Sharma, P., Deka, M., & Bora, U. (2016). Green synthesis of gold nanoparticles using aqueous extract of *Dillenia indica*. *Advances in Natural Sciences: Nanoscience and Nanotechnology*, 7(2), 1-8.

Sondi, I., & Salopek-Sondi, B. (2004). Silver nanoparticles as antimicrobial agent: a case study on *E. coli* as a model for Gram-negative bacteria. *Journal of colloid and Interface Science*, *275*(1), 177-182.

Song, H. Y., Ko, K. K., Oh, I. H., & Lee, B. T. (2006). Fabrication of silver nanoparticles and their antimicrobial mechanisms. *European Cells and Materials*, *11*(Suppl 1), 58.

Stankovic, M. S. (2011). Total phenolic content, flavonoid concentration and antioxidant activity of *Marrubium peregrinum* L. extracts. *Kragujevac Journal of Science*, 33(2011), 63-72.

Stockert, J. C., Blázquez-Castro, A., Cañete, M., Horobin, R. W., & Villanueva, Á. (2012). MTT assay for cell viability: Intracellular localization of the formazan product is in lipid droplets. *Acta Histochemica*, 114(8), 785-796.

Tapia, V. R., Tizapa, M. S., Mora, E. R., Martínez, M. L. O., Franco, A., & Calva, E. B. (2016). Solvent-Induced Morphological Changes of Polyhedral Silver Nanoparticles in Epoxy Resin. *Plasmonics*, 11(6), 1417-1426.

URL: https://webspectra.chem.ucla.edu/irtable.html

URL:http://www2.ups.edu/faculty/hanson/Spectroscopy/IR/IRfrequencies.html,

CHAPTER 3

Green Synthesis of Zinc Oxide Nanoparticles using *Heteropanax fragrans* Leaf Extract and their Applications

CHAPTER 3

Green Synthesis of Zinc Oxide Nanoparticles using *Heteropanax fragrans* Leaf Extract and their Applications

3.1 INTRODUCTION

Nanoparticles (NPs) have unique physical and chemical properties than their counter bulk material due to a larger surface area to volume ratio and wider band gap (Sangeetha et al., 2011; Deng et al., 2008; Yang & Park, 2007). NPs of metal oxides are of great importance which is evident from their applications in various fields such as catalysis, molecular sensing, environmental remediation, medicine, biology, cosmetics, electronics, sporting, equipment, magnetic storage media and solar energy transformation industries. (Jeevanandam et al., 2016; Koupaei et al., 2016). Zinc oxide (ZnO) NP is a semiconductor having a wide band gap (3.37eV) and large exciton-binding energy (60meV) (Sangeetha et al., 2011). Due to their unique optical and electronic properties, ZnO NPs have diverse applications including solar cells, UV light-emitting devices, gas sensors, photo-catalysts, pharmaceutical and cosmetic industries (Sangeetha et al., 2011). ZnO NPs are also used in sunscreens and cosmetics as they can efficiently absorb UV-A and UV-B light without scattering visible light (Ramesh et al., 2015). ZnO NPs are low cost, ecofriendly, non-toxic, self-cleansing, antimicrobial, and offer easy fabrication. Further, US Food and Drug Administration has listed ZnO as generally recognized as safe materials (GRAS) (Jamdagni et al., 2016). They are one of the semiconductors used in photocatalysis for the removal of dyes from waste water. However, ZnO has structure dependent

properties which can vary with respect to size, shape, morphology, orientation and aspect ratio of the NP.

Methylene blue, one of the important members of the thiazine dyes is widely used in industries such as textiles, paper, plastics, leather, food, and cosmetic to color products. Methylene blue (MB), present in these industry effluents, possesses risk of bioaccumulation and eco-toxicity (Ayad and El-Nasr, 2010). Therefore, their removal from waste water is essential. Various techniques are used for dye removal such as reverse osmosis, ion exchange, precipitation, adsorption, ultrasonic decomposition, advanced chemical oxidation, and nanofiltration (Sivasubramanian et al., 2016). Nano-catalysts such as photocatalyst, electrocatalyst, Fenton based catalyst, and chemical oxidant have shown the potential for removing both organic and inorganic contaminants (Anjum et al., 2016). Therefore ZnO NP is evaluated for its photocatalytic activity in this study.

ZnO NP synthesis methods include physical, chemical and biological methods. Physical methods include high energy ball milling, melt mixing, physical vapor deposition, laser ablation, sputtering deposition, electric arc deposition, and ion implantation processes. Chemical methods include processes such as liquid phase synthesis (precipitation, co-precipitation method, colloidal methods, sol-gel processing, water–oil micro-emulsions method, hydrothermal synthesis, solvothermal, and sonochemical, and polyol method), and gas phase synthesis (pyrolysis and inert gas condensation) (Naveed Ul Haq et al., 2017). Biological methods of ZnO NP synthesis involve the use of plants, or plant extracts, microorganisms, enzymes, and waste materials, etc. and hence is an ecofriendly and

cost effective (Ramesh et al., 2015; Agarwal et al., 2017). Generally, plants and plant extracts are used for NP synthesis as they are easily available and low cost. Plants can uptake metal ions from soil and water and convert them to NP. This in vivo method of bio-reduction is explored for phytoremediation or phytomining. In vitro, plant extracts prepared from different plant parts such as leaves, stem bark, roots, flower, fruits and seeds are also used to synthesize NP (Naveed Ul Haq et al., 2017). Phenolic compounds, tannins, flavonoids, terpenoids, starch etc. present in the plant extract act as reducing and capping agent which converts metal ions to NPs and stabilizes them (Naveed Ul Haq et al., 2017). ZnO NP were synthesized using leaf extract *Calotropis procera.* Several reports of ZnO NP synthesis using plant extract have been reviewed in Chapter 1.

In this study, we have used *Heteropanax fragrans* leaves, also known as Kesseru for the synthesis of ZnO NP. *H. fragrans* leaves are used to feed eri silkworms when there is a scarcity of castor leaves (URL: http://www.cmerti.res.in/faq.html; Chutia et al. 2014). The *H. fragrans* plant is perennial in nature, small, soft wooded ever green tree. This plant has medicinal value and it is reported that the Chakma community of Bangladesh uses this plant to treat cancer. Its root and bark are also used for detoxification, blood activation, detumescence and pain easing (Changmai et al., 2015).

The ZnO NP synthesized using an aqueous extract of *H. fragrans* leaves were characterized with biophysical techniques. Their application in photocatalytic degradation of methylene blue in aqueous solution was also studied.

3.2 OUTLINE OF THE RESEARCH STUDY

i) Green synthesis zinc oxide nanoparticles (ZnO) using *H. fragrans* (Kesseru) leaf extract.

ii) Characterization of the green synthesized ZnO NP (KeZnONPs).

iii) Degradation of methylene blue using KeZnONPs under UV light illumination.

3.3 EXPERIMENTAL SECTION

3.3.1 Preparation of *H. fragrans* leaf extract

Fresh leaves were collected from Boko, Assam, India. The leaves were washed to remove dust particles and dried under shade. Then the dried leaves were ground to powder in a mixer grinder. Aqueous extract of the leaf powder was prepared by adding 100 ml of distilled water to 5 g of *H. fragrans* leaf powder and boiled at 100°C for 20 minutes. The extract was filtered through Whatman filter paper. The extract was collected and stored at 4°C for ZnO NP synthesis.

3.3.2 Total phenolic content analysis

The aqueous extract of *H. fragrans* leaves was dried and total phenolic content was estimated using Folin-Ciocalteu reagent (Stankovic, 2011). 0.5 ml of leaf extract (1 mg/ml) was mixed with 2.5 ml of 10% Folin-Ciocalteu reagent. Further to it, 2.5 ml of $NaHCO_3$ was added followed by incubation at 45°C for 45 minutes. Absorbance was then measured at 765 nm using UV-Visible spectrophotometer (Tecan i-control, 1.11.1.0). Gallic acid was used as standard in this assay. Different concentrations of gallic acid (10-100 µg/ml) were prepared in methanol. Total phenolic content was

estimated for each gallic acid dilutions and a standard curve was plotted. The total phenolic content of the *H. fragrans* leaf extract was determined from the linear equation obtained from gallic acid standard curve (Alhakmani et al., 2014).

3.3.3 Zinc Oxide nanoparticle synthesis

Zinc oxide nanoparticle was synthesized using *H. fragrans* leaf extract and zinc nitrate as described in Devi and Gayathri, (2014). The leaf extract was heated to 60-80°C in a stirrer-heater and 1.25 g of zinc nitrate hexahydrate was added to it when the temperature reached 60°C. The solution was boiled at stirring condition till all the solvent was evaporated. A yellow color paste was obtained which was collected and kept in a silica crucible. The paste was calcined at 400°C for 2 hours in a furnace. After calcination white colored powder (KeZnONP) was obtained which was kept for further characterization.

3.3.4 Characterization of KeZnONP

UV-Visible spectroscopy

KeZnONP obtained after calcination was ground to powder using a mortar and pestle. The nanoparticles were dispersed in distilled water using sonicator and then absorbance was measured at 300-800 nm wavelength using UV-Visible spectrophotometer (Tecan i-control, 1.11.1.0). Band gap energy of KeZnONP can be calculated from the absorption peak in UV-Visible spectroscopy using the following relation (Anbuvannan et al., 2015**;** Balcha et al., 2016).

$$E_g = \frac{hc}{\lambda} eV \quad (1)$$

$$Eg = \frac{1240}{\lambda} \quad (2)$$

Where E_g is the band gap energy (eV), *h* is the Planck's constant (6.626 × 10^{-34} Js), *c* is the light velocity (3 × 10^8 m/s) and λ is the wavelength (nm).

Microscopy studies

The morphology of the zinc oxide nanoparticle was studied using FESEM (Make-ZEISS). TEM studies were carried out to analyze the size and crystallinity of the nanoparticle. A drop of water dispersed zinc oxide nanoparticle was put onto a copper grid and dried. Then the NP were analyzed using TEM (Model: JEM-2100) at SAIF, NEHU.

X-Ray Diffraction (XRD) analysis

XRD analysis of KeZnONP was carried out to evaluate the crystallinity and phase purity of the nanoparticle. KeZnONP powder was kept in a glass slide and X-ray Diffraction analysis was performed at 2theta/ theta scanning mode, 50 kV operational voltage, 180 mA current and CuKα radiation λ=1.540 Å.

Fourier Transform Infrared Spectroscopy (FTIR) analysis

Green synthesis causes capping of nanoparticles with phytoconstituents which was confirmed by FTIR analysis that identified the functional groups present on the nanoparticle surface. *H. fragrans* leaf extract and KeZnONP was analyzed in FTIR (Make Perkin Elmer) in transmittance mode from 450 cm^{-1} to 4000 cm^{-1}.

Thermogravimetric (TGA) analysis

The thermal stability of the synthesized KeZnONP was studied by TGA analysis of using NETZSCH STA 449F3, Thermal analysis system (make Hitachi). The alumina crucible is cleaned with acetone and kept next to the reference crucible without touching each other. 5.79 mg of the KeZnONP powder was placed in the alumina crucible and heated at a temperature ranging from 25°C to 1000°C with 10°C per minute increase rate.

3.3.5 Application of KeZnONP

3.3.5.1 Photocatalytic activity of KeZnONP

The photocatalytic activity of KeZnONP was demonstrated by degradation of water soluble dye methylene blue (MB). In this process degradation of 5 mg/L of MB in distilled water using 0.5 mg/ml and 1 mg/ml KeZnONP was studied separately. 5 mg/L of methylene blue without nanoparticle was kept as control. The solutions were stirred in dark for 15 minutes for the equilibrium of the system. All the samples along with control were irradiated with UV light. Aliquot of sample was withdrawn from each reaction after 20-minute interval and centrifuged to remove nanoparticle residues. The degradation of MB was assessed by measuring the absorbance of the supernatant at 500-750 nm wavelength range using UV-Visible spectrophotometer.

Effect of pH on the MB degradation by KeZnONP was also evaluated. KeZnONP powder was added at 1 mg/ml concentration to 5 mg/L of MB solution and pH was adjusted. In this experiment effect of four pH conditions i.e. 3, 5, 7 and 9 were studied.

The solutions were kept in dark for 15 minutes and then irradiated with UV light. Absorbance was measured at 500-750 nm using UV-Visible spectrophotometer.

According to Beer Lambert's law absorbance is directly proportional to the concentration. Therefore, the degradation efficiency can be calculated following the formula (Chen et al., 2011):

$$Degradation\ Efficiency\ (\%) = \frac{(C_i - C_f)}{C_i} \times 100 \quad (3)$$

Where C_i is the initial MB concentration and C_f is the MB concentration during irradiation. The photocatalytic reaction rate depends on the concentration of MB and can be described by the following expression (Soltani et al., 2012):

$$Rate = -\frac{dC}{dt} = \frac{kKC}{1 + KC} \quad (4)$$

Where C is the concentration of MB (mg/L) at any time, t is the irradiation time, k is the first-order rate constant of the reaction and K is the adsorption constant of the dye on the photocatalyst. This equation can be simplified to a pseudo first order equation (Soltani et al., 2012):

$$Ln\left(\frac{C}{C_0}\right) = -kKt = k_{obs}t \quad (5)$$

3.4 RESULTS AND DISCUSSIONS

3.4.1 Estimation of total phenolic content and Zinc oxide nanoparticle synthesis

The image of *H. fragrans* leaves is presented in **Figure 3.2a.** The total phenolic of *H. fragrans* leaf extract is calculated from the standard curve (**Figure 3.1**) and found to

be 4.5 GAE/mg. The phenolic compounds are the reducing agents responsible for nanoparticle synthesis. During synthesis process, after the addition of zinc nitrate hexahydrate precipitations were visible. A yellow colored paste was obtained after the evaporation of solvent. When the paste was calcinated a white colored powder (**Figure 3.2b**) was obtained which was further characterized to confirm the synthesis of zinc oxide nanoparticles. The synthesized nanoparticles is mentioned as KeZnONP in this thesis.

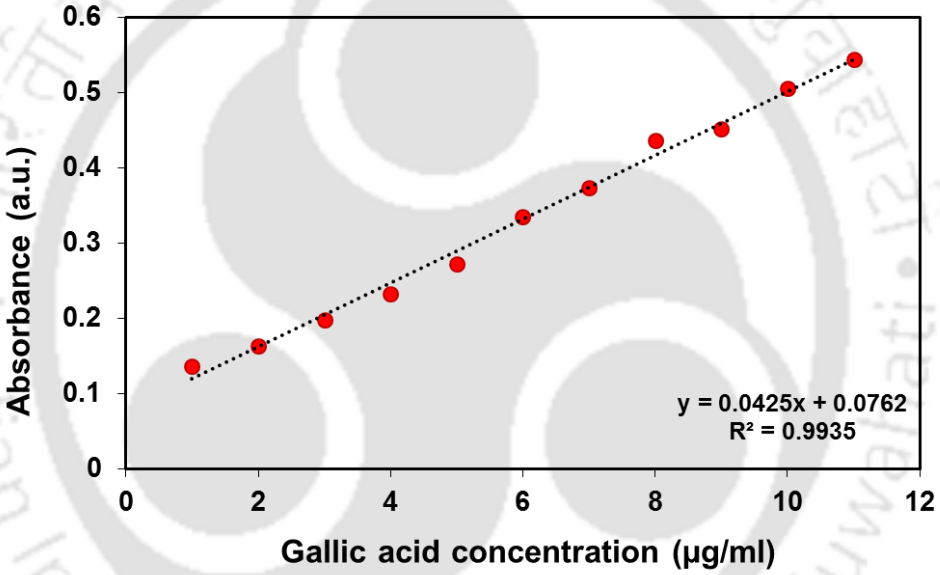

Figure 3.1 Gallic acid standard curve of total phenolic content.

3.4.2 Characterization of KeZnONP

UV-Visible spectroscopy

UV-Visible spectrum of KeZnONP is presented in **Figure 3.2c**. An absorbance peak at 382 nm was obtained in the UV-visible spectrum which corresponds to the band gap energy (E_g) of value 3.24 eV, calculated using equation 1. The result is in agreement to that of reported in the literature (Sáenz-Trevizo et al., 2016).

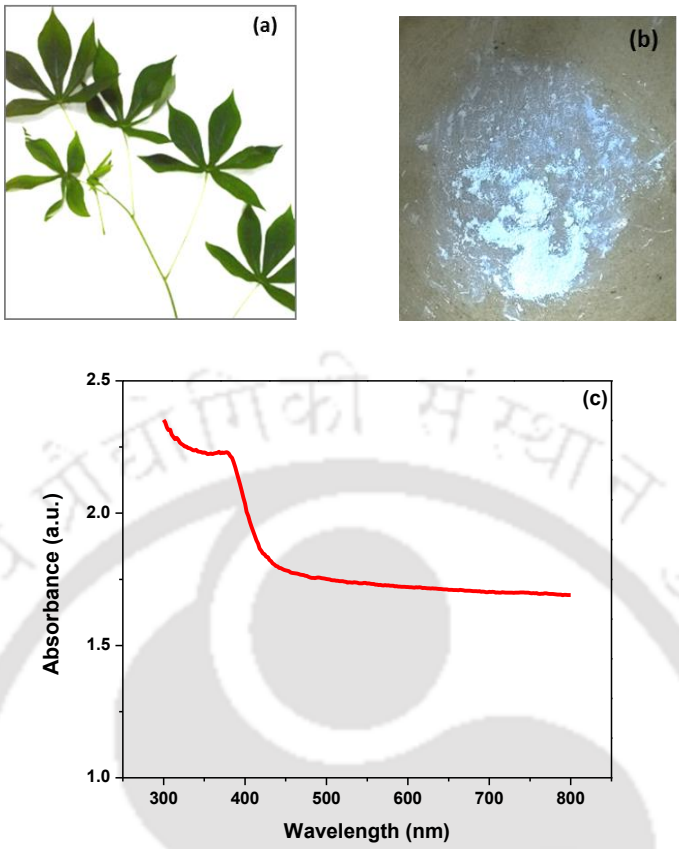

Figure 3.2 Green synthesis of KeZnONP using (a) *H. fragrans* leaves, (b) KeZnONP powder and (c) UV-Visible spectrum of KeZnONP showing peak at 382 nm.

Microscopy studies

Microscopy analysis was carried out to study the shape, size and crystallinity of the KeZnONPs. **Figure 3.3a** represents FESEM image of KeZnONP which shows that the NPs are mostly spherical. **Figure 3.3b** represents the TEM image of KeZnONP and the size of nanoparticles is calculated using Image J software which is found to be 19-22 nm. The UHRTEM image of KeZnONP is presented in **Figure 3.3c** shows clear lattice fringes on the NP with 0.28 nm interplane distance, corresponding to the (100) plane of wurtzite structure of ZnO nanoparticles (Darabdhara et al., 2016).

Figure 3.3d represents SAED pattern of KeZnONP showing concentric rings with bright spots which infers the crystallinity of the nanoparticle.

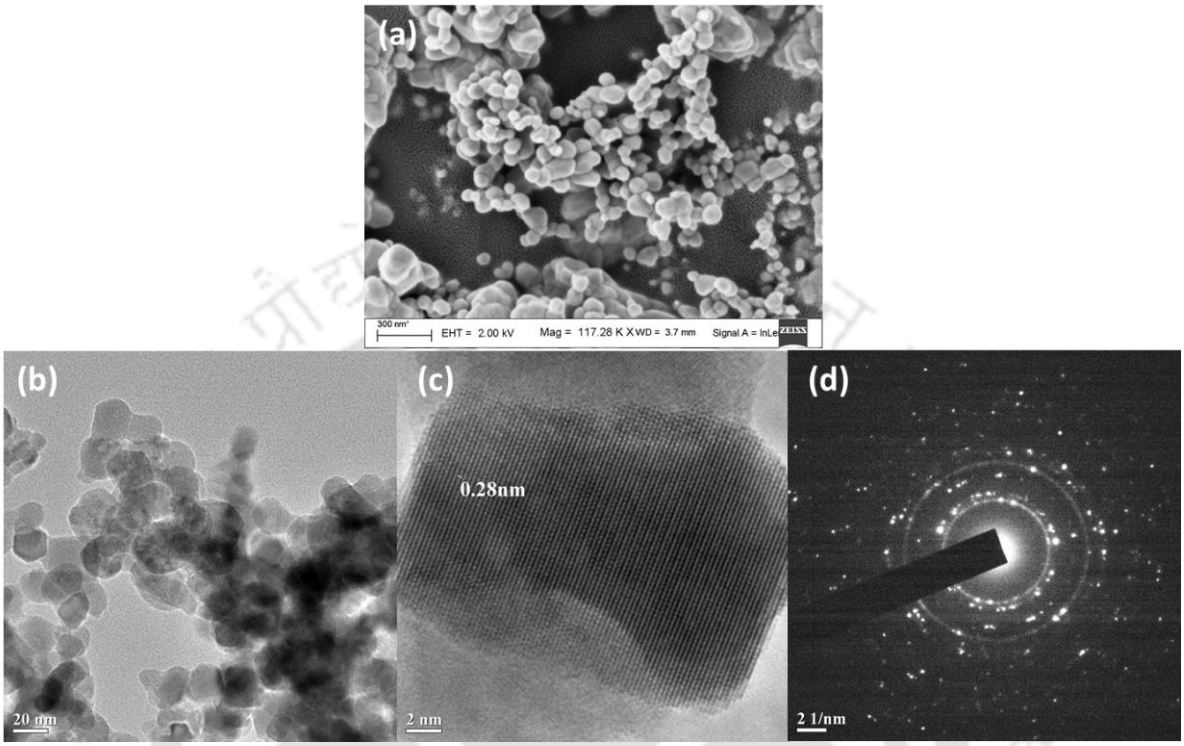

Figure 3.3 Images of KeZnONP (a) FESEM, (b) TEM, (c) UHRTEM, and (d) SAED

XRD studies

The crystallinity of the KeZnONP was analyzed by XRD studies, which is represented in **Figure 3.4.** The XRD spectrum of KeZnONP shows Braggs peak at 2θ values 31.83°, 34.53°, 36.33°, 47.67°, 56.67°, 62.97°, 66.57°, 68.13°, 69.15° corresponding to (100), (002), (101), (102), (110), (103), (200), (112) and (201) planes of wurtzite structure of zinc oxide nanoparticle (Akhtar et.al., 2012; Anubhavannan et al., 2015; Rahimi et al., 2013).

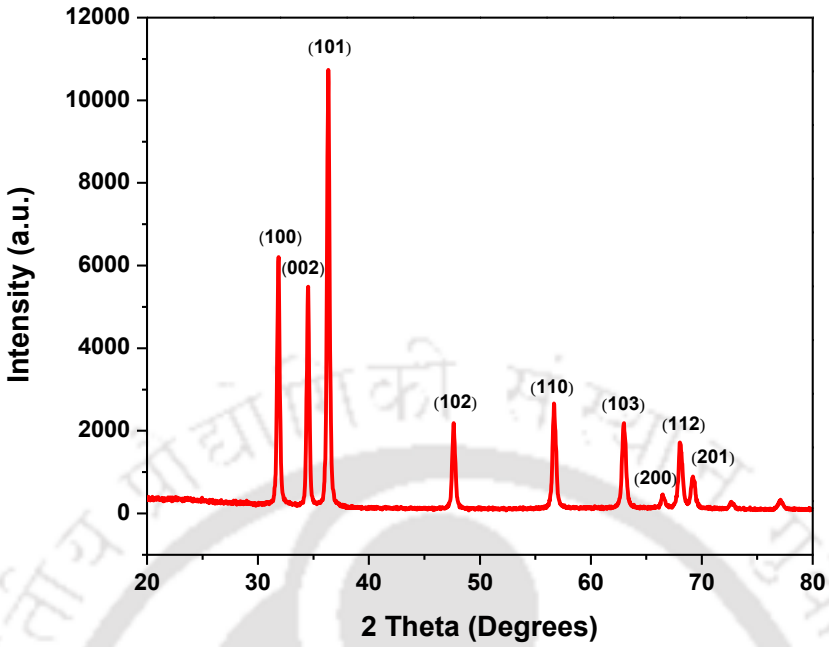

Figure 3.4. XRD analysis of KeZnONP

FTIR analysis

Figure 3.5 represents the FTIR analysis of *H. fragrans* leaf extract and KeZnONP. The IR peaks and the corresponding functional groups have been mentioned in **Table 3.1**. This reveals that the phytochemicals present in the leaf extract are the source of the functional groups present on the KeZnONP. The functional groups present on the NP can be utilized for further conjugation with other molecules for various applications.

TGA analysis

TGA analysis was performed to assess the stability of the KeZnONP**. Figure 3.6** shows the TGA analysis curve of KeZnONP synthesized. TGA analysis was carried out at 25°C to 1000°C in static air. There was 16% weight loss at 333°C, which might be due to the decomposition of organic compounds present in the KeZnONP

(Nagajyothi et al., 2014). This suggests capping of nanoparticles with phytoconstituents. There was gradual weight loss between 400°C to 1000°C.

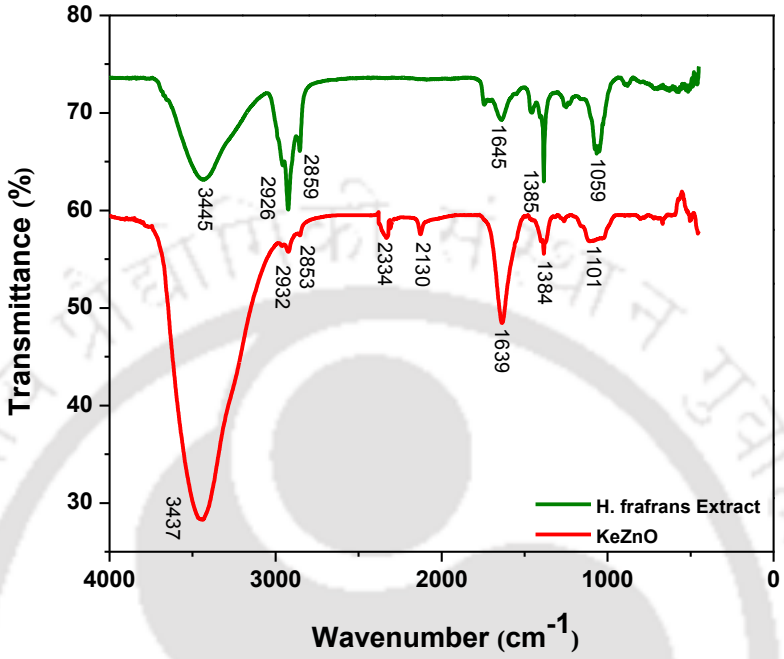

Figure 3.5 FTIR analysis of *H. fragrans* leaves extract and KeZnONP

Table No. 3.1 List of FTIR peaks and their corresponding functional groups.

Functional groups	*H. fragrans* leaves extract	KeZnONP	References
Alcohol (O-H) stretch	3445	3437	http://www2.ups.edu/faculty/hanson/Spectroscopy/IR/IRfrequencies.html. https://webspectra.chem.ucla.edu/irtable.html
Alkane (C-H) stretch	2926	2932	
Alkane (C-H) stretch	2859	2853	
Alkynes (C≡C)	-	2334	
Alkynes (C≡C)	-	2130	
Amide (C=O) stretch	1645	1639	
Nitro (N-O) stretch	1385	1384	
C-O-H stretch	1059	1101	

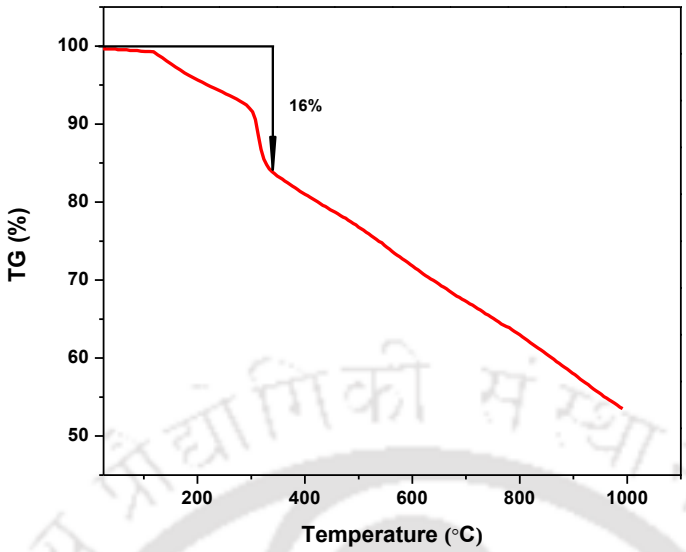

Figure 3.6 TGA analysis of KeZnONP

3.4.3 Application of KeZnONP

3.4.3.1 Photocatalytic activity of KeZnONP

The photocatalytic activity of KeZnONP was assessed by decolorization of MB under UV light illumination. MB degradation efficiency under UV light was 36%. The degradation efficiency is increased to 65% and 76% respectively when KeZnONPs were added. Photodegradation of MB is caused by the free radicals generated during UV illumination in presence of zinc oxide. The free radicals react with the MB molecules and degrade them into CO_2 and H_2O.

Photodegradation process

ZnO NPs are photocatalysts and generate electron and hole pair when irradiated with appropriate light. The electrons are produced in the conduction band and leave positive holes in the valence band which leads to a series of chemical reactions resulting in degradation of pollutant.

The series of chemical reactions which follows after UV irradiation on ZnO nanoparticles are described below (Rajamanickam and Shanthi, 2016; Mondal and Sharma, 2014):

$$\text{Photocatalysts (ZnO)} + h\gamma \rightarrow e^- + h^+ \quad (6)$$

$$h^+ + H_2O \rightarrow H^+ + OH\cdot \quad (7)$$

$$h^+ + OH^- \rightarrow OH\cdot \quad (8)$$

$$e^- + O_2 \rightarrow O_2^- \quad (9)$$

$$2e^- + O_2 + 2H^+ \rightarrow H_2O_2 \quad (10)$$

$$e^- + H_2O_2 \rightarrow OH\cdot + OH^- \quad (11)$$

$$\text{Organic} + \cdot OH + O_2 \rightarrow CO_2 + H_2O + \text{other degradation productions} \quad (12)$$

In the valence band h^+ is created by photons, which reacts with H_2O or OH^- to produce ·OH radicals. In the conduction band the free electron e^- reacts with O_2 adsorbed on the ZnO surface and generates radicals such as OH· and O_2^-. Finally the radicals react with the dye and degrade them to CO_2 and H_2O along with other products. These reactions are observed by decolorization of the MB and decreased absorbance.

Effect of catalyst

In this study, KeZnONP are assessed for their photocatalytic activity. **Figure 3.7** represents the absorbance spectra of 5 mg/L MB in presence of KeZnONP under UV light with respect to time. The intersection of the normalized MB concentration change and degradation efficiency curves (C/C_0 and $1-C/C_0$) shows the half-life of MB that is the time taken to decrease the concentration of MB by half (Soltani et al., 2012). It can be observed from **Figure 3.7,** that the intensity of MB absorbance peak

decreased gradually when MB was illuminated with UV light and it is more pronounced in presence of KeZnONP than in control. The concentration of MB decreased by half after 80 minutes in presence of 0.5 mg/ml KeZnONP and the degradation efficiency reached 68% after 160 minutes. In presence of 1 mg/ml KeZnONP the half-life of MB was 61 minutes and the degradation efficiency reached 76% after 160 minutes, whereas the degradation efficiency was only 36% in absence of KeZnONP.

Linear plots of $Ln(C/C_0)$ vs time for the photo-degradation of MB (5 mg/L) under UV light in presence of KeZnONP at different concentrations has been shown in **Figure 3.8a**. The slope of the plots represents the rate of MB degradation process in presence of varying amount of KeZnONP. The rate constant for MB (5 mg/L) degradation increases from 8.11×10^{-3} min^{-1} to 9.79×10^{-3} min^{-1} with the increase in KeZnONP concentration from 0.5 mg/ml to 1 mg/ml. The rate of degradation for control was 3.17×10^{-3} min^{-1}. The degradation efficiencies of KeZnONP based on their concentration has been represented in **Figure 3.8b**. Therefore, the rate of MB degradation is dependent on KeZnONP concentration.

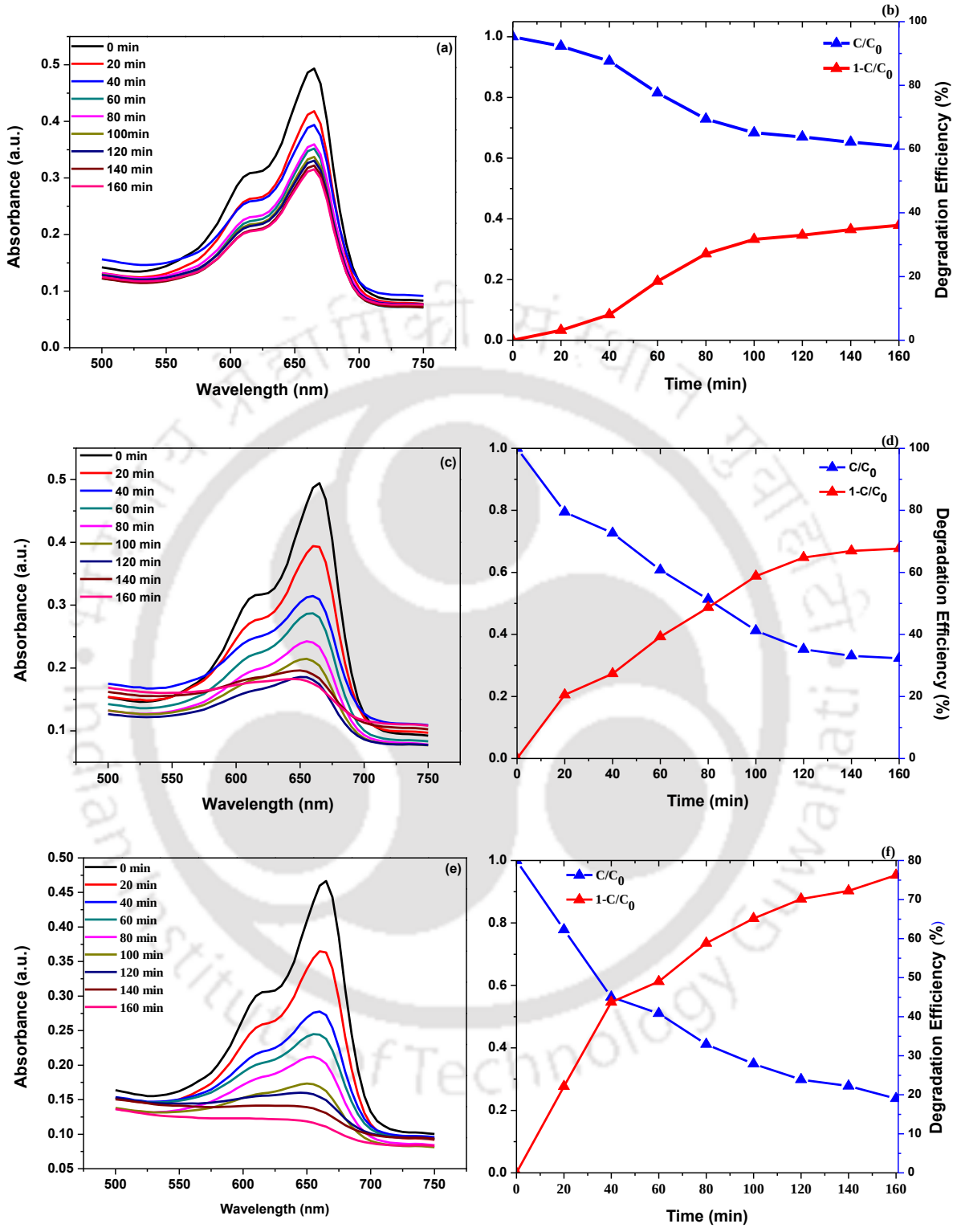

Figure 3.7. Absorption spectral changes and photocatalytic degradation of MB at different time intervals. (a), (b) Control MB without catalyst; (c), (d) MB with 0.5 mg/ml KeZnONP and (e), (f) MB with 1 mg/ml KeZnONP.

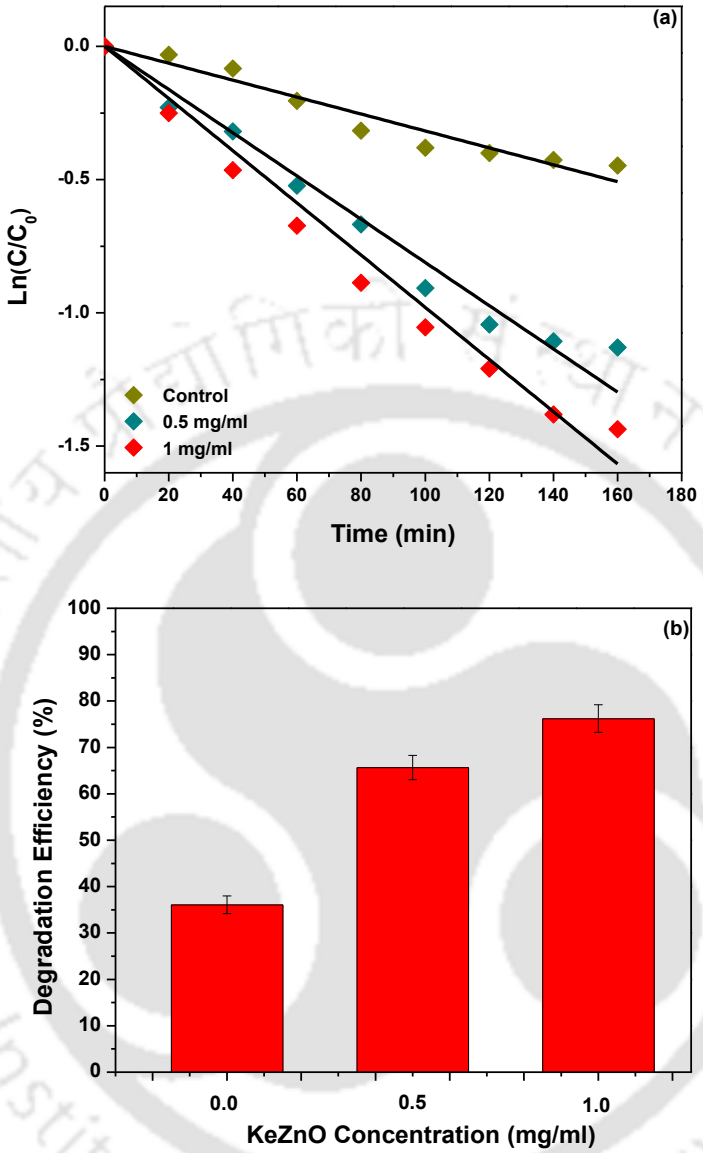

Figure 3.8 Photocatalytic degradation of MB by KeZnONP at different concentrations, (a) Linear plots of Ln(C/C_0) of MB degradation, (b) Degradation efficiency of MB with different KeZnONP concentration.

Effect of pH

The effect of pH on KeZnONP (1 mg/ml) catalyzed MB (5 mg/L) degradation was studied at pH 3, 5, 7 and 9 under UV light illumination. **Figure 3.9** represents the

photocatalytic degradation of MB for 160 minutes at different pH conditions. It is visible that there is a fast increase in degradation efficiency with the increase in pH i.e. up to pH 7 followed by a slight decrease at pH 9. Oxides are amphoteric in nature, which means that they are soluble in both acidic and alkaline conditions. The low initial reaction rates can be attributed to the dissolution and photodissolution of KeZnONP. It is reported that the pH of zero point charge for ZnO is 9 (Abdollahi et al., 2011). When pH value is lower than 5, the ZnO surface is favorably covered by the dye molecules. When pH increases generation of hydroxyl radicals increases which again enhances photodegradation. However, at higher pH electrostatic repulsion between MB anion and oxide surface increases and diffusion of surface generated OH ions towards lower MB concentration decreases (Ghule et al., 2011). Therefore, due to the competition of these two factors highest degradation efficiency was obtained at pH 7.

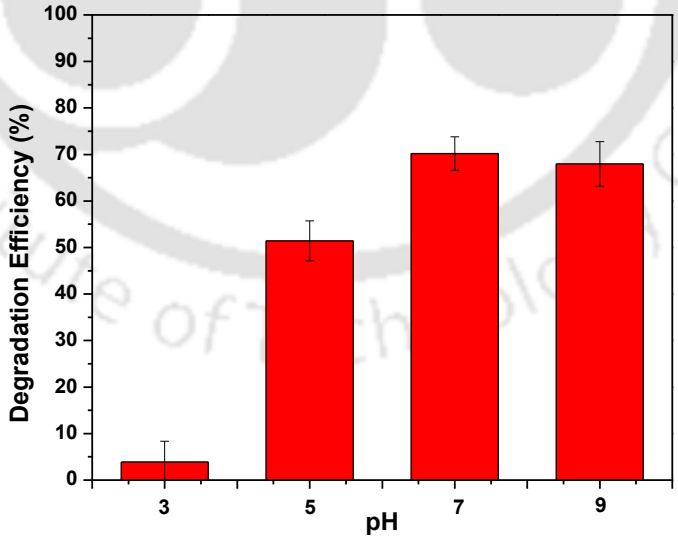

Figure 3.9 Photocatalytic degradation of 5 mg/L MB by 1 mg/ml KeZnONP at different pH conditions (3, 5, 7 and 9).

Effect of initial Concentration

The effect of initial dye concentration was studied at 5-20 mg/L MB concentration, using 1 mg/ml of KeZnONPs at pH 7 for 160 minutes under UV light. The results obtained has been represented in **Figure 3.10.** From the figure it is observed that photodegradation of MB was inversely proportional to its concentration. This is evident from the decrease in degradation efficiency of KeZnONP from 76% to 30% when MB concentration was increased from 5-20 mg/L. The decrease in degradation efficiency is due to a rise in dye adsorbance on the catalyst surface and decrease in free active sites on the catalysts surface. This leads to lesser adsorption of OH^- ions on the catalyst surface and lesser generation of OH· radicals. Moreover, when dye concentration increases fewer photons reach the catalyst's surface which leads to limited holes and hydroxyl radicals production (Mohamed et al., 2011).

Reuse of KeZnONP

Figure 3.11 shows the percentage degradation of MB when treated with KeZnONP reused for three times for photocatalytic degradation of 5 mg/L MB. The MB degradation process was carried out for 160 mins using 1 mg/ml KeZnONP under UV light. At the fourth cycle of MB degradation percentage removal was 75% which is comparable with the first cycle of MB degradation i.e. 78%. Therefore KeZnONP can be reused for the photodegradation of MB.

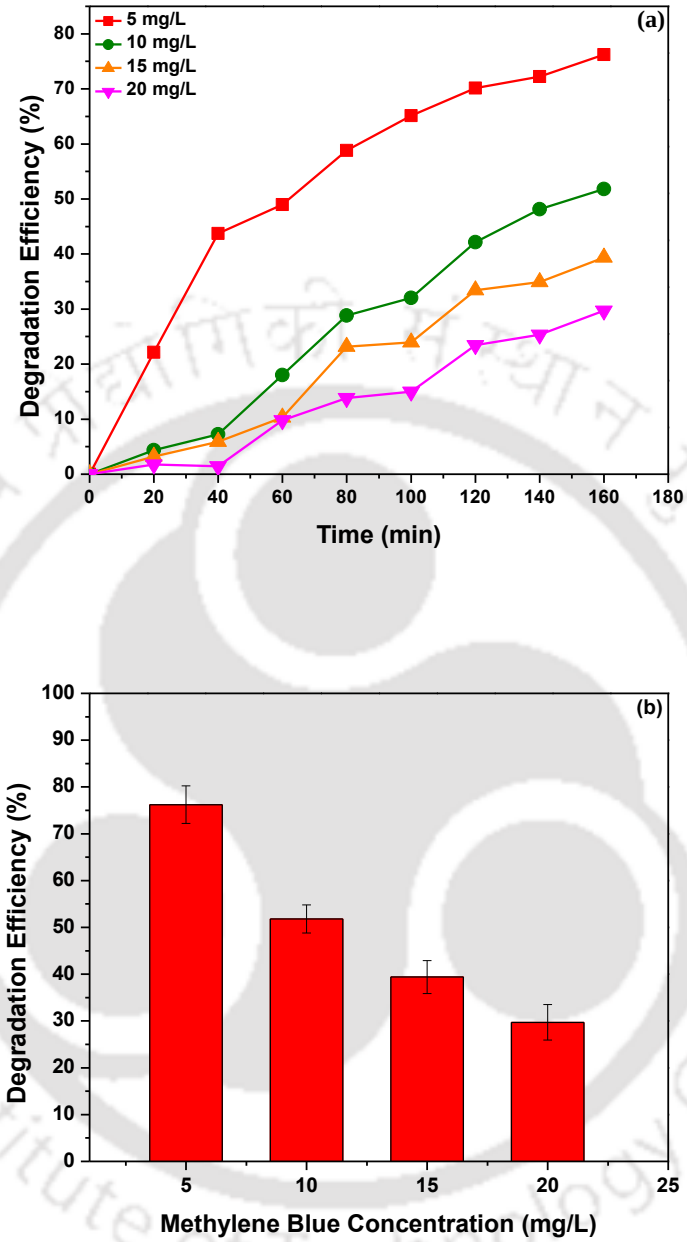

Figure 3.10 Photocatalytic degradation of MB at 5-20 mg/L concentrations by 1 mg/ml KeZnONP at pH 7, (a) Degradation of MB at different time point and (b) Degradation Efficiency of MB at 160 minutes.

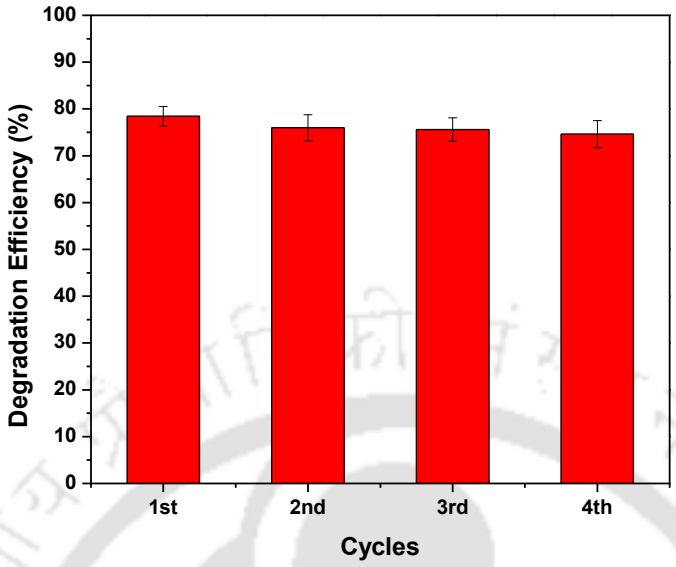

Figure 3.11 Reuse of KeZnONP for photocatalytic degradation of MB for 3 times.

3.5 CONCLUSION

In this study, we have discussed the green synthesis of zinc oxide NP using leaf extract of *H. fragrans* and its application in degradation of MB as a photocatalyst.

The synthesis of KeZnONP was confirmed by various techniques. From the UV-visible spectroscopy the band gap energy of KeZnONP was found to be 3.24 eV. Other characterizations such as FESEM, TEM, FTIR, XRD, TGA analysis were carried out. The size and shape of the KeZnONP was obtained from microscopy analysis and found to be in nano-range with spherical morphology. Wurtzite structure of KeZnONP was concluded from XRD studies. The nanoparticles were stabilized by capping with phytoconstituents which was confirmed by FTIR and TGA analysis. TGA analysis also confirmed the thermal stability of the synthesized KeZnONP.

The rate of degradation of MB (5 mg/L), by KeZnONP (1 mg/ml) at 25°C and pH 7 was 9.79×10^{-3} min^{-1}. Zinc oxide nanoparticles with photocatalytic properties are synthesized by an inexpensive and ecofriendly method can be used to for candle for water purification.

3.6 REFERENCES

Abdollahi, Y., Abdullah, A. H., Zainal, Z., & Yusof, N. A. (2011). Photocatalytic degradation of p-Cresol by zinc oxide under UV irradiation. *International journal of molecular sciences*, 13(1), 302-315.

Agarwal, H., Kumar, S. V., & Rajeshkumar, S. (2017). A review on green synthesis of zinc oxide nanoparticle–An eco-friendly approach. *Resource-Efficient Technologies*, 1-10

Akhtar, M. J., Ahamed, M., Kumar, S., Khan, M. M., Ahmad, J., & Alrokayan, S. A. (2012). Zinc oxide nanoparticle selectively induce apoptosis in human cancer cells through reactive oxygen species. *International Journal of Nanomedicine*, 7, 845-857.

Alhakmani, F., Khan, S. A., & Ahmad, A. (2014). Determination of total phenol, in-vitro antioxidant and anti-inflammatory activity of seeds and fruits of Zizyphus spina-christi grown in Oman. Asian Pacific *Journal of Tropical Biomedicine*, 4, S656-S660.

Anbuvannan, M., Ramesh, M., Viruthagiri, G., Shanmugam, N., & Kannadasan, N. (2015). Synthesis, characterization and photocatalytic activity of ZnO nanoparticle prepared by biological method. *Spectrochimica Acta Part A: Molecular and Biomolecular Spectroscopy*, 143, 304-308.

Anjum, M., Miandad, R., Waqas, M., Gehany, F., & Barakat, M. A. (2016). Remediation of wastewater using various nano-materials. *Arabian Journal of Chemistry*, 1-23.

Ayad, M. M., & El-Nasr, A. A. (2010). Adsorption of cationic dye (methylene blue) from water using polyaniline nanotubes base. *The Journal of Physical Chemistry C*, 114(34), 14377-14383.

Balcha, A., Yadav, O. P., & Dey, T. (2016). Photocatalytic degradation of methylene blue dye by zinc oxide nanoparticle obtained from precipitation and sol-gel methods. *Environmental Science and Pollution Research*, 23(24), 25485-25493.

Changmai, M., Chetia J., Upadhyaya, S., Yadav, R. N. S., Bhuyan, M. (2015) Phytochemical and biochemical analysis of two host plants of eri silkworm, *Samia ricini* (D.) *International. Journal of Pharmaceutical Sciences Review Research*, 32(2), 187-192.

Chen, C., Liu, J., Liu, P., & Yu, B. (2011). Investigation of photocatalytic degradation of methyl orange by using nano-sized ZnO catalysts. *Advances in Chemical Engineering and Science*, 1(1), 9-14.

Chutia, P., Kumar, R., & Khanikar, D. P. (2014). Host plants relationship in terms of cocoon colour and compactness of eri Silkworm (*Samia ricini*). *In Biological Forum- An International Journal*, 6(2), 340-343.

Darabdhara, G., Boruah, P. K., Borthakur, P., Hussain, N., Das, M. R., Ahamad, T., Alshehri, S.M., Malgras, V., Wu, K.C.W. & Yamauchi, Y. (2016). Reduced

graphene oxide nanosheets decorated with Au–Pd bimetallic alloy nanoparticles towards efficient photocatalytic degradation of phenolic compounds in water. *Nanoscale*, 8(15), 8276-8287.

Deng, Z., Chen, M., Gu, G., & Wu, L. (2008). A facile method to fabricate ZnO hollow spheres and their photocatalytic property. *The Journal of Physical Chemistry B*, 112(1), 16-22.

Devi, R. S., & Gayathri, R. (2014). Green Synthesis of zinc oxide nanoparticles by using Hibiscus rosa-sinensis. *International Journal of Current Engineering and Technology*, 4(4), 2444-2446.

Ghule, L. A., Patil, A. A., Sapnar, K. B., Dhole, S. D., & Garadkar, K. M. (2011). Photocatalytic degradation of methyl orange using ZnO nanorods, *Toxicological & Environmental Chemistry*, 93(4), 623-634.

Jamdagni, P., Khatri, P., & Rana, J. S. (2016). Green synthesis of zinc oxide nanoparticle using flower extract of *Nyctanthes arbor-tristis* and their antifungal activity. *Journal of King Saud University-Science*. 1-8.

Jeevanandam, J., Chan, Y. S., & Danquah, M. K. (2016). Biosynthesis of Metal and Metal Oxide NP. *ChemBioEng Reviews*, 3(2), 55-67.

Luo, W., Zhu, L., Wang, N., Tang, H., Cao, M., & She, Y. (2010). Efficient removal of organic pollutants with magnetic nanoscaled BiFeO3 as a reusable heterogeneous Fenton-like catalyst. *Environmental science & technology*, 44(5), 1786-1791.

Mohamed, R. M., Mkhalid, I. A., Baeissa, E. S., & Al-Rayyani, M. A. (2012). Photocatalytic degradation of methylene blue by Fe/ZnO/SiO2 nanoparticles under visible light. *Journal of Nanotechnology*, *2012*, 1-5.

Mondal, K., & Sharma, A., (2014). Photocatalytic oxidation of pollutant dyes in wastewater by TiO_2 and ZnO nano-materials—a mini-review. *Nanoscience & Technology for Mankind*, 36-72.

Nagajyothi, P. C., Sreekanth, T. V. M., Tettey, C. O., Jun, Y. I., & Mook, S. H. (2014). Characterization, antibacterial, antioxidant, and cytotoxic activities of ZnO NP using *Coptidis Rhizoma*. *Bioorganic & Medicinal Chemistry Letters*, 24(17), 4298-4303.

Naveed Ul Haq, A., Nadhman, A., Ullah, I., Mustafa, G., Yasinzai, M., & Khan, I. (2017). Synthesis Approaches of Zinc Oxide nanoparticle: The Dilemma of Ecotoxicity. *Journal of Nanomaterials*, (2017), 1-14.

Rahimi, R., Shokrayian, J., & Rabbani, M. (2013). Photocatalytic removing of methylene blue by using of Cu-doped ZnO, Ag-doped ZnO and Cu, Ag-codoped ZnO nanostructures. In The 17th International Electronic Conference on Synthetic Organic Chemistry. Multidisciplinary Digital Publishing Institute.

Rajamanickam, D., & Shanthi, M. (2016). Photocatalytic degradation of an organic pollutant by zinc oxide–solar process. *Arabian Journal of Chemistry*, 9, S1858-S1868.

Ramesh, M., Anbuvannan, M., & Viruthagiri, G. (2015). Green synthesis of ZnO nanoparticle using *Solanum nigrum* leaf extract and their antibacterial activity. *Spectrochimica Acta Part A: Molecular and Biomolecular Spectroscopy*, 136, 864-870.

Sáenz-Trevizo, A., Amézaga-Madrid, P., Pizá-Ruiz, P., Antúnez-Flores, W., & Miki-Yoshida, M. (2016). Optical band gap estimation of ZnO nanorods. *Materials Research*, 19, 33-38.

Sangeetha, G., Rajeshwari, S., & Venckatesh, R. (2011). Green synthesis of zinc oxide NP by aloe barbadensis miller leaf extract: Structure and optical properties. *Materials Research Bulletin*, 46(12), 2560-2566.

Sivasubramanian, V. (Ed.). (2016). *Environmental Sustainability Using Green Technologies*. CRC Press.

Soltani, N., Saion, E., Hussein, M. Z., Erfani, M., Abedini, A., Bahmanrokh, G., Navasery, M. & Vaziri, P. (2012). Visible light-induced degradation of methylene blue in the presence of photocatalytic ZnS and CdS nanoparticle. *International Journal of Molecular Sciences*, 13(10), 12242-12258.

Stankovic, M. S. (2011). Total phenolic content, flavonoid concentration and antioxidant activity of *Marrubium peregrinum* L. extracts. *Kragujevac Journal Science*, 33(2011), 63-72.

Yang, S. J., & Park, C. R. (2007). Facile preparation of monodisperse ZnO quantum dots with high quality photoluminescence characteristics. *Nanotechnology*, 19(3), 1-4.

CHAPTER 4

Green Synthesis of Iron Oxide Nanoparticles using *Persea bombycina* Leaf Extract and their Applications

CHAPTER 4

Green Synthesis of Iron Oxide Nanoparticles using *Persea bombycina* Leaf Extract and their Applications

4.1 INTRODUCTION

Nanoscale iron oxide particle synthesis has gained importance as they are magnetic, biocompatible and biodegradable. The most common forms of Iron oxides existing nature are magnetite (Fe_3O_4), maghemite (γ-Fe_2O_3), and hematite (α-Fe_2O_3) (Majewski and Thierry, 2007). Magnetic NPs have wide applications in different areas such as catalysis, bioremediation, magnetic storage media, magnetic resonance imaging (MRI), biosensors, and targeted drug delivery (Mahdavi et al., 2009; Yew et al., 2016). Fe_3O_4 NPs as modified Fenton's reagent are studied for degradation of organic pollutants. Reuse of these magnetic NPs is one of the advantages as the magnetic NPs can easily be separated from the solutions using external magnet after the catalysis or adsorption process (Es'haghi et al., 2016). Catalytic degradation of organic pollutant through fenton's reaction is known long ago. It involves use of Fe^{2+} and H_2O_2 for the degradation of the pollutants. However, these reactions generates sludge as a byproduct of the treatment. This challenge can be overcome by use Fe_3O_4 NPs in place of Fe^{2+} which can be separated using magnet and subsequently reused. Thus magnetite is suitable as a heterogeneous Fenton catalyst for organic pollutant removal (Zhou et al., 2014).

The toxicity of methylene blue has already been dicussed in chapter 3.

Various synthesis methods of magnetite (Fe_3O_4) NPs include co-precipitation, sol–gel method, flow injection, electrochemical, solvothermal, hydrothermal, microwave-assisted, thermal decomposition of iron (III) acetylacetonate in tri(ethylene glycol), etc (Basavegowda et al., 2014; Chaki et al., 2015). However, these methods are time consuming involving toxic chemicals and complicated steps. Greener way of iron oxide NP synthesis is easier and safe as it uses plants and microorganisms for the synthesis. There are several studies on plant mediated iron oxide nanoparticles synthesis. For instance, fruit extract of *Artemisia annua* (Basavegowda et al., 2014), leaf extract of *Perilla frutescens* (Basavegowda et al., 2014), *Tridax procumbens* (Senthil and Ramesh, 2012) and *caricaya papaya* (Latha and Gowri, 2014). Peel extract of plantain (Venkateswarlu et al., 2013), seed extract of grape *proanthocyanidin* (Narayanan et al., 2011), leaf extract *Kappaphycus alvarezii* (Yew et al., 2016), extract of sea weed *Padina pavonica* (Linnaeus) Thivy and *Sargassum acinarium* (Linnaeus) Setchell 1933 (El-Kassas et al., 2016), and tangerine peel extract (Ehrampoush et al., 2015) are also used to synthesize iron oxide nanoparticles.

Iron oxide NPs are low cost, biocompatible, scalable and can combat enviromental pollution (Saif et al., 2016). In this study, we have used *Persea bombycina* leaf extract for the synthesis of iron oxide NPs and studied their application in degradation methylene blue from aqueous solution.

4.2 OUTLINE OF THE RESEARCH STUDY

i) Green synthesis iron oxide (Fe_3O_4) NPs by coprecipitation method using *P. bombycina* leaf extract in alkaline condition and room temperature.

ii) Characterization of the green synthesized iron oxide nanoparticles (PbFeONPs) by biophysical techniques

iii) Degradation of methylene blue using PbFeONPs and H_2O_2.

4.3 EXPERIMENTAL SECTION

4.3.1 Preparation of plant extract

Aqueous extract of *Persea bombycina* leaves were prepared for the synthesis of iron oxide nanoparticle. The leaves were collected from Central silk Board, Khanapara, Assam India. The leaves were cleaned and dried under shade. When the leaves were completely dried, ground to powder using a mixer grinder. 60 ml water was added to 5 g of *P. bombycina* leaf powder and left overnight. After 12 hours the aqueous extract was separated by using muslin cloth. The aqueous extract was stored at 4°C for later use.

4.3.2 Estimation of total phenolic content

The phytochemicals in the plant extract act as reducing agent in NP synthesis process. Total phenolic content of *P.bombycina* leaf extract was estimated by Folin-Ciocalteu's method as described by Stankovic (2011) . Gallic acid was used as standard in this assay. The aqueous extract was dried and used for total phenolic

content estimation. A series of concentrations of gallic acid and *P. bomycina* extract were prepared from 1 mg/ml gallic acid stock solution. 10% of Folin-Ciocalteu's (FC) reagent was added to each gallic acid concentration along with the *P. bombycina* leaf extract and a control. Further to it, 2.5% $NaHCO_3$ was added and the solution was kept for incubation at 45°C for 20 minutes. After the incubation, absorbance was measured at 765 nm. Standard curve was plotted using absorbance of gallic acid and gallic acid equivalent phenolic content of the extract was determined from the linear equation obtained from the standard curve.

4.3.3. Green synthesis of iron oxide nanoparticle (PbFeONP) using *P. bombycina* leaf extract

Iron oxide nanoparticle was synthesized using *P. bombycina* leaf extract as described by Yew et al. (2016). A solution containing Fe^{3+} and Fe^{2+} at 2:1 molar ratio was prepared and *P. bombycina* leaf extract was added to it at different concentration. Three different preparations were made with varying the volume of the leaf extract (1 ml, 2 ml and 3 ml) and the total volume of the reaction were kept constant with addition of water. The colloidal solutions were stirred constantly and the pH was adjusted to 11 by dropwise addition of 1.0 M NaOH. The reaction was allowed to proceed for one hour. Using a magnet nanoparticles were separated out from the solution. The nanoparticles were washed three times with distilled water and dried at 50°C. The iron oxide nanoparticles (PbFeONPs), obtained in powder form, were stored for further characterization and applications.

4.3.4. Characterization of PbFeONPs

The nanoparticles were characterized for their magnetic and structural properties. Magnetic properties of the iron oxide nanoparticles were assesed by Vibrating sample magnetometer (VSM) analysis. FESEM and TEM studies were carried out to analyze the size, morphology and crystallinity of the iron oxide nanoparticles. X-Ray diffraction (XRD) analysis were performed to analyze the phase purity and crystallinity. Capping of PbFeONPs with phytoconstituents of *P. bombycina* leaf extract was characterized by FTIR analysis of the extract and the synthesized iron oxide NP. Thermal stability of PbFeONP was characterized by thermogravimetric analysis (TGA). The cytotoxicity of PbFeONP was assesed by MTT assay using mouse fibroblast cell line (L929).

Magnetic property analysis

The lyophilized iron oxide nanoparticles were analyzed for their magnetic properties using vibrating sample magnetometer (VSM). The samples were weighed accurately on a teflon tape and then placed on the sample holder of the VSM instrument. VSM analysis was performed at room temperature.

Microscopy studies

FESEM analysis was carried out to study the morphology of the iron oxide NPs and TEM analysis was carried out to confirm the size and crystallinity of the NPs. The iron oxide NPs in powder form was used for FESEM studies. For TEM studies the NPs were suspended in distilled water and sonicated to obtain a well dispersed

suspension. A drop of this suspension was then was put on copper grid and kept in a oven for drying. TEM analysis was carried out at SAIF, NEHU, Shillong, India.

X-Ray Diffraction (XRD) studies

XRD analysis was carried out to assess the phase purity and crystallinity. The iron oxide NPs were characterized by X-ray diffractometer studies at 2theta/theta scanning moderanging from 20-80° (operational voltage 50 kV and current 180 mA, CuKα radiation λ=1.540 A° with 0.05° s−1).

Fourier Transform Infrared Spectroscopy (FTIR) analysis

FTIR spectroscopy of the *P. bombycina* leaf extract and the iron oxide nanoparticles were carried out using IRAffinity-1 (Shimadzu) by ATR method in transmittance mode from 450 cm^{-1} to 4000 cm^{-1} with resolution at 4.0 cm^{-1}

Thermogravimetric (TGA) analysis

High temperature differential scanning calorimetry (DSC)/Thermo Gravimetric (TG) System (make: Netzsch , model: STA449F3A00) was used to assess the thermal stability of the nanoparticles. The iron oxide NPs were kept in a clean alumina crucible. The crucible was kept near to the reference crucible without touching each other. After taring well the nanoparticles were subjected to a heat ranging from 25°C to 1200°C at 10°C per minute increasing rate.

4.3.5 Cytotoxic assay

Biocompatibility of the PbFeONPs was assessed by MTT (3-[4, 5-dimethylthiazole-2-yl]-2, 5-diphenyl tetrazolium bromide) reduction assay using mouse fibroblastic cell line L929 as mentioned in Sett et al. (2016). The L929 cell lines were maintained on Dulbecco's Modified Eagle's Medium (DMEM) with 10% fetal serum in a 5% CO_2 incubator at 37°C. The cells were harvested and suspended DMEM media containing 10% fetal bovine serum. The suspended cells were added to the wells of a 94 well plate such that each well contains 10^4 cells. The cells were allowed to grow for 24 hours at 37°C in the incubator with 5% CO_2. PbFeONPs were dispersed in DMEM media at 1 mg/ml concentration and sonicated to prepare a uniformly dispersed nanoparticle suspension. The NP suspension was sterilized by UV irradiation. After sterilization various dilutions of the PbFeONPs were made in a serum free DMEM media. Media from the wells containing cells were discarded after incubation and added with 100µl DMEM media containing PbFeONP. Triplicate wells for every dilution of PbFeONPs were prepared and incubated for 24 and 48 hours. Negative control wells were added with serum free DMEM media without NPs. 0.5 mg/ml MTT was freshly prepared in serum free media and stored in dark. After 24 hours or 48 hours of incubation the media was discarded and 100 µl of MTT was added including negative controls and incubated for 4 hours in CO_2 incubator. After incubation MTT was discarded and 100µl DMSO was added. Absorbance was measured at 570 nm with reference wavelength at 690 nm using Elisa Plate Reader (Tecan i-control, 1.11.1.0). Cell viability was calculated using following equation:

$$Viability\ (\%) = \frac{N_T}{N_C} \times\ 100 \quad (1)$$

Where N_T and N_C are the absorbance of the treated and negative control cells respectively.

4.3.6. Application of PbFeONPs

4.3.6.1 Methylene blue (MB) degradation by PbFeONPs

Methylene blue (MB) degradation by iron oxide nanopaticles was studied as studied by Badmapriya and Asharani (2016) with some varriations. PbFeONP was added 0.3 mg/ml dose to methylene blue of 20 mg/L concentration followed by addition of 0.1 mM of H_2O_2. Optimizing experiments were performed to study the effects of various parameters such as pH, NP dose, H_2O_2 concentration, duration of the reaction and MB concentration. Recyclabilty of the PbFeONPs was evaluated by performing MB degradation for multiple cycles. All the experiments were conducted at room temperature i.e. 25°C. Absorbance were measured using UV-Visible spectrophotometry. Degradation efficiency was calculated using the following expression (Abkenar et al., 2014).

$$Degradation\ efficiency = \frac{C_i - C_f}{C_i} \times 100 \quad (2)$$

Where C_i and C_f are the MB concentrations at time 0 and t respectively. The degradation rate depends on the concentration of the dye which can be described by the following kinetic model (Taghvaei et al., 2010)

$$rate = -\frac{dC}{dt} = \frac{kKC}{1 + KC} \quad (3)$$

where C is the concentration of MB (mg/L) at any time, t is time duration, k is the first-order rate constant of the reaction and K is the adsorption constant of MB on the NP. This equation can be simplified to a pseudo-first-order equation (Xu et al., 2011)

$$Ln\left(\frac{C}{C_0}\right) = -kKt = k_{obs}t \quad (4)$$

k_{obs} is the first order rate constant obtained from the slope of $Ln(C/C_0)$ versus time plot.

4.4 RESULTS AND DISCUSSIONS

4.4.1 Estimation of total phenolic content of *P. bombycina* leaf extract and green synthesis of iron oxide nanoparticle

The image of *P. bomycina* is presented in **Figure 4.1a**. The total phenolic content of *P. bombycina* leaf extract was estimated using Folin-Ciocalteus's reagent. Standard curve was plotted using gallic acid and total phenolic content of the extract was calculated from the standard curve. Total phenolic content of *P. bombycina* leaf extract was calculated and found to be 21.58 GAE/mg. These phenolic compounds act as reducing agent for the green synthesis of nanoparticles.

P. bombycina leaf extract when mixed with the solution containing $FeCl_3$ and $FeCl_2$ at 2:1 molar ratio, a colloidal solution was formed. The viscosity of the solution changed when 1 M NaOH was added gradually. After one hour the nanoparticles from the three preparations each with different amount of *P. bombycina* extract were separated using magnet (**Figure 4.1b**) followed by washing with deionized water and subsequent drying at 50°C to obtain powdered iron oxide nanoparticles.

4.4.2. Characterization of Iron oxide nanoparticles

Magnetic property analysis

VSM analysis was carried out to study the magnetic property of the iron oxide nanoparticles synthesized using *P. bombycina* leaf extract (PbFeONP). **Figure 4.2** represents the hysteresis loop of PbFeONPs obtained from VSM analysis. The ferromagnetic parameters such as coercivity (H_c) and magnetization (M_S) are listed in **Table 4.1**.

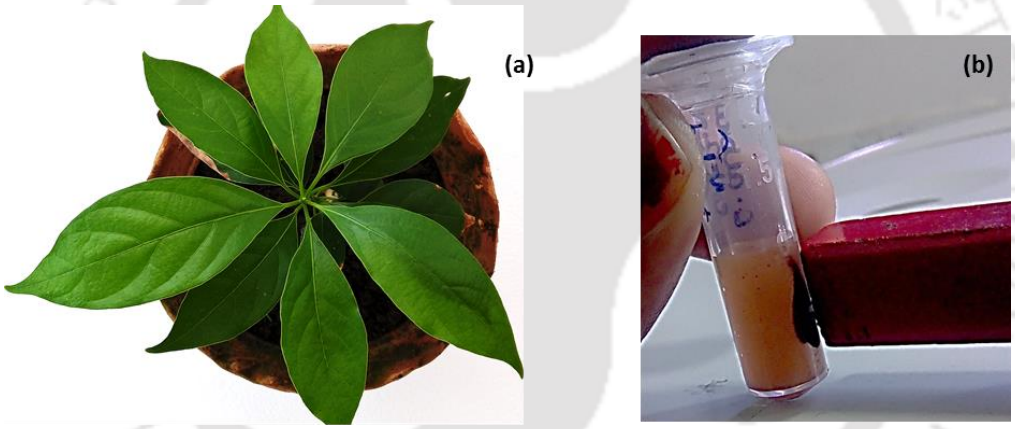

Figure 4.1 Green synthesis of iron oxide nanoparticles using (a) *P. bombycina*, (b) Magnetic separation of PbFeONPs

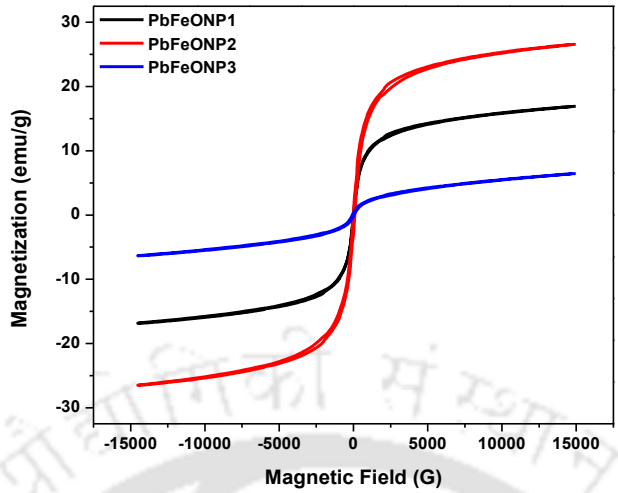

Figure 4.2 VSM analysis of iron oxide nanoparticles.

PbFeONPs synthesized using different ratios of *P. bombycina* extract have different magnetization and coerciveness. Based on the magnetization (M_s), PbFeONPs synthesized using 2 ml volume of *P. bombycina* extract in a 5 ml reaction volume along with $FeCl_3$ and $FeCl_2$ at 2:1 molar ratio were selected for further characterization and application studies. PbFeONP2 had the highest magnetization among the other two preparation with 26.5 emu/g magnetization, therefore characterized further and used in other studies. Due to the ferromagnetic property of the nanoparticles it is expected that the material can be easily separated and reused for various applications. (Venkateswarlu and Yoon, 2015). In the next section, PbFeONP2 is written as PbFeONP.

Table 4.1 List of magnetic properties of PbFeONPs.

Iron Oxide NPs	Coercivity (G)	Magnetization (Ms) (emu/g)
PbFeONP1	50.428	16.876
PbFeONP2	50.534	26.526
PbFeONP3	58.803	6.4008

Microscopy Studies

Figure 4.3a illustrating FESEM image of PbFeONPs shows that the NPs are predominantly spherical in shape. **Figure 4.3b** represents the TEM image of the PbFeONPs and the size of the iron oxide nanoparticles was found to be in 12-15 nm range calculated using image J software. **Figure 4.3c** illustrates UHRTEM image of PbFeONP. The lattice fringes are clearly visible with 0.28 nm interplane distance corresponding to (311) planes of inverse spinel Fe_3O_4 NP (Bhandari et al., 2015). SAED image of PbFeONP in **Figure 4.3d** shows bright spots with concentric circles confirming the crystallinity of the PbFeONP.

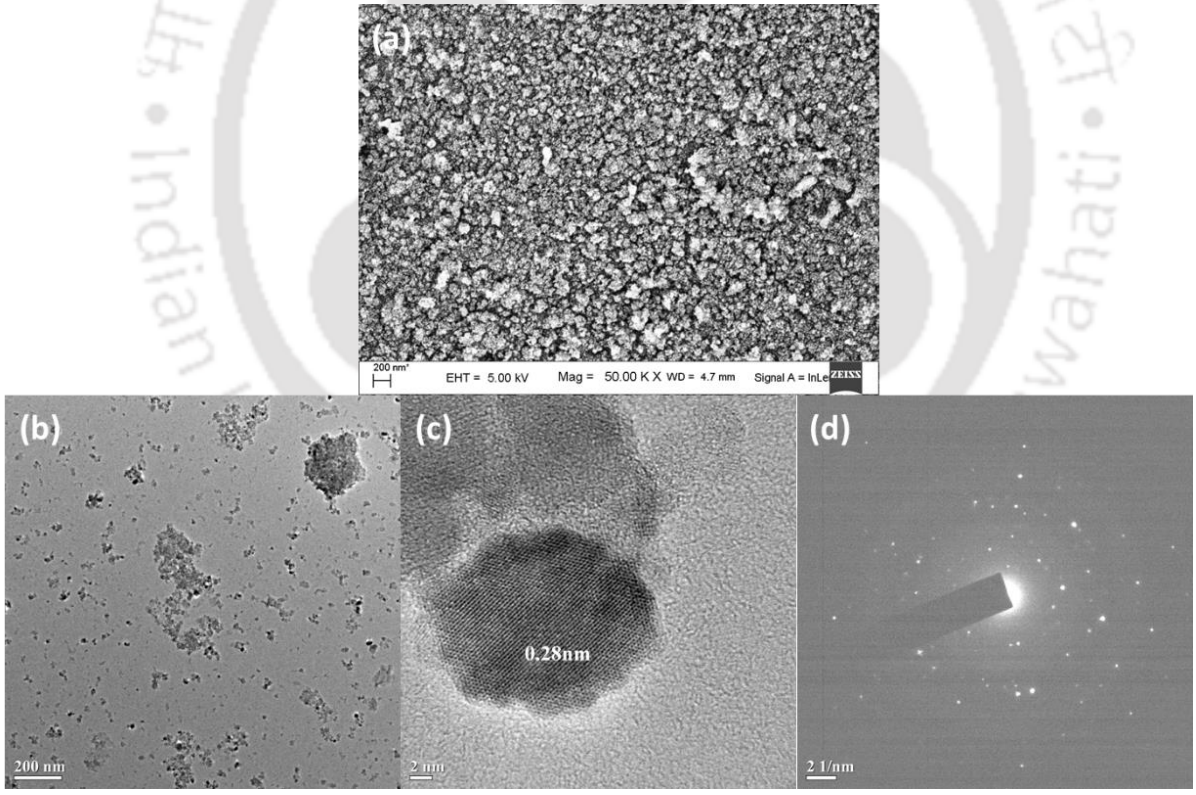

Figure 4.3 Images of PbFeONPs (a) FESEM, (b) TEM, (c) UHRTEM and (d) SAED.

XRD studies

The X-ray Diffraction pattern of the PbFeONP has been presented in **Figure 4.4**. Braggs peaks at 2θ values, 35.5°, 43.4°, 57.45°, 62.85° was obtained from the XRD analysis correspond to (311), (400), (511) and (440) planes of Fe_3O_4 nanoparticles respectively. Thus the XRD spectrum confirms the crystallinity of the iron oxide nanoparticles (Wu and Chen, 2012).

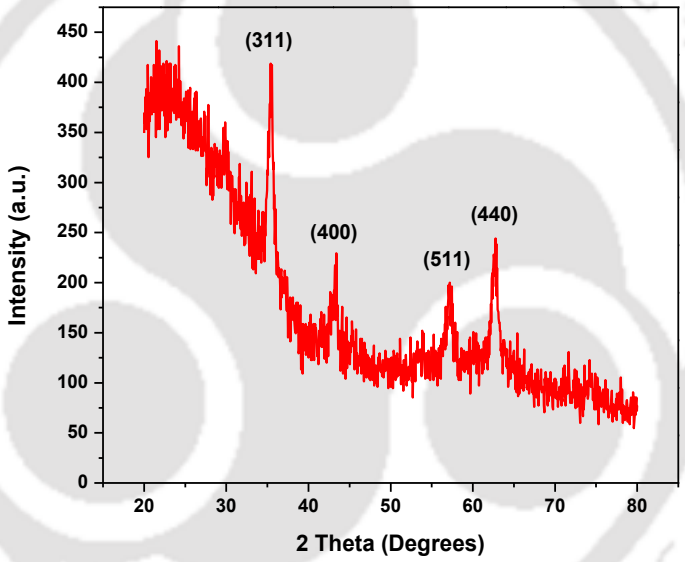

Figure 4.4 XRD analysis of PbFeONP

FTIR analysis

FTIR analysis of *P. bombycina* leaf extract and PbFeONP has been represented in **Figure 4.5**. The list of FTIR peaks obtained and their corresponding functional groups are listed in **Table 4.2**. Peaks at 1122 cm^{-1}, 1274 cm^{-1}, 1383 cm^{-1} and 1634 cm^{-1} were observed in FTIR analysis of *P.bombycina* leaf extract which correspond to C-O, C-

N, N-O and C=C stretch. FTIR analysis of PbFeONP presented peaks at 1080 cm^{-1}, 1370 cm^{-1} and 1626 cm^{-1} corresponds to C-O, N-O, and C=C stretch, respectively. Peaks corresponding to C-O stretch, N-O stretch, and C=C stretch suggest the presence of these functional groups on PbFeONP surface which originates from *P. bombycina* extract. These functional groups can be used for functionalization with other compounds for various application in future.

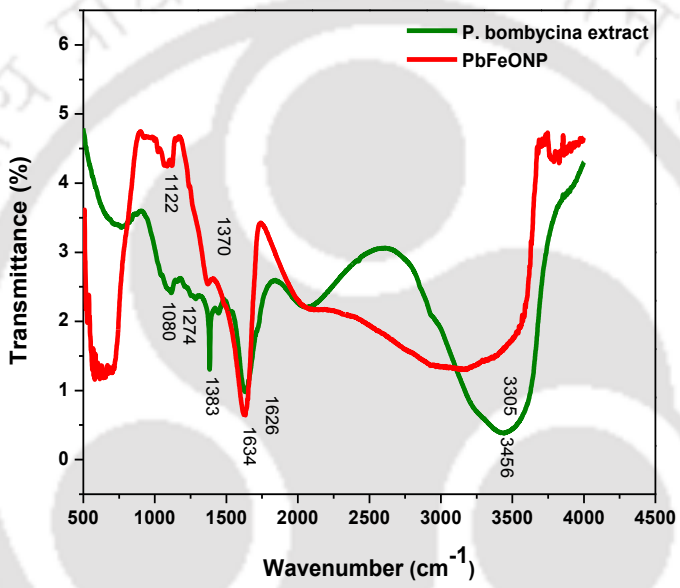

Figure 4.5 FTIR Analysis of *P. bombycina* leaf extract and PbFeONP.

Table 4.2 List of FTIR peaks and their corresponding functional groups.

Functional Groups	IR Peaks of *P. bombycina* extract	IR Peaks of PbFeONP	References
Alcohol (C-O) stretch	1080	1122	http://www2.ups.edu/faculty/hanson/Spectroscopy/IR/IRfrequencies.html
Amine (C-N) stretch	1274	--	
Nitro (N-O) stretch	1383	1370	
Alkene (C=C) stretch	1634	1626	
Alcohol (O-H) stretch	3456	3305	

TGA analysis

Figure 4.6 represents the TGA curve of PbFeONP. In the TGA curve, loss of nanoparticles occured in two phases. In first phase 4.2% of mass was lost till 135.4°C and 31.2% of the mass were lost in the second phase from 135.4°C to 1040.4°C. In the whole process total 35.4% of the nanoparticle mass was lost. The initial loss was due to the loss of moisture content and in next phase the loss might be due to the organic matter present in the nanoparticles. The thermal stability of the PbFeONP was also ensured.

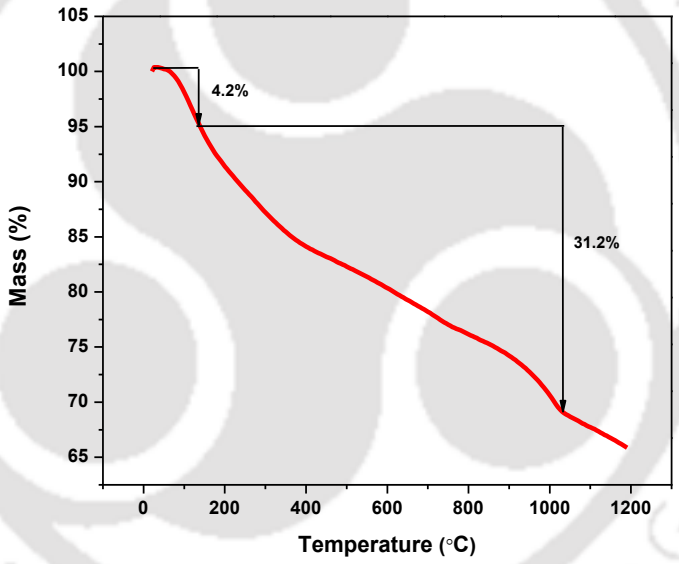

Figure 4.6. TGA Curve of PbFeONP.

4.4.3 Cytotoxic assay

In MTT assay, viable cells are capable of metabolizing MTT (3-(4, 5-dimethylthiozol-2-yl)-2,5-diphenyl tetrazolium bromide) dye into a purple colored precipitate called formazan, with the help mitochondrial dehydrogenase enzymes (VIjaykumar and Ganesan, 2012). After treatment the cells which were not viable were in capable of

metabolizing MTT, thus no purple colored precipitate was formed. In **Figure 4.7** it is clearly visible that PbFeONPs are less toxic to cells during 24 hrs of treatment and become cytotoxic at 48hrs of the treatment. Cell viability was maintained above 75% at <50 µg/ml concentrations of PbFeONPs proving that they are biocompatible or nontoxic to mouse fibroblast cell line in the same range of concentrations. However, they are moderately toxic at 60-90 µg/ml and toxic at >90 µg/ml concentration during 24 hrs of treatment.

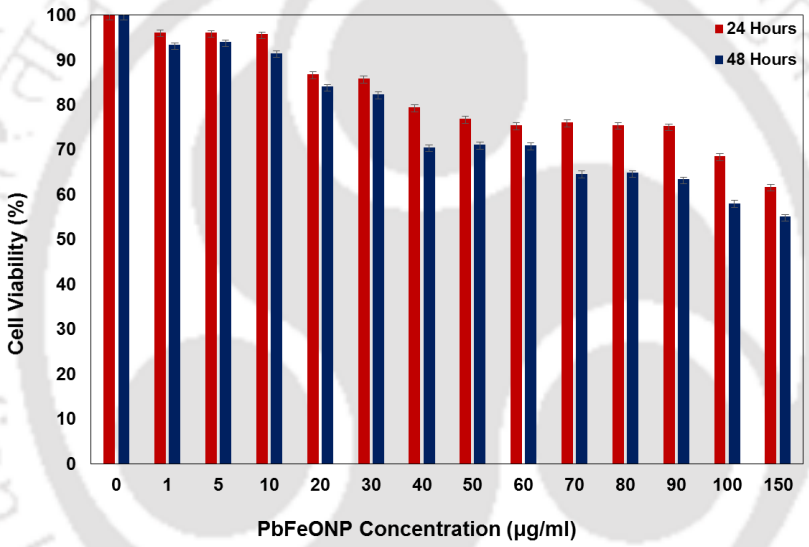

Figure 4.7 Cytotoxicity assay of PbFeONP in L929 cell line at 24 hours and 48 hours.

4.4.4 Application of PbFeONP

4.4.4.1 Methylene Blue (MB) Degradation Studies

Fenton-like mechanism

Chemical oxidation method is a powerful method for degradation of organic pollutants in contaminated water. The oxidation is based on the hydroxyl radical generation

when Fe^{2+} and H_2O_2 are combined in aqueous solution and this combination is known as fenton's reagent. The disadvantages of using Fe^{2+} for the degradation include generation of large amount of sludge and formation of high concentrations of anions in the treated water. In our study, we have replaced Fe^{2+} with iron oxide nanoparticle (PbFeONP) for the degradation of MB.The reactions that causes degradation of MB are mentioned below (Jiang et al., 2011).

$$\equiv Fe^{III} + H_2O_2 \rightarrow \equiv Fe^{III} \cdots H_2O_2 \rightarrow H^+ + \equiv Fe^{II} + \cdot O_2H \quad (5)$$

$$\equiv Fe^{II} + H_2O_2 \rightarrow \equiv Fe^{II} \cdots H_2O_2 \rightarrow OH^- + \equiv Fe^{III} + \cdot OH \quad (6)$$

$$\equiv Fe^{III} + H_2O_2 \rightarrow \equiv Fe^{III} \cdots H_2O_2 \rightarrow H^+ + \equiv Fe^{II} + \cdot O_2H \quad (7)$$

$$MB + \cdot OH \rightarrow\rightarrow CO_2 + H_2O \quad (8)$$

$$MB + \cdot O_2H \rightarrow\rightarrow CO_2 + H_2O \quad (9)$$

$$\cdot OH + H_2O_2 \rightarrow H_2O + \cdot O_2H \quad (10)$$

$$\cdot O_2H + H_2O_2 \rightarrow H_2O + \cdot OH + O_2 \quad (11)$$

$$\equiv Fe^{II} + \cdot OH \rightarrow \equiv Fe^{III} + OH^- \quad (12)$$

$$\equiv Fe^{III} + \cdot O_2H \rightarrow \equiv Fe^{II} + H^+ + O_2 \quad (13)$$

$$\cdot OH + \cdot O_2H \rightarrow H_2O + O_2 \quad (14)$$

$$\cdot O_2H + \cdot O_2H \rightarrow H_2O_2 + O_2 \quad (15)$$

At first, H_2O_2 was adsorbed on Fe_3O_4 NPs surface to form precursor surface complex $\equiv Fe^{III}\ldots H_2O_2$ and $\equiv Fe^{II}\ldots H_2O_2$, which might possess an inner- or an outer sphere surface coordination. The electron transfer between precursor surface complex produces $\equiv Fe^{II}$, $\cdot O_2H$, $\equiv Fe^{III}$, $\cdot OH$ (eq. (5), (6)). Radicals of $\cdot O_2H$ and $\cdot OH$ present in the H_2O_2- Fe_3O_4 nanoparticle system as shown in eqs (7), (8). Both $\cdot O_2H$ radicals and $\cdot OH$ radicals, having high oxidizing ability, can directly attack MB, resulting degradation and mineralization of MB. Further, the $\cdot O_2H$ and $\cdot OH$ radicals may react with the adsorbed H_2O_2 (eqs. (9), (10)), Fe(III), and Fe(II) sites on the nanoparticle surface (eqs. (11), (12)) or with each other (eqs. (13), (14)) to either terminate the chain or extend the reactions.

MB degradation by PbFeONPs were carried out in various sets of experiments to optimize the dose of iron oxide nanoparticle, H_2O_2 concentration, pH of the solution and duration for the dye degradation. MB degradation by PbFeONP alone was slow in absence of hydrogen peroxide. Upon addition of H_2O_2, MB was degraded almost completely after 140 minutes. This confirms degradation of MB by free radical pathway. In both the cases, MB degradation was more with increase in nanoparticle dosage. The effects of various parameters on MB degradation using PbFeONPs and H_2O_2 has been discussed below.

Effect of pH

The effect of pH on the degradation efficiency of methylene blue was studied at pH 3, 5, 7 and 9. As shown in **Figure 4.8**, MB degradation is effective at wide range of pH. However, at pH 3, MB degradation is 93.6% which is comparable to that of pH 9 i.e. 90.5 %. The degradation of MB is lower at pH 5 and 7. As explained in eqs. (5)-(13), presence of ferrous ion is important to initiate the reactions, leading to hydroxyl radical production which then degrades MB. Iron oxide and zero valent iron can be used as a source of ferrous ions in Fenton like process. Therefore, acidic pH is crucial for Fenton oxidation system. In acidic conditions the surface of the iron oxide nanoparticles corrodes and generates OH· radicals which is the reason for the maximum degradation efficiency at pH 3. In alkaline conditions H_2O_2 is unstable and perhydroxyl anion is easily formed which acts as a bleaching agent and due to which degradation efficiency increases at pH 9. Thus pH for MB degradation process was optimized at 3 which is in agreement with other studies (Reza et al., 2016; Jiang et al, 2011)

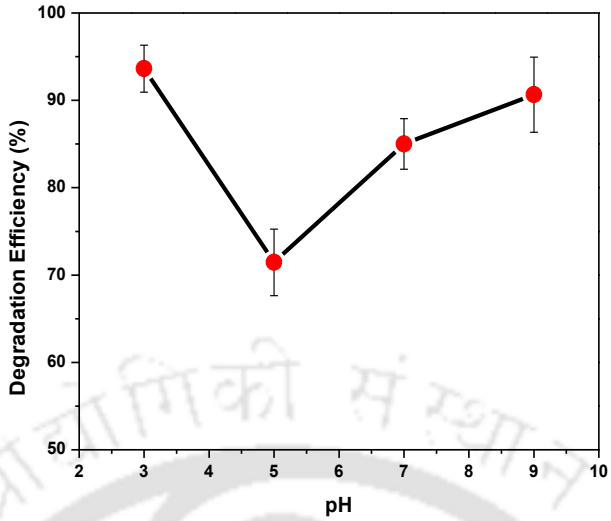

Figure 4.8 MB (20 mg/L) degradation by 0.3 mg/L PbFeONP at different pH conditions (3, 5, 7 and 9).

Effect of H_2O_2 and PbFeONP concentration

In this experiment, the effect of H_2O_2 concentration and effect of PbFeONP was studied simultaneously. Degradation of 20 mg/L MB is studied using varying concentration of H_2O_2 and PbFeONP at a range of 0.1-0.5 mM and 0.1-0.5 mg/ml, respectively along with negative controls. The pH of the solution was adjusted to 3 and reaction was allowed to proceed for 140 minutes at 25°C. **Figure 4.9** represents the effect of H_2O_2 and PbFeONP concentrations on MB degradation. This result depicts combined effect of different concentrations of PbFeONPs and H_2O_2. It can be inferred that highest degradation of 20 mg/L MB was observed at 0.3 mg/ml PbFeONPs and 0.1 mM H_2O_2.

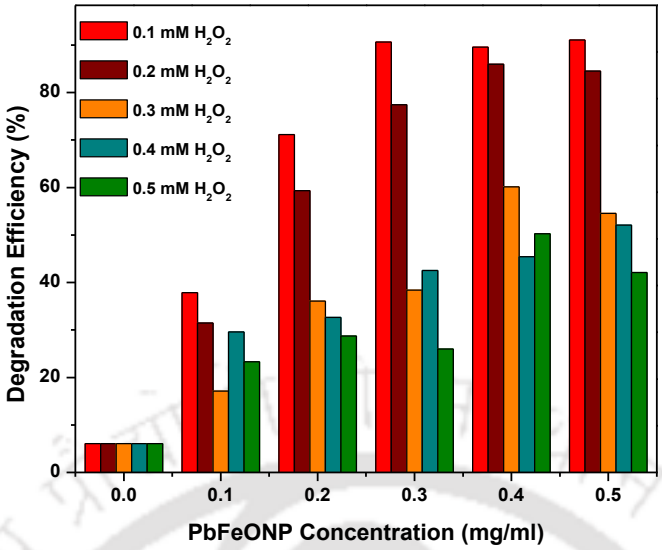

Figure 4.9 Effect of H_2O_2 and PbFeONP concentration on MB (20 mg/L) degradation.

The degradation efficiency of MB in presence of 0.3 mg/ml PbFeONP and varying concentration H_2O_2 has been represented in **Figure 4.10**. In this study, it is observed that the degradation process was highest at 0.1 mM concentration and the degradation efficiency decreased with the increasing concentration of H_2O_2 from 0.2-0.5 mM. The excessive adsorption of H_2O_2 on PbFeONP surface limits the degradation of MB dye. Moreover excessive H_2O_2 could induce OH· radical scavenging effect lessening the degradation efficiency (Luo et al., 2010). Therefore H_2O_2 concentration was optimized at 0.1 mM, as higher concentration reduced the degradation efficiency of MB. The degradation efficieny increased when PbFeONP concentration increased from 0.1-0.3 mg/ml in presence 0.1 mM H_2O_2 presented in **Figure 4.11**. However, the degradation efficiency remained constant when PbFeONP concentration increased further from 0.3-0.5 mg/ml. The percentage degradation of the MB was negligible in absence of PbFeONP. With the addition of PbFeONP the

efficiency increased significantly as the nanoparticle acted as peroxidase-like catalyst and accelerated the decomposition of the H_2O_2 resulting in burst of oxidizing radical species (Jiang et al., 2011). However, when PbFeONP dose increased beyond 0.3 mg/ml there was very less change in degradation and equilibrium was achieved.Therefore the optimized concentration of H_2O_2 and PbFeONP were 0.1 mM and 0.3 mg/ml, respectively.

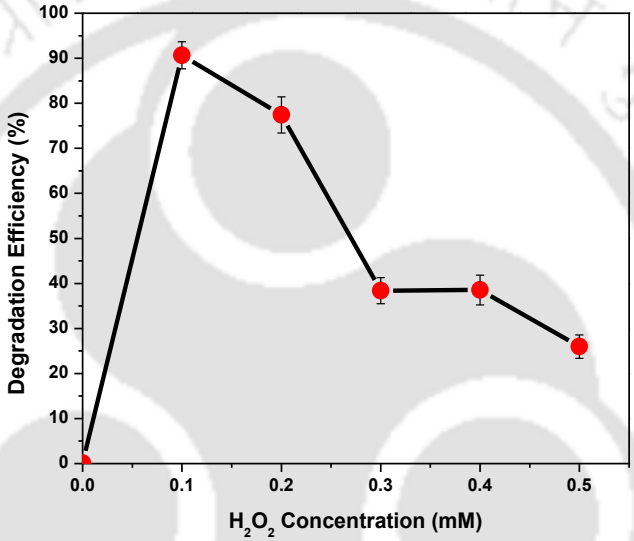

Figure 4.10 Effect of H_2O_2 concentration on MB (20 mg/L) degradation by PbFeONP

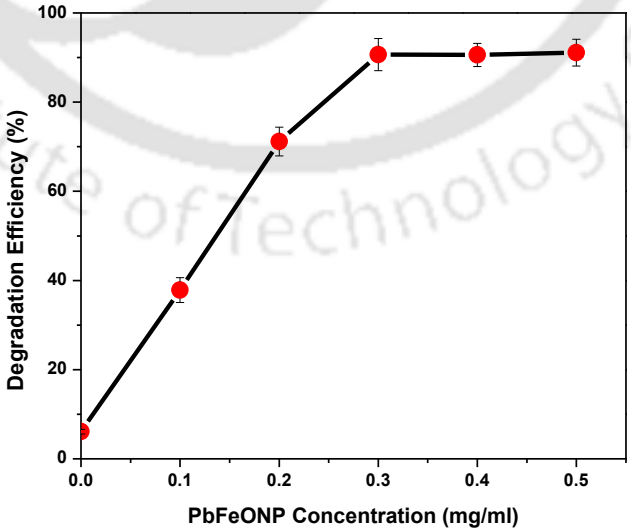

Figure 4.11 Effect of PbFeONP dose on MB (20 mg/L) degradation.

Effect of time

MB degradation was studied at different time interval in presence of 0.3 mg/ml PbFeONP, 0.1 mM H_2O_2 and pH at 3 . The result is depicted in **Figure 4.12.** The experiments were carried out with controls including the one with MB and PbFeONP and another with MB and H_2O_2. There was almost no degradation of MB in absence of Fenton's catalysts and very less i.e. 2.4% of MB was degradaed when added with PbFeONP. However, 24.2% of MB was degraded in presence of 0.1 mM H_2O_2 alone. 91.3 % of 20 mg/L of MB was degraded after 140 minutes of PbFeONP and H_2O_2 addition. The results suggest that as the time progresses degradation efficiency of MB increased exponentially from 0% to 73% in 0-80 minutes interval. However, the degradation efficiency increased slowly after 80 minutes from 83%-91% at 100-140 minutes interval.

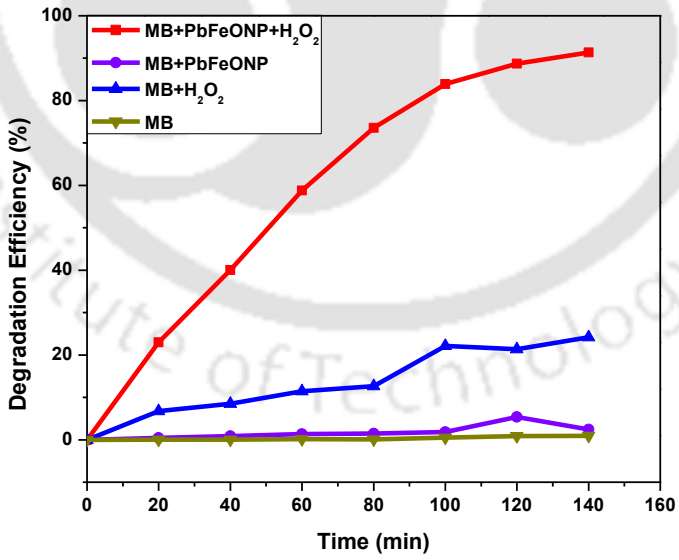

Figure 4.12 MB (20 mg/L) degradation by PbFeONP (0.3 mg/L) at different time intervals.

The experimental data were fitted with first-order model to understand the reaction kinetics of MB degradation by PbFeONP. First-order kinetic model is expressed by eq (16), where C and C_0 are the initial and apparent concentrations of MB, respectively, and K is the kinetic rate constant, which can be calculated from the slope of the straight line (Yang et al., 2009).

$$ln\left(\frac{C}{C_0}\right) = -Kt \quad (16)$$

A first order linear relationship was obtained when Ln(C/C_0) versus reaction time was plotted from the experimental data obtained from the degradation of 20 mg/L MB using 0.3 mg/ml PbFeONP and 0.1 mM H_2O_2 at pH 3 and 25°C **(Figure 4.13)**. The MB degradation followed first order kinetics The rate constant was calculated from the slope i.e. 18.5 × 10^{-3} min^{-1} which is much higher than 4.34 × 10^{-4} min^{-1}, reported by Yang et al. (2009), using magnetite as an catalyst and 300 mmol L^{-1} H_2O_2.

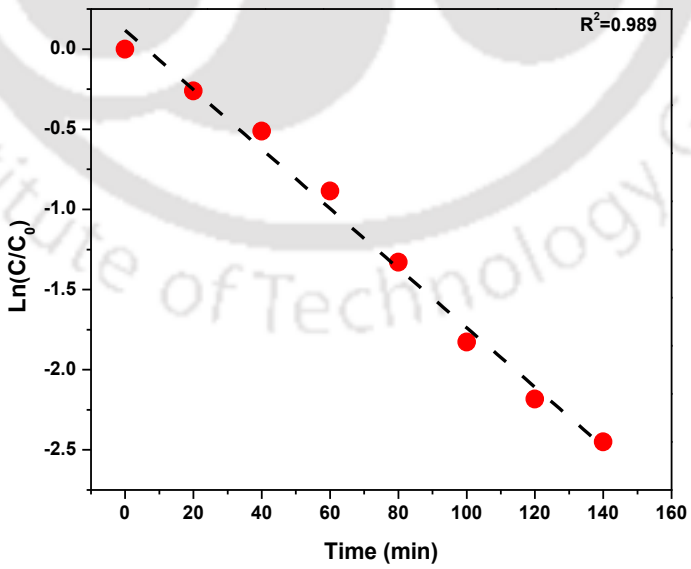

Figure 4.13 First order kinetics of MB degradation.

Effect of MB concentration

The degradation efficiencies of the MB at different initial concentrations were presented in **Figure 4.14**. The figure illustrates decreasing trend of MB degrdation efficincies with increasing initial concentrations. The experiments were performed at pH 3, using 0.3 mg/ml PbFeONP, 0.1 mM H_2O_2 and varying concentrations of MB from 20-50 mg/L. Degradation efficiency decreased with the increase in MB concentration at 140 minutes. However, the degradation efficiencies of MB were equal when duration of the reaction increased. From this it can be interpreted as rate of the degradation decreased as the number of moles of MB was increased for a constant amount of hydroxyl radicals generated at given time interval.

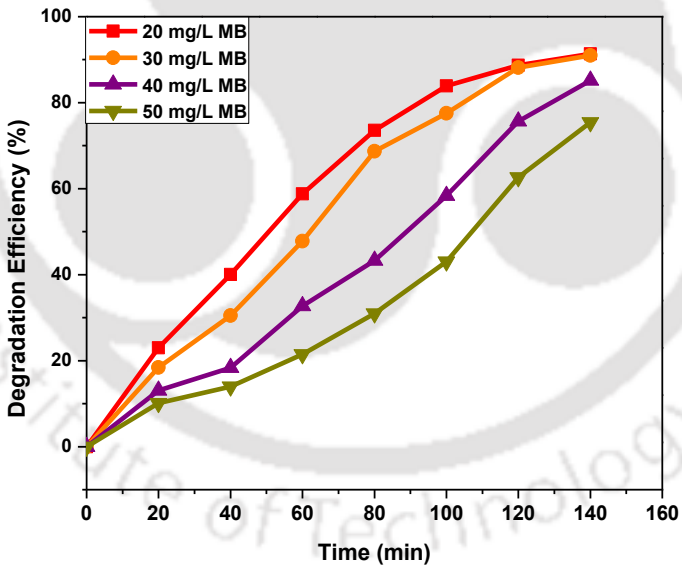

Figure 4.14 MB degradation by PbFeONP (0.3 mg/ml) at different initial concentrations.

Reuse of PbFeONPs

To evaluate the stablility of the PbFeONPs, degradation of MB at 20 mg/L concentration were carried out using 0.3 mg/ml PbFeONP in the presence of H_2O_2 for four cycles. After each cycle the nanoparticles were separated, dried and used for the next cycle of MB degradation process. After fourth cycle the removal of MB was 90% within 140 minutes **(Figure 4.15)**. Therefore PbFeONPs with H_2O_2 can be reused for MB degradation.

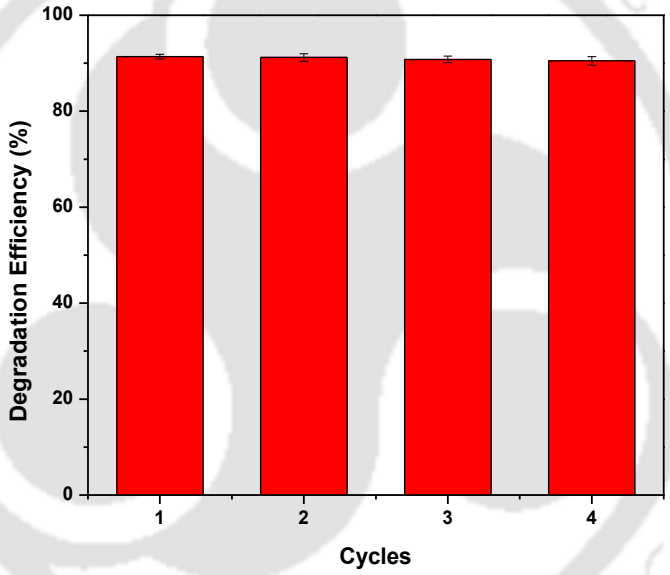

Figure 4.15 Reuse of PbFeONP for MB (20 mg/L) degradation

4.5 CONCLUSION

Persea bombycina, the primary host plant of muga silkworm was explored for the synthesis of iron oxide nanoparticles. Thus synthesized PbFeONPs were characterized for their physical, chemical and magnetic properties. PbFeONPs synthesized were ferromagnetic with 26.5 emu/g magnetization. TEM studies

confirmed their size to be in nano-range. The crystallinity and the phase purity of the nanoparticles were confirmed by XRD studies and supported by UHRTEM and SAED studies. Presence of functional groups was studied using FTIR spectroscopy which insisted the successful capping of the nanoparticles. PbFeONPs are thermally stable and can sustain at higher temperature which was concluded from TGA analysis. Cell toxicity of the PbFeONPs on mouse fibroblast cell lines L929, was studied by MTT assay and found to be biocompatible at concentrations <50 μg/ml.

Its applications as Fenton's catalyst in methylene blue dye degradation was also studied. 90% of 20 mg/L MB dye was degraded when added with 0.3 mg/ml PbFeONP was added along with 0.1 mM H_2O_2 after 140 minutes. Effect of pH, initial concentrations, nanoparticle doses, H_2O_2 concentrations and time were studied for MB removal. The PbFeONPs were reusable as 90% of MB was removed after 4^{th} cycle of reuse. Synthesis of metallic nanoparticles using plant extract has lowered the cost of synthesis largely. In further research, these magnetic nanoparticles can be surface coated to minimize their cytotoxicity.

4.6 REFERENCES

Abkenar, S. D., Khoobi, M., Tarasi, R., Hosseini, M., Shafiee, A., & Ganjali, M. R. (2014). Fast removal of methylene blue from aqueous solution using magnetic-modified Fe_3O_4 nanoparticles. *Journal of Environmental Engineering*, 141(1), 1-7.

Badmapriya, D., & Asharani, I. V. (2016). Dye degradation studies catalysed by green synthesized Iron oxide nanoparticles. *International Journal of ChemTech Research*, 9(06), 409-416.

Basavegowda, N., Magar, K. B. S., Mishra, K., & Lee, Y. R. (2014). Green fabrication of ferromagnetic Fe_3O_4 nanoparticles and their novel catalytic applications for the synthesis of biologically interesting benzoxazinone and benzthioxazinone derivatives. *New Journal of Chemistry*, 38(11), 5415-5420.

Basavegowda, N., Mishra, K., & Lee, Y. R. (2014). Sonochemically synthesized ferromagnetic Fe_3O_4 nanoparticles as a recyclable catalyst for the preparation of pyrrolo [3, 4-c] quinoline-1, 3-dione derivatives. *RSC Advances*, 4(106), 61660-61666.

Bhandari, S., Khandelia, R., Pan, U. N., & Chattopadhyay, A. (2015). Surface complexation-based biocompatible magnetofluorescent nanoprobe for targeted cellular imaging. *ACS Applied Materials & Interfaces*, 7(32), 17552-17557.

Chaki, S. H., Malek, T. J., Chaudhary, M. D., Tailor, J. P., & Deshpande, M. P. (2015). Magnetite Fe3O4 nanoparticles synthesis by wet chemical reduction and their characterization. *Advances in Natural Sciences: Nanoscience and Nanotechnology*, *6*(3), 1-6.

Ehrampoush, M. H., Miria, M., Salmani, M. H., & Mahvi, A. H. (2015). Cadmium removal from aqueous solution by green synthesis iron oxide nanoparticles with tangerine peel extract. *Journal of Environmental Health Science and Engineering*, 13(1), 1-7.

El-Kassas, H. Y., Aly-Eldeen, M. A., & Gharib, S. M. (2016). Green synthesis of iron oxide (Fe_3O_4) nanoparticles using two selected brown seaweeds: characterization and application for lead bioremediation. *Acta Oceanologica Sinica*, 35(8), 89-98.

Es'haghi, Z., Vafaeinezhad, F., & Hooshmand, S. (2016). Green synthesis of magnetic iron nanoparticles coated by olive oil and verifying its efficiency in extraction of nickel from environmental samples via UV–vis spectrophotometry. *Process Safety and Environmental Protection*, 102, 403-409.

Jiang, J., Zou, J., Zhu, L., Huang, L., Jiang, H., & Zhang, Y. (2011). Degradation of methylene blue with H_2O_2 activated by peroxidase-like Fe_3O_4 magnetic nanoparticles. *Journal of Nanoscience and Nanotechnology*, 11(6), 4793-4799.

Latha, N., & Gowri, M. (2014). Biosynthesis and characterisation of Fe_3O_4 nanoparticles using Caricaya papaya leaves extract. *International Journal of Scientific Research*, 3(11), 1551-1556.

Luo, W., Zhu, L., Wang, N., Tang, H., Cao, M., & She, Y. (2010). Efficient removal of organic pollutants with magnetic nanoscaled $BiFeO_3$ as a reusable heterogeneous Fenton-like catalyst. *Environmental Science & Technology*, 44(5), 1786-1791.

Majewski, P., & Thierry, B. (2007). Functionalized magnetite nanoparticles—synthesis, properties, and bio-applications. *Critical Reviews in Solid State and Materials Sciences*, 32(3-4), 203-215.

Narayanan, S., Sathy, B. N., Mony, U., Koyakutty, M., Nair, S. V., & Menon, D. (2011). Biocompatible magnetite/gold nanohybrid contrast agents via green chemistry for MRI and CT bioimaging. *ACS Applied Materials & Interfaces*, 4(1), 251-260.

Reza, K. M., Kurny, A. and Gulshan, F. (2016) Photocatalytic Degradation of Methylene Blue by Magnetite+H_2O_2+UV Process. *International Journal of Environmental Science and Development*, 7(5), 325-329.

Saif, S., Tahir, A., & Chen, Y. (2016). Green synthesis of iron nanoparticles and their environmental applications and implications. *Nanomaterials*, 6(11), 209.

Senthil, M., & Ramesh, C. (2012). Biogenic synthesis of fe_3O_4 nanoparticles using *Tridax procumbens* leaf extract and its antibacterial activity on *Pseudomonas aeruginosa*. Digest *Journal of Nanomaterials & Biostructures*, 7(3), 1655-1660.

Sett, A., Gadewar, M., Sharma, P., Deka, M., & Bora, U. (2016). Green synthesis of gold nanoparticles using aqueous extract of *Dillenia indica*. *Advances in Natural Sciences: Nanoscience and Nanotechnology*, 7(2), 1-8.

URL:https://www.boundless.com/chemistry/textbooks/virtual-textbook-of-organic-chemistry/spectroscopy-8/infrared-spectroscopy-49/group-frequencies-186-16073/

Venkateswarlu, S., Rao, Y. S., Balaji, T., Prathima, B., & Jyothi, N. V. V. (2013). Biogenic synthesis of Fe_3O_4 magnetic nanoparticles using plantain peel extract. *Materials Letters*, 100, 241-244.

Vijayakumar, S., & Ganesan, S. (2012). In vitro cytotoxicity assay on gold nanoparticles with different stabilizing agents. *Journal of Nanomaterials*, 2012, 1-9.

Wu, C.C., and Chen, D. H., (2012) Spontaneous synthesis of gold nanoparticles on gum arabic-modified iron oxide nanoparticles as a magnetically recoverable nanocatalyst. *Nanoscale Research Letters* 7, 317, 1-7

Yang, S., He, H., Wu, D., Chen, D., Ma, Y., Li, X., Zhu, J. & Yuan, P. (2009). Degradation of methylene blue by heterogeneous Fenton reaction using titanomagnetite at neutral pH values: process and affecting factors. *Industrial & Engineering Chemistry Research*, 48(22), 9915-9921.

Yew, Y. P., Shameli, K., Miyake, M., Kuwano, N., Khairudin, N. B. B. A., Mohamad, S. E. B., & Lee, K. X. (2016). Green synthesis of magnetite (Fe_3O_4) nanoparticles using seaweed (*Kappaphycus alvarezii*) extract. *Nanoscale research letters*, 11(1), 1-7.

Zhang, Y., Chen, Y., Westerhoff, P., Hristovski, K., & Crittenden, J. C. (2008). Stability of commercial metal oxide nanoparticles in water. *Water research*, 42(8), 2204-2212.

Zhou, L., Shao, Y., Liu, J., Ye, Z., Zhang, H., Ma, J., Jia, Y., Gao, W. & Li, Y. (2014). Preparation and characterization of magnetic porous carbon microspheres for removal of methylene blue by a heterogeneous Fenton reaction. *ACS Applied Materials & Interfaces*, 6(10), 7275-7285.

CHAPTER 5

Summary and Future prospects

CHAPTER 5

Summary and Future Prospects

5.1 SUMMARY

The present study was focused on the exploration of silkworm host plants for the synthesis of metallic nanoparticle employing their reducing and stabilizing capabilities. The synthesized nanoparticles were characterized using various biophysical techniques. Various applications of these synthesized nanoparticles were studied. A summary of the chapters is provided below.

5.1.1 Green synthesis of silver nanoparticles using *Ricinus communis* var *carmencita* leaf extract and their applications.

Ricinus communis var carmencita (Red castor) is one of the primary host plant of eri silkworm (*Samia cynthia ricini*). A peak at 442 nm was obtained in UV visible spectroscopy, when methanolic extract of *R. communis* leaves was added to 1 mM $AgNO_3$ solution at 1:3 ratio at room temperature. The time required for the synthesis of silver nanoparticle was optimized for 24 hours. The synthesized silver nanoparticles (RcAgNPs) were characterized by biophysical techniques. TEM studies confirmed the size of the RcAgNPs ranging between 30-40 nm. UHRTEM images and SAED studies confirmed the crystallinity of the nanoparticle. XRD result was in agreement with the literature and confirmed the crystallinity of the nanoparticle. The stability of the RcAgNPs depends on the capping of the nanoparticles which was studied by FTIR and TGA analysis. The presence of functional groups such as amide

groups indicated by FTIR peak analysis. Similarly TGA analysis also suggested presence of organic compounds on nanoparticle surface due to the mass loss at 440°C. RcAgNPs were non-toxic to mouse fibroblast cell lines at lower concentrations. RcAgNPs has antibacterial activity against both gram positive (*Bacillus subtillis, Streptococcus zooepidemicus, and Staphylococcus aureus*) and gram negative (*Escherichia coli and Enterobacter aerogenes*) bacteria.

5.1.2 Green synthesis of zinc oxide nanoparticles using *Heteropanax fragrans* leaf extract and their applications.

Heteropanax fragrans (Kesseru) is also a primary host plant of eri silk worm. Zinc oxide nanoparticles (KeZnONP) were prepared using aqueous extract of *H. fragrans* leaves and zinc nitrate hexahydrate. Zinc oxide powder was obtained after calcination of the precipitate obtained. A peak at 382 nm was obtained in UV-visible spectroscopy studies of KeZnONP and the band gap was calculated to be 3.24 eV. The size of the nanoparticle was evaluated by TEM studied and found to be 19-22 nm. UHRTEM and SAED studies supported the crystallinity of the nanoparticle. XRD data revealed the wurtzite structure of the synthesized KeZnONP. FTIR peaks suggest presence of functional groups such as amide group (C=O), alkane (C-H) and alkyne (C≡C) groups, which ensured capping of the nanoparticles with various phytochemicals and hence their stability. TGA analysis also confirmed the presence of organic compounds on KeZnONP surface. The rate of degradation of 5 mg/L methylene blue, by 1 mg/ml KeZnONP at 25°C and pH 7 was calculated to be 9.79×10^{-3} min^{-1}.

5.1.3 Green synthesis of iron oxide nanoparticles using *Persea bombycina* leaf extract and their applications.

Persea bombycina (Som) is a primary host plant of muga silkworm (*Antheraea assamensis*). Iron oxide nanoparticles were synthesized using aqueous extract *P. bombycina* leaves. 2 ml of the extract was added to a solution containing $FeCl_3$ and $FeCl_2$ (2:1 molar ratio). The iron oxide nanoparticles (PbFeONPs) precipitated when the pH was adjusted to 11. Magnetization of value 26.5 emu/g and coercivity of value 50.5 G were obtained from VSM analysis. The size of PbFeONPs were in 12-15 nm range as confirmed by TEM analysis. XRD analysis confirmed the presence of Fe_3O_4 nanoparticles and the crystallinity of the nanoparticles. UHRTEM and SAED analysis further supported the crystallinity of PbFeONP. Presence of several FTIR peaks corresponding to alcohol, amine, nitro and alkene functional groups on PbFeONP surface indicated successful capping and their stability. TGA analysis also suggested the presence of organic compounds and hence their stability. The biocompatibility of the PbFeONPs was studied by MTT assay and found that these were non toxic to mouse fibroblast cell line at concentrations <50 μg/ml and moderately toxic at 60-90 μg/ml concentrations.

90% of methylene blue of 20 mg/L concentration was degraded after 140 minutes of adding PbFeONP (0.3 mg/ml dose) along with H_2O_2 (0.1 mM). The degradation rate of methylene blue was 18.5×10^{-3} min^{-1} . The PbFeONPs can be recycled as 90% of methylene blue was removed after 4^{th} cycle of reuse.

5.2 FUTURE PROSPECTS

Our attempt to synthesize metallic nanoparticles using indigenous plants extracts discovered the potential of these plants in nanoparticle biosynthesis. We have successfully characterized the synthesized nanoparticles with biophysical techniques. We have also evaluated their applications in various areas. However, at the end of the investigations we could foresee many areas in which further studies could yield potentially new and beneficial information as summarized below.

- The RcAgNPs synthesized, exhibited antibacterial activity against gram positive and gram negative bacterial strains and were non-toxic to normal mouse fibroblast cell lines. Therefore an antibacterial ointment or band aid can be formulated using these silver nanoparticles.
- The synthesized KeZnONPs exhibited photocatalytic property. Therefore in future, these ZnO nanoparticles can be used for waste water treatment.
- The synthesized PbFeONPs exhibited catalytic activity and magnetic property. As catalyst these iron oxide nanoparticles can be used for degradation of organic pollutant. The magnetic PbFeONPs can also be tested for their efficiency in bio-imaging such as MRI and drug delivery in future.
- Together these particles can be combined into a candle for water purification so that the three nanoparticles can act simultaneously to decontaminate the water.

List of Publications

1. Ojha, S., Sett, A., & Bora, U. (2017). Green Synthesis of Silver NPs by *Ricinus communis* var. *carmencita* Leaf Extract and its Antibacterial Study. *Advances in Nanosciences: Nanoscience and Nanotechnology*, 8, 1-8.
2. Ojha, S., Singh, D., Sett, A., Chetia, H., Kabiraj, D. & Bora, U (2018). Nanotechnology in Crop Protection. In *Nanomaterials in Plants, Algae and Micro-organism: Concepts and Controversies (Vol 1)*. Academic Press, 345-390.

Manuscript Submitted

3. Ojha, S., Saikia, D. & Bora, U. (2018). Nanopharmaceuticals: Synthesis, Characterization and Challenges. In *Nanopharmaceuticals: Principles and Applications*. Environmental Chemistry for a Sustainable World.

Manuscript under preparation/review

1. Green synthesis, characterization and application of Zinc Oxide NPs using *Heteropanax fragrans* (Roxb) leaf extract (Under Preparation)
2. Green synthesis, characterization and application of Iron Oxide NPs using *Persea bombycina* (King ex Hook. F.) leaf extract (Under Preparation)

List of Presentations

Oral Presentation

1. Ojha, S. and Bora, U. International Conference on Advances in Nanotechnology 2017, held at Assam Don Bosco University, Guwahati during 9th-13th January, 2017.
2. Ojha, S. and Bora, U. Omics Technology and Biodiversity, 2017 held at IIT Guwahati on 19th June 2017.

Poster Presentation

1. Ojha, S. and Bora, U. North East Pharmaceutical Convention 2017, held at Girijananda Chowdhury Institute of Pharmaceutical Science, Guwahati during 6th -7th May 2017.
2. Ojha, S. International Conference on Disease Biology and Therapeutics 2014 held at IASST, Guwahati during 3rd -5th December, 2014.

Training/Workshop

1. Next Generation Sequencing and Data Analysis, organized by Biotech Hub, Centre for the Environment, IIT Guwahati, held during 14th -17th May, 2014
2. Techniques in Metagenomics, organized by Institutional Biotech Hub, IASST, Guwahati on 26th-28th November 2013.
3. Exploitation of Seribiodiversity for Novel Product Development, organized by Unit of Excellence on Seribiodiversity, Centre for the Environment, IIT Guwahati (sponsored by DBT Govt. of India) during 29th-30th November 2014.

Vitae

Sunita Ojha was born on May 15, 1988 in the silver city of India, Cuttack, (Odisha). She completed her Secondary Examination conducted by Odisha Board of Secondary Education (10th Class), Odisha in 2003 and Higher Secondary Examination conducted by Odisha Council of Higher Secondary Education (12th Class), Odisha in 2005. She completed her Bachelor in Science with Botany honors in 2009 from Khallikote Autonomous College, Berhampur under Berhampur University. She completed her M.Sc. (Biotechnology) from VIT University, Vellore, Tamil Nadu, India in 2011. The author joined the Ph.D. program in July, 2012 at Department of Biosciences and Bioengineering, Indian Institute of Technology Guwahati, Guwahati-781 039, Assam, India. She successfully completed the course work with 8.6/10 CPI. She received Institute Fellowship (IIT Guwahati) under the funding by Ministry of Human Resource and Development (MHRD), New Delhi. Her thesis work focusses on green synthesis of metallic nanoparticles and their various applications. She has synthesized silver, zinc oxide and iron oxide nanoparticles using silkworm host plants. During her thesis work she has published one research article. She has published a book chapter on “Nanotechnology in Crop Protection”. She has also submitted another book chapter on “Nanopharmaceuticals: Synthesis, Characterization and Limitation”.

Green synthesis of silver nanoparticles by *Ricinus communis* var. *carmencita* leaf extract and its antibacterial study

2017 Adv. Nat. Sci: Nanosci. Nanotechnol. 8 035009

(http://iopscience.iop.org/2043-6262/8/3/035009)

OPEN ACCESS
IOP Publishing
Advances in Natural Sciences: Nanoscience and Nanotechnology
Adv. Nat. Sci.: Nanosci. Nanotechnol. **8** (2017) 035009 (8pp)
https://doi.org/10.1088/2043-6254/aa724b

Green synthesis of silver nanoparticles by *Ricinus communis* var. *carmencita* leaf extract and its antibacterial study

Sunita Ojha[1], Arghya Sett[1] and Utpal Bora[1,2]

[1] Bioengineering Research Laboratory, Department of Biosciences and Bioengineering, Indian Institute of Technology Guwahati, Guwahati, Assam 781039, India
[2] Mugagen Laboratories Pvt. Ltd, Technology Incubation Centre, Indian Institute of Technology Guwahati, Guwahati, Assam 781039, India

E-mail: ubora@iitg.ernet.in

Received 25 August 2016
Accepted for publication 10 April 2017
Published 17 July 2017

Abstract

In this study, we report synthesis of silver nanoparticles (RcAgNPs) from silver nitrate solution using methanolic leaf extract of *Ricinus communis* var. *carmencita.* The polyphenols present in the leaves reduce Ag^{++} ions to Ag^{0} followed by a color change. Silver nanoparticle formation was ensured by surface plasmon resonance between 400 nm to 500 nm. Crystallinity of the synthesized nanoparticles was confirmed by UHRTEM, SAED and XRD analysis. The capping of phytochemicals and thermal stability of RcAgNPs were assessed by FTIR spectra and TGA analysis, respectively. It also showed antibacterial activity against both gram positive and gram negative strains. RcAgNPs were non-toxic against normal cell line (mouse fibroblast cell line L929) at lower concentrations (80 μg ml^{-1}).

Keywords: *Ricinus communis* var. *carmencita*, silver nanoparticles, green synthesis, TEM studies, anti-bacterial activity
Classification numbers: 2.04, 4.02

1. Introduction

Nanotechnology being an interdisciplinary research area imparts broad spectrum applications in medicines, biomedical sciences, drug and gene delivery, cosmetics, food and feed, mechanics, optics, electronics, energy science, optoelectronic applications, single electron transistors, space industries and chemical industries. The unique physicochemical characteristics such as size, distribution and morphology, surface plasmon resonance (SPR) of the nanoparticles have been explored to meet the current research trends. Among other metallic nanoparticles, silver nanoparticles (AgNPs) offer various applications in biomedical field. Although non-toxic to animal cells, the toxicity of silver nanoparticle to bacterial cells makes them a safe and effective bactericidal agent [1]. Apart from medicines/drugs, they are also used in household products like toothpaste, shampoo, washing machines, water purifiers, humidifiers, cloth, paints, electronics etc [2]. Considering their wide applications, synthesis of silver nanoparticles of unique size with a characteristic dispersity and composition is a key area of research [3]. The silver nanoparticles can be synthesized by physical, chemical or biological cues. Vapor condensation and arc discharge are common physical methods of AgNPs synthesis [4]. AgNPs are also chemically synthesized by reduction process, photochemical method (irradiation), electrochemical (electrolysis) and pyrolysis method. Plants and microorganisms are explored as biological source for nanoparticle synthesis which is referred as 'green synthesis' of silver nanoparticles [5]. Microorganisms trap metal ions from environment and convert them to nanoparticles by enzymatic process. Plants contain strong reducing agents such as polyphenols, terpenoids, phenolic acids, alkaloids, sugars

and proteins which are key players for bio reduction of silver ions (Ag^{++}) due to presence of several −OH groups [6]. In contrary to physical and chemical method, green synthesis of nanoparticles uses and generates minimal environmentally harmful chemicals. Thus this is an efficient, inexpensive and environment friendly method to synthesize immensely important nanoparticles [7].

Silver nanoparticles have been widely explored as antimicrobials along with other application areas such as optoelectronics, biosensors, catalysis and surface enhanced Raman scattering (SERS) [8]. Ag^{+} ion as an anti-bacterial agent is delimited by it's easy inactivation through complexation and precipitation, whereas silver nanoparticle possess higher bactericidal activity due to its larger surface area [9, 10]. These nanoparticles inhibit bacterial cell division causing membrane damage and increased cell permeability which finally leads to cell death [11]. Bacterial proliferation also decreases when the functional groups present on nanoparticle surface interact with bacterial membrane proteins, phospholipids, lipoproteins and lipotechoic acids and declining their colonization and surface adherence [12].

Recent reports suggest the synthesis of silver nanoparticles using *Averrhoa carambola* fruit extract and *Solidago altissima* leaf extract having antibacterial and photocatalytic properties [13, 14]. Moreover green synthesis of silver nanoparticles has also been carried out using an endophytic fungi *Penicillium* species of *Glycosmis mauritiana* [15]. The extract from *Padina tetrastromaticai* and carbohydrates secreted from microalgae *Chlorella vulgaris* has also been used to synthesize silver nanoparticles having anticancer activities [16, 17].

In this paper we have exploited *Ricinus communis* var. *carmencita* leaf extract as 'green chemical' to synthesize silver nanoparticle (RcAgNP). We further characterized its physical, optical and thermal property along with its antibacterial activity against gram positive and gram negative strains.

2. Materials and methods

2.1. Preparation of leaf extract

Ricinus communis var. *carmencita* leaves were collected from the IIT Guwahati campus, Guwahati, India. Leaves were cleaned, dried in shade and ground to fine powder. Methanolic extract of the leaves was prepared by cold maceration process [18]. The extract was evaporated to dryness under reduced pressure and further solubilized in methanol to a final concentration of 1.0 mg ml^{-1}.

2.2. Estimation of antioxidant activity of leaf extract

Antioxidant activity of *Ricinus communis* var. *carmencita* leaf extract was assessed by 2, 2-diphenyl-1-picrylhydrazyl (DPPH) standard method with minor modifications [19]. Various concentrations (10–100 μg ml^{-1}) of ascorbic acid and extract were prepared from 1 mg ml^{-1} concentration in methanol. 0.1 mM DPPH was mixed with extract in 9:1 (v/v) ratio and kept for 30 min in dark at room temperature. In this assay ascorbic acid was used as standard and DPPH as blank. Absorbance was measured at 517 nm in UV–Vis spectrophotometer (Tecan i-control, 1.11.1.0). The percentage inhibition was calculated using the following formula

$$\text{Inhibition}(\%) = \frac{A_C - A_S}{A_C} \times 100,$$

where A_C is absorbance of control and A_S is absorbance of sample at 517 nm.

2.3. Estimation of total phenolic content of leaf extract

Total phenolic content was estimated using Folin–Ciocalteu reagent [20]. 0.5 ml of leaf extract (1 mg ml^{-1}) was mixed with 2.5 ml of 10% Folin–Ciocalteu reagent. Another 2.5 ml of sodium carbonate was added followed by incubation at 45 °C for 45 min. Then absorbance was measured at 765 nm using UV–Vis spectrophotometer (Tecan i-control, 1.11.1.0). Different concentrations of gallic acid standard (10–100 μg ml^{-1}) were prepared in methanol. The total phenolic content of the extract was determined from the linear equation obtained from gallic acid standard curve [21].

2.4. Green synthesis of silver nanoparticle using Ricinus communis var. carmencita leaf extract

In a 1 ml reaction mixture, 10 μg ml^{-1} leaf extract (in methanol) was added to 1 mM silver nitrate solution (in miliQ) at different ratios 1:1, 1:2 and 1:3, and the volume was made up by addition of water. The solution was mixed by gentle shaking and kept at room temperature for 24 h. Then absorbance was scanned from 300–800 nm wavelength by UV–Vis spectrophotometer (Tecan i-control, 1.11.1.0)

After 24 h, the reaction mixture was centrifuged at 13 000 rpm for 10 min to pellet down the silver nanoparticles (RcAgNPs). Then the pellet was washed with deionized water to remove leaf extract residues. This step was repeated twice and lyophilized to obtain RcAgNPs in powder form to be used for further characterization.

2.5. Characterization of RcAgNP

2.5.1. UV–Vis spectroscopy. In a 1 ml reaction volume, varying ratio (1:1, 1:2 and 1:3) of leaf extract and silver nitrate solution were mixed and kept for 24 h at room temperature. Absorbance of synthesized silver nanoparticle was measured at UV–Vis spectrum i.e. 300 nm–800 nm wavelength using UV–Vis spectrophotometer (Tecan i-control, 1.11.1.0).

2.5.2. Transmission electron microscope (TEM) studies. The silver nanoparticles were suspended in deionized water and sonicated. A drop of dispersed RcAgNP was placed on a copper grid and kept at 37 °C for drying. Transmission electron microscopy was performed to confirm the size of the nanoparticles (Make: JEOL, Model: JEM-100 CX II).

2.5.3. X-ray diffraction (XRD) studies. A thin film of uniformly water suspended RcAgNP was prepared on a glass slide and kept for drying. X-ray diffraction (XRD) studies of

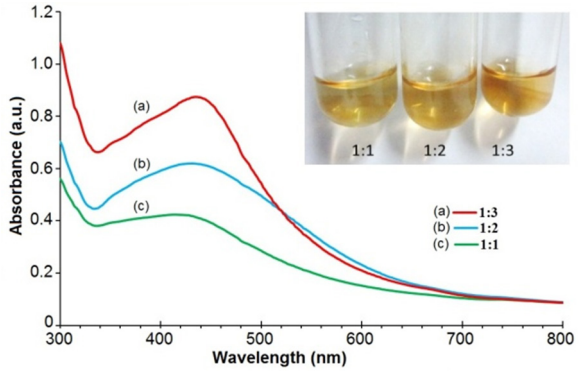

Figure 1. UV–Vis absorption spectra of nanoparticle synthesized at different ratios (1:1, 1:2 and 1:3) of leaf extract (10 μg ml^{-1}) to $AgNO_3$ solution (1 mM) at room temperature. Inset: silver nanoparticle synthesis showing color change with change in ratio of plant extract and $AgNO_3$ solution.

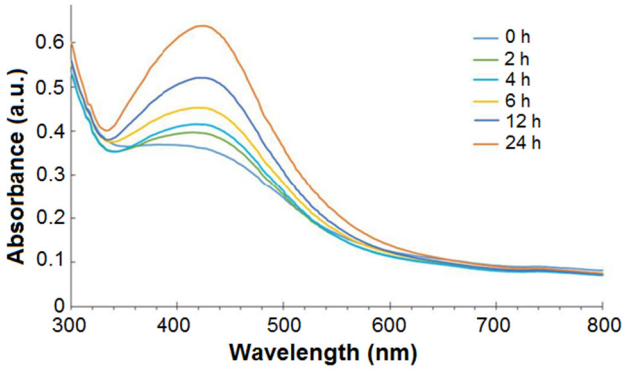

Figure 2. UV–Vis absorption spectrum of RcAgNPs at different time intervals.

the RcAgNP thin film was carried out in x-ray diffractometer at 2theta/theta scanning mode (operational voltage 50 kV and current 180 mA, Cu-Kα radiation $\lambda = 1.540$ Å with 20 min^{-1} scanning rate).

2.5.4. Fourier transform infrared (FTIR) analysis. Leaf extract dissolved in methanol was used for FTIR analysis. RcAgNPs were suspended in water and sonicated to get a uniform suspension. FTIR analysis of leaf extract and RcAgNPs was carried out using IRAffinity-1 (Shimadzu) by ATR method in transmittance mode from 600 cm^{-1} to 4000 cm^{-1} with resolution at 4.0 cm^{-1}.

2.5.5. Thermogravimetric analysis (TGA) and differential thermal analysis (DTA). The STA7200 thermal analysis system, Hitachi was used to perform TGA and DTA studies. The RcAgNPs in powder form obtained after lyophilization was used for TGA and DTA analysis. An alumina crucible tied with another crucible (reference) was cleaned with acetone and kept next to the other without touching each other. 8.6 mg of RcAgNP was kept in the crucible and subjected to heating at 10 °C min^{-1} increasing rate from 40 °C to 900 °C with constant flow of nitrogen gas at a flow rate 40 ml min^{-1}. Nitrogen gas level was checked regularly in between the analysis.

2.5.6. Antibacterial studies. Antibacterial studies were carried out by resazurin method with two gram negative strains (*Enterobacter aerogenes* (*E. aerogenes*) and *Escherichia coli* (*E. coli*)) and three gram positive strains (*Bacillus subtilis* (*B. subtilis*), *Streptococcus zooepidemicus* (*S. zooepidemicus*) and *Staphylococcus aureus* (*S. aureus*)).

2.5.6.1. Antibacterial assay by resazurin method. The antibacterial activity of RcAgNP were evaluated by resazurin method [22]. Both gram positive and gram negative strains were tested for antibacterial activity of RcAgNPs. A uniform number of bacterial cells i.e. 5×10^5 cfu ml^{-1} was maintained in this assay. RcAgNPs were suspended in deionized water at a concentration of 1 mg ml^{-1}. The nanoparticle suspension was sonicated to disperse nanoparticles uniformly and various dilutions were prepared from 1 mg ml^{-1} RcAgNP stock suspension. Resazurin solution was prepared by dissolving 270 mg resazurin in 40 ml water. Sterile 96 well plate was used for the assay. Each well contained 50 μl of the nanoparticle, 10 μl of resazurin solution, 30 μl of Luria Bertani broth and 10 μl bacterial suspensions. Positive control contained kanamycin of same concentrations as that of nanoparticles along with other components. One set without nanoparticles or antibiotic and another set without bacteria were considered as negative controls. The plates were sealed with parafilm and kept at 37 °C for 24 h in static condition.

2.5.6.2. Growth curve analysis of RcAgNP treated E. aerogenes. Growth curve analysis of *E. aerogenes* treated with different concentrations of RcAgNPs (0, 20, 50 and 100 μg ml^{-1}) was carried out to understand their growth pattern under RcAgNP treatment with time. Bacteria was inoculated in Luria Bertani broth and kept overnight at 37 °C temperature and shaking at 180 rpm. Then growth medium was inoculated to obtain 5×10^5 cfu ml^{-1} of bacterial cells. Uniformly dispersed nanoparticle from 1 mg ml^{-1} stock suspension was diluted to obtain desired dilution. Bacterial culture without any treatment was considered as negative control and kept along with the treated ones at 37 °C and 180 rpm. Absorbance was measured at 600 nm for 10 h starting from the 0th hour i.e. just after the nanoparticle addition.

2.5.7. Cell viability assay. Cytotoxicity of RcAgNP was assessed by 3-(4, 5-dimethylthiazole-2-yl)-2,5-diphenyltetrazolium bromide (MTT) assay in mouse fibroblastic cell line L929 as mentioned in [23]. In a 96 well plate, each well was seeded with 1×10^4 cells in 100 μl cell culture medium (Dulbecco's modified eagle medium (DMEM)) with 10% fetal bovine serum. A series of RcAgNP dilutions (5–100 μg ml^{-1}) were prepared in serum free culture medium from 1 mg ml^{-1} stock suspension for the treatment. After 24 h of seeding each well was treated with 100 μl of UV sterilized uniformly suspended RcAgNP. Negative control did not contain any test material. After 24 and 48 h incubation culture medium was discarded and 100 μl of MTT at 0.5 mg ml^{-1} concentration in serum free culture medium was added and kept for 4 h incubation. Blue formazan crystals formed thereafter were solubilized in 100 μl of DMSO. The absorbance was measured at 570 nm with reference wavelength at 690 nm using Elisa plate reader (Tecan i-control,

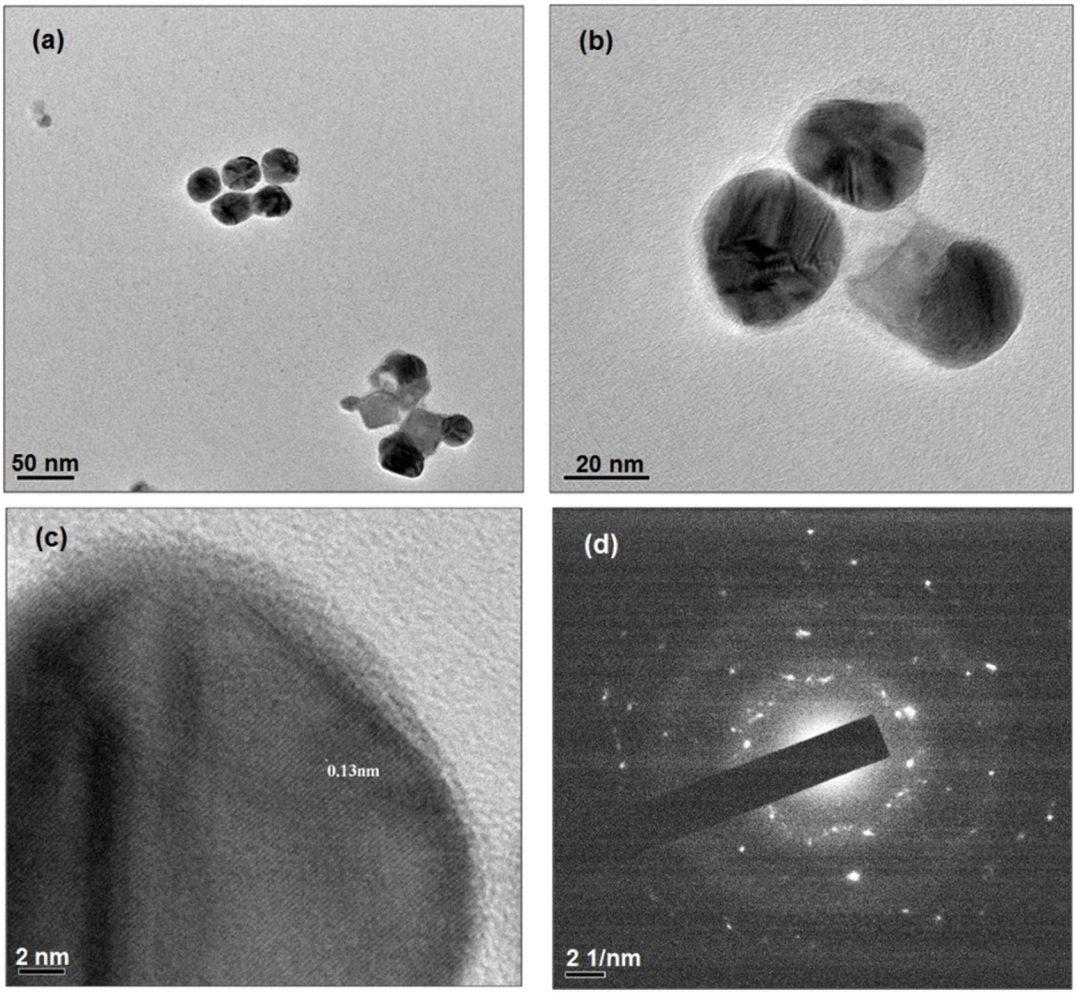

Figure 3. TEM images at (a) lower magnification, (b) higher magnification; (c) UHRTEM image and (d) SAED image of RcAgNPs.

1.11.1.0). Cell viability assay was expressed with the following equation

$$\text{Viability}(\%) = \frac{N_T}{N_C} \times 100,$$

where N_T, N_C are absorbance of nanoparticle treated and negative control cells, respectively.

3. Results and discussions

3.1. Reducing capacity R. communis var. carmencita leaf extract and RcAgNP synthesis

Antioxidant activity of the *R. communis* var. *carmencita* leaf extract was assessed by DPPH method. A linear curve was obtained on plotting percentage inhibition against concentration separately for standard and extract. Half maximal inhibitory concentration (IC_{50}) was calculated using linear equation obtained from standard curve and was found to be 7.45 μg ml^{-1} whereas for ascorbic acid the value was 2.84 μg ml^{-1}. The total phenolic content of the leaves was found to be 12.42 GAE mg^{-1}.

The color change of silver nitrate solution from clear solution to golden yellow color upon addition of *Ricinus communis* var. *carmencita* leaf extract indicates the reducing potency of phytochemicals present in it which is related to the total phenolic content of the leaves.

3.2. Physical and optical properties of RcAgNPs

3.2.1. UV–Vis spectroscopic analysis. The color change of the silver nitrate solution from transparent to golden yellow color was observed after addition of leaf extract at an optimal ratio. This color change is due to the excitation of surface plasmonic vibrations of silver nanoparticles [24]. Absorbance spectra of all the prepared solutions containing varying ratios of leaf extract (10 μg ml^{-1}) and silver nitrate (1 mM) has been depicted in figure 1. A peak at 442 nm wavelength indicated the SPR of the synthesized silver nanoparticles in the solution containing leaf extract and silver nitrate at 1:3 ratio. The SPR peak reached its maxima at 430 nm after 24 h of addition of all the components which articulates maximum reduction of silver ions after 24 h. UV–Vis absorption spectrum of the reaction mixture was measured for 24 h at 2 h interval. From the absorbance spectra (figure 2) it has been observed that the absorbance of nanoparticles intensified with time at 430 nm. Highest absorbance was recorded at 24 h of the synthesis of nanoparticle at room temperature.

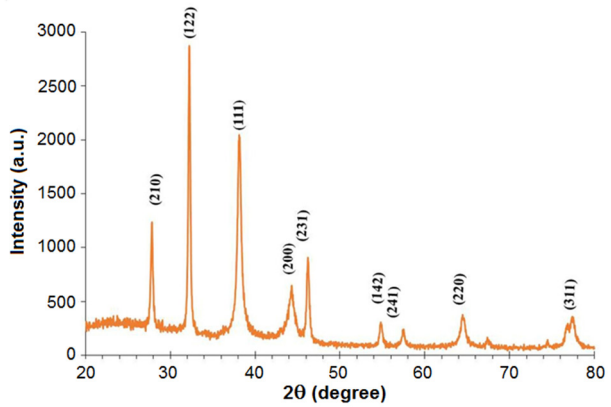

Figure 4. XRD pattern of RcAgNPs.

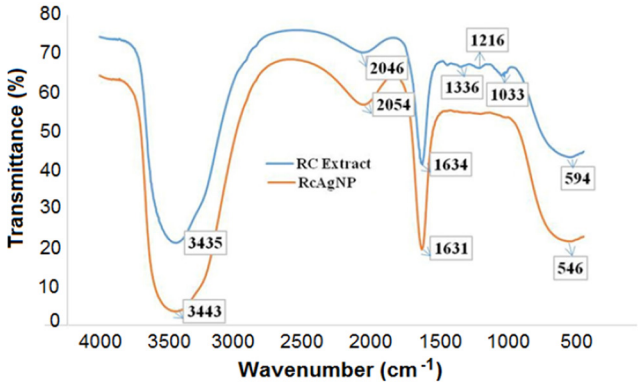

Figure 5. FTIR analysis of RcAgNPs and *Ricinus communis* var. *carmencita* leaf extract.

3.2.2. TEM analysis. Transmission electron microscope (TEM) study was performed to estimate the shape and size of the nanoparticles. RcAgNPs synthesized were mostly seen in spherical shape (figures 3(a) and (b)). Size varied from 30–40 nm when analyzed under TEM model JEM-2100. Lattice fringes with 0.13 nm spacing were observed on the nanoparticle surface in ultra-high resolution TEM (UHR-TEM) images (figure 3(c)) which correspond to the (2 2 0) crystal planes of silver nanoparticle [25]. Selected area electron diffraction pattern image (figure 3(d)) showed concentric rings with bright spots due to Braggs reflection coming from separate crystals thereby affirming the crystallinity of the RcAgNPs [26].

3.2.3. XRD analysis. XRD pattern of RcAgNP is presented in figure 4. XRD analysis of RcAgNPs showed presence of Bragg's peaks at 2θ values 27.81°, 32.19°, 38.16°, 44.43°, 46.23°, 54.93°, 57.39, 64.65°, 77.61° corresponding to (2 1 0), (1 2 2), (1 1 1), (2 0 0), (2 3 1), (1 4 2), (2 4 1), (2 2 0) and (3 1 1) planes of silver metals based on face centered cubic structure as per described in [27, 28]. Thus the XRD studies confirm the crystallinity of RcAgNPs.

3.2.4. FTIR analysis. Green synthesized nanoparticles are stabilized by capping with phenolic constituents of leaf extract which are responsible for the Ag^{++} reduction. Therefore FTIR studies of RcAgNPs and leaf extract was performed to distinguish plant phenolic compounds capping on RcAgNP surface. Figure 5 showed common absorbance at 3443 cm^{-1} and 1631 cm^{-1} corresponding to alcohol O–H stretch, and N–H bond of amine groups respectively which ensures capping of the nanoparticles with these functional groups. Absorbance at 2054 cm^{-1} in RcAgNP spectrum and at 2046 cm^{-1} in leaf extract spectrum were also observed which correspond to C = O stretch. Due to capping of the nanoparticles with these functional groups the stability of nanoparticles was maintained.

3.2.5. TGA and DTA analysis. Thermal analysis was carried out to study thermal characteristics of RcAgNPs. TGA reports

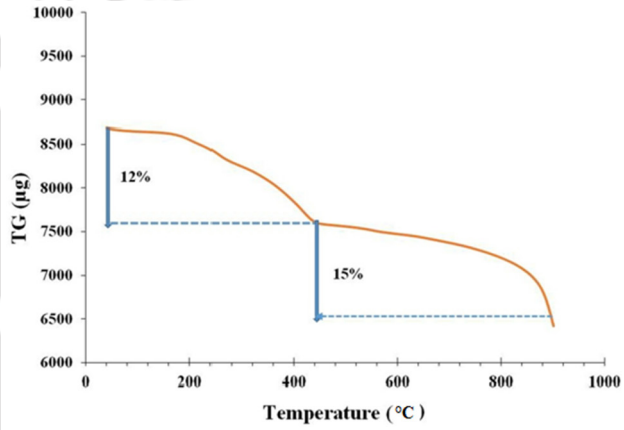

Figure 6. TGA analysis of RcAgNPs.

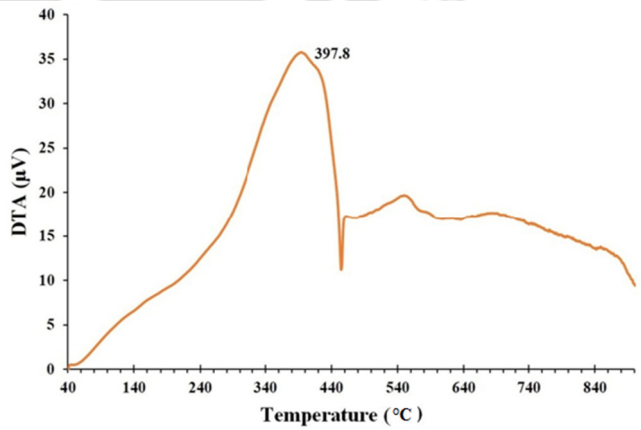

Figure 7. DTA analysis of RcAgNPs.

change in mass with temperature, which in turn indicates thermal stability, material purity and moisture content of the nanoparticles. From the thermo gravimetric curve shown in the figure 6, it is visible that loss of nanoparticle weight was two stage process. In the first stage 12% of the initial weight of nanoparticles was lost between 200 °C to 440 °C and in the second stage, 15% weight was lost between 440 °C to 900 °C. There was almost no loss of weight till 180 °C. The weight

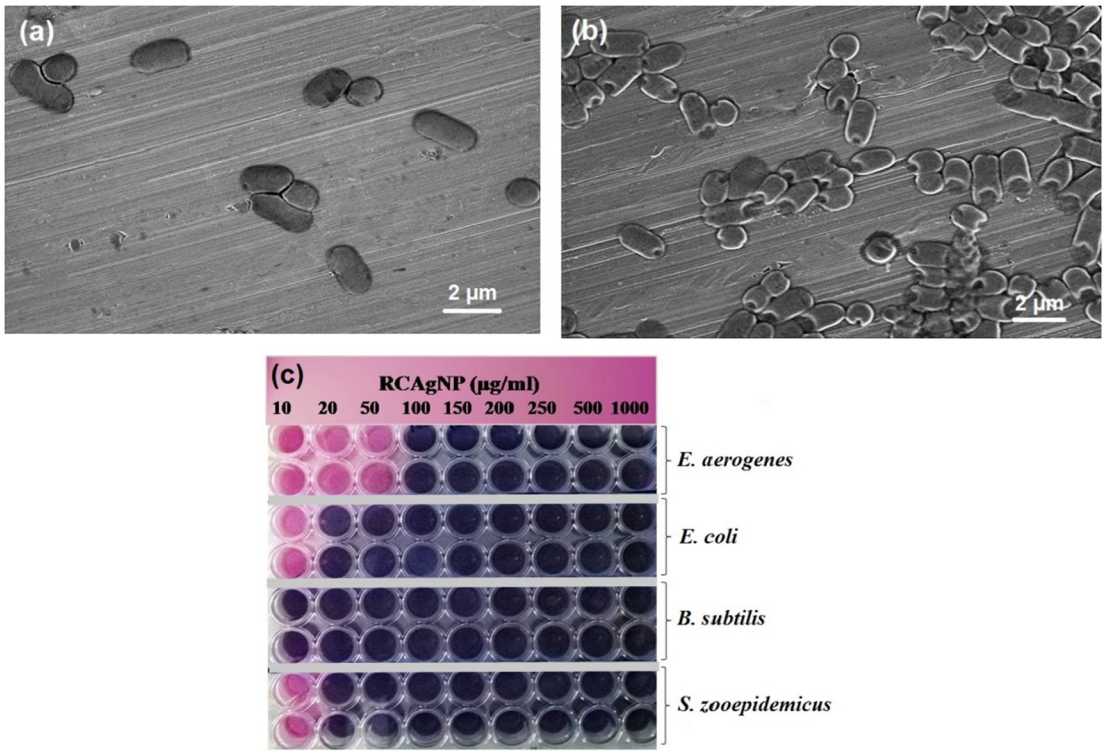

Figure 8. FESEM images of (a) untreated *E. aerogenes*, (b) RcAgNP treated *E. aerogenes*; (c) antibacterial assay by Resazurin method.

Table 1. List of minimum inhibitory concentrations of RcAgNP and kanamycin against bacterial strains.

No.	Bacterial strain (5×10^5 cfu ml^{-1})	MIC of RcAgNP (μg ml^{-1})	MIC of kanamycin (μg ml^{-1})
1	*E. aerogenes* (MTCC No. 2824)	100	10
2	*E. coli* (MTCC No. 443)	20	10
3	*B. subtilis* (BS168GW)	10	10
4	*S. zooepidemicus* (SZ3523)	20	250
5	*S. aureus* (NCIM 2901)	10	10

loss of RcAgNPs might be due to the presence of moisture content and organic residues sourced from leaf extract [23].

Another thermal analysis, DTA reports change in temperature of sample with respect to reference when subjected to heat. In the DTA curve (figure 7), a peak at 398 °C temperature infers that the weight loss due to decomposition of organic residues was an exothermic reaction [28]. Both TGA and DTA analysis suggests that RcAgNPs were stable up to 200 °C.

3.2.6. Antibacterial assay. Resazurin method. The minimum inhibitory concentration was determined from the color of resazurin which is an indicator of the bacterial growth. Oxidoreductase enzymes present in viable cells reduce non-fluoresent and non-toxic resazurin dye to resorfurin which is pink in color. Resorufin on further reduction becomes hydroresorufin which is colorless [22]. Therefore blue color indicates no bacterial growth whereas pink color denotes presence of viable bacterial cells (figure 8). The MICs of RcAgNP and kanamycin for bacterial strains at 5×10^5 cfu ml^{-1} were listed in table 1. Membrane damage and distorted morphology in

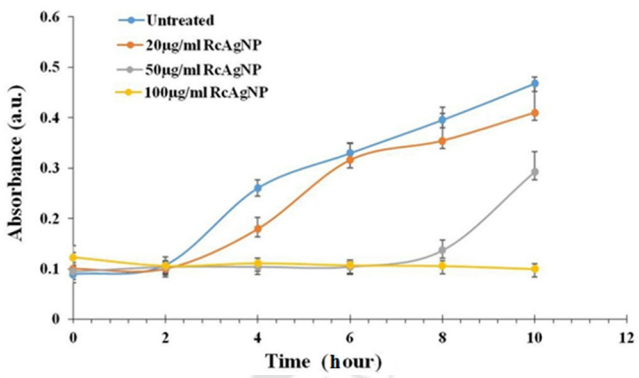

Figure 9. Growth curve of *E. aerogenes* treated with RcAgNP at different concentrations.

RcAgNP treated *E. aerogenes* was observed in FESEM images (figure 8) whereas the untreated bacterial cells had intact cell membrane.

From the resazurin antibacterial assay, it can be inferred that RcAgNPs possess bactericidal activity against both gram positive and gram negative strains listed above. RcAgNPs has the maximum inhibition against *B. subtilis* and *S. aureus* in comparison to other strains used in this experiment. RcAgNP inhibited growth of *E. aerogenes* at 100 μg ml^{-1}. However RcAgNP inhibited *E. coli* and *S. zooepidemicus* growth at a little higher concentration. Interestingly kanamycin had lesser inhibitory effect on *S. zooepidemicus* at 10 μg ml^{-1} which was the MIC value for RcAgNP. Figure 9 shows growth curve of *E. aerogenes* treated with RcAgNPs of different concentrations (0, 20, 50 and 100 μg ml^{-1}) for 10 h. From the growth curve it was evident that growth of *E. aerogenes* increased

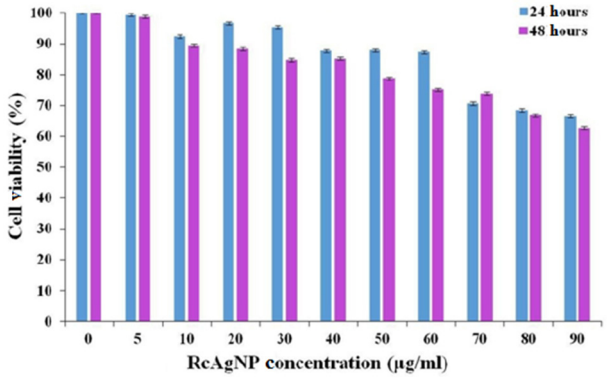

Figure 10. Cytotoxicity assay of RcAgNP in L929 cell line at 24 h and 48 h.

with time in case of negative control, however *E. aerogenes* treated with nanoparticle had inhibited growth. Additionally *E. aerogenes* was not able to grow in presence of 100 μg ml^{-1}. Absorbance at 0th hour of 100 μg ml^{-1} treated bacteria was higher due to the absorbance of nanoparticle suspended in the culture. It is also observed that at 50 μg ml^{-1} growth of *E. aerogenes* was inhibited similar to 100 μg ml^{-1} but, after 8th hour some of the viable bacteria could resist the nanoparticle treatment and started to grow.

3.2.7. Cell viability assay. In this method, MTT is reduced to purple color formazan by mitochondrial dehydrogenase enzymes present in viable cells. This reduction reaction does not occur in the dead cells due to inactivity of mitochondrial dehydrogenase enzyme; hence no blue color is produced. After 24 h of the RcAgNP treatment at 0–60 μg ml^{-1} concentration, 80% mouse fibroblast cells were alive (figure 10) which shows that RcAgNPs were non-toxic to normal cells at 60 μg ml^{-1}.

4. Conclusion

Ricinus communis var *carmencita* is explored as a sustainable green chemical to synthesize silver nanoparticle. Essentially its phenolic elements are pivotal for silver ion reduction and antioxidant activity. The shape and size of the nanoparticle was found mostly spherical and in nanorange by TEM analysis. The crystallinity nature of the nanoparticles was confirmed by XRD and SAED analysis. FTIR analysis showed capping of the nanoparticle that ensures stability of the nanoparticles synthesized. Thermal analyses such as TGA and DTA establish their stability at higher temperature. Although the antibacterial activity of silver and silver nanoparticles are well-known but their activity depends on the size of the nanoparticles. Antibacterial activity of the RcAgNPs was evaluated against gram positive and gram negative bacteria by resazurin reduction assay and the results found to be noteworthy. Biocompatibility of the RcAgNPs were tested by MTT assay and was found to be non-toxic to normal mouse fibroblast cell lines at lower concentrations. Their activity against bacterial strains shows that RcAgNPs has the potential to be used as antimicrobial formulations.

Acknowledgment

We would like to thank Department of Biotechnology, New Delhi Government of India for providing us support and facility to carry out our research work at Institutional Biotech Hub, Centre for the Environment, IIT Guwahati (Project No. BT/04/NE/2009). SO and AS would also like to thank IITG and MHRD for the financial support in the form of fellowship. We extend our thanks to Department of Biosciences and Bioengineering, IIT Guwahati.

References

[1] Abdel-Aziz M S, Shaheen M S, El-Nekeety A A and Abdel-Wahhab M A 2014 *J. Saudi Chem. Soc.* **18** 356
[2] Kim Y S *et al* 2010 *Part. Fibre Toxicol.* **7** 20
[3] Iravani S, Korbekandi H, Mirmohammadi S V and Zolfaghari B 2014 *Res. Pharm. Sci.* **9** 385
[4] Ghorbani H R, Safekordi A A, Attar H and Sorkhabadi S M 2011 *Chem. Biochem. Eng. Q.* **25** 317
[5] Banerjee P, Satapathy M, Mukhopahayay A and Das P 2014 *Bioresour. Bioprocess.* **1** 3
[6] Rodríguez-León E, Iñiguez-Palomares R, Navarro R E, Herrera-Urbina R, Tánori J, Iñiguez-Palomares C and Maldonado A 2013 *Nanoscale Res. Lett.* **8** 318
[7] Makarov V V, Love A J, Sinitsyna O V, Makarova S S, Yaminsky I V, Taliansky M E and Kalinina N O 2014 *Acta Nat.* **6** 35
[8] Agnihotri S, Mukherji S and Mukherji S 2014 *RSC Adv.* **4** 3974
[9] Lee W, Kim K J and Lee D G 2014 *Biometals* **27** 1191
[10] Salem W, Leitner D R, Zingl F G, Schratter G, Prassl R, Goessler W, Reidl J and Schild S 2015 *Int. J. Med. Microbiol.* **305** 85
[11] Ma J, Zhang J, Xiong Z, Yong Y and Zhao X S 2011 *J. Mater. Chem* **21** 3350
[12] Arakha M, Pal S, Samantarrai D, Panigrahi T K, Mallick B C, Pramanik K, Mallick B and Jha S 2015 *Sci. Rep.* **5** 14813
[13] Gavade S M, Nikam G H, Dhabbe R S, Sabale S R, Tamhankar B V and Mulik G N 2015 *Adv. Nat. Sci.: Nanosci. Nanotechnol.* **6** 045015
[14] Kumar V A, Uchida T, Mizuki T, Nakajima Y, Katsube Y, Hanajiri T and Maekawa T 2016 *Adv. Nat. Sci.: Nanosci. Nanotechnol.* **7** 015002
[15] Govindappa M, Farheen H, Chandrappa C P, Rai R V and Raghavendra V B 2016 *Adv. Nat. Sci.: Nanosci. Nanotechnol.* **7** 035014
[16] Selvi B C G, Madhavan J and Santhanam A 2016 *Adv. Nat. Sci.: Nanosci. Nanotechnol.* **7** 035015
[17] Ebrahiminezhad A, Bagheri M, Taghizadeh S M, Berenjian A and Ghasemi Y 2016 *Adv. Nat. Sci.: Nanosci. Nanotechnol.* **7** 015018
[18] Raaman N 2006 *Phytochemical Technique* (NewDelhi: New India Publishing) p 9
[19] Sahu R K, Kar M and Routray R 2013 *J. Med. Plants Stud.* **1** 21
[20] Stankovic M S 2011 *Kragujevac J. Sci.* **33** 63

[21] Alhakmani F, Khan S A and Ahmad A 2014 *Asian Pac. J. Trop. Biomed.* **4** S656
[22] Sarker S D, Nahar L and Kumarasamy Y 2007 *Methods* **42** 321
[23] Sett A, Gadewar M, Sharma P, Deka M and Bora U 2016 *Adv. Nat. Sci. Nanosci.: Nanotechnol.* **7** 025005
[24] Awwad A M, Salem N M and Abdeen A O 2013 *Int. J. Ind. Chem.* **4** 29
[25] Tapia V R, Tizapa M S, Mora E R, Martínez M L O, Franco A and Calva E B 2016 *Plasmonics* **11** 1417
[26] Sathyaseelan B, Baskaran I and Sivakumar K 2013 *Soft Nanosci. Lett.* **3** 69
[27] Meng Y 2015 *Nanomaterials* **5** 1124
[28] Khan M A M, Kumar S, Ahamed M, Alrokayan S A and Alsalhi M S 2011 *Nanoscale Res. Lett.* **6** 434

CHAPTER

16

Nanotechnology in Crop Protection

Sunita Ojha, Deepika Singh, Arghya Sett, Hasnahana Chetia, Debajyoti Kabiraj, Utpal Bora

Indian Institute of Technology Guwahati, Guwahati, India

16.1 INTRODUCTION

Nanoparticles (NPs) are particles in a nanorange structure with unique optical, magnetic, electrical, and thermal properties (Luo et al., 2015). Compared to their bulk materials they have more strength with superior conductivity and reactivity (Annadhasan et al., 2014). The large number of surface atoms alters the surface-related properties of the particle in their nanosize. These surface atoms make these NPs very reactive for use as catalysts. In addition, high surface energy and spatial confinement properties of the NPs aid in quantum effects. Quantum confinement alters the energy band structure and charge carrier density, which in turn alters the optical and electronic properties (Buzea et al., 2007; Roduner, 2006).

Nanotechnology utilizing these nanomaterials is a multifaceted technology that has been applied in material science, electronics, energy sectors, biotechnology, medicine, and many other sectors. In agriculture, it has gained momentum over time with an abundance of public funding and government policies to combat food crises. Numerous scientific reports and patents filed in this field suggest the advancement of nanotechnology in crop protection and disease management (Parisi et al., 2015). In farming, nanointervention improves yield by increasing the efficiency of nutrient uptake and protects crops from pests through nanoformulations of pesticides. Development of new-generation pesticides with better carrier systems and decontamination of water and soil using nanotechnology also helps in crop protection. Moreover, bionanotechnology helps in better understanding host–parasite interaction at the molecular level. Preservation and packaging of food are some of the other applications of nanotechnology. It is a boon to the concept of precision farming, which aims for targeted delivery, firm attachment, and controlled release of the active material. Encapsulation or entrapment of agrochemicals using polymers and dendrimers by surface ionic attachment helps in their controlled release and improves solubility and stability. Because of their antimicrobial activity, nanoparticles of metals such as silver, zinc oxide, and titanium oxide, and nonmetals such as silica and sulfur can be used to eradicate bactericide- and fungicide-resistant pathogens (Chowdappa and Gowda, 2013; Aziz et al., 2015, 2016).

Nanomaterials in Plants, Algae, and Microorganisms
http://dx.doi.org/10.1016/B978-0-12-811487-2.00016-5